INELASTIC STATIC AND DYNAMIC RESPONSE

OF

FRAME TUBE STRUCTURES

By

© BASSAM ABDUL RAHMAN HALABIEH, B.Sc, M.Sc.

A Thesis

Submitted to the School of Graduate Studies

in Partial Fulfilment of the Requirements

for the Degree of

Doctor of Philosophy

McMaster University

July 1989

ISBN 0-315-52139-2

INELASTIC STATIC AND DYNAMIC RESPONSE OF FRAME TUBE STRUCTURES

TO MY PARENTS AND MY WIFE

DOCTOR OF PHILOSOPHY (1989)
(Civil Engineering and Engineering Mechanics)

McMaster University
Hamilton, Ontario

TITLE: Inelastic Static and Dynamic Response of Frame Tube Structures.

AUTHOR: Bassam Abdul Rahman Halabieh, B.Sc. University of Louisiana
M.Sc. University of California, Berkeley.

SUPERVISOR: Professor Wai K Tso

NUMBER OF PAGES: xiv, 183

ABSTRACT

A study has been made for the inelastic response of a thirty story frame tube structure subjected to static loading as well as dynamic excitation. The intent of this study was (i) to develop a simplified model for frame tube structures in order to compute both elastic and inelastic responses of such structures when subjected to lateral loadings, (ii) to identify the parameters that govern the behavior of frame tube structures, (iii) to assess the significance of the tube action on the elastic as well as inelastic responses, and (iv) to provide guidelines to estimate the structural responses when subjected to multiple components of earthquake ground motions.

The simplified model reduces the 3-D frame tube system into sets of plane frames, interconnected by 3-D beam column elements. It is shown that this model gives good accuracy for each of the static and dynamic loading cases when compared with the results based on a 3-D model. The computer time involved with the planar model is at least one third that for the 3-D model. Therefore, it is believed that the proposed model is a viable tool for the inelastic analysis of frame tube structures.

The tube action is referred to as the forces developed in the two frames that are orthogonal to the direction of loading and which provide partial resistance to the applied loading. In order for this tube action to be effective, it is found that the frame tube should deflect like a cantilever with linear variation of axial force in the columns of the longitudinal frames and almost uniform axial force in the columns of the transversal frames. The key parameter that governs the inelastic dynamic response of frame tube structure was found to be the change of the post elastic story stiffness from the elastic story stiffness. For a large change of story stiffness, the bottom stories suffered large interstory drift. However, by decreasing

such changes, the interstory drift became more evenly distributed along the height of the structure.

The inelastic response when the frame tube is subjected to a bidirectional excitation is finally presented. It is found that the approximate estimates suggested by design codes underestimate the response. An alternative was proposed to give a more realistic estimate. Such scheme is the simple summation rule.

ACKNOWLEDGEMENTS

I would like to express my sincere gratitute to Dr. W.K. Tso for his guidance, advice and interest during the course of this study.

Special thanks are due to Dr. F. A. Mirza, Dr. A. Ghobarah, and Dr. M. Dokainish, members of my supervisory committee, for their valuable comments and suggestions.

I wish to thank my wife Sawsan for her help, patience and encouragement towards the completion of this thesis. Special thanks are to my mother for her inspiration. Finally, I wish to thank my brothers for their encouragement too.

Particular acknowledgement is due to the Natural Sciences and Engineering Research Council of Canada (NSERC) and to McMaster University for providing the financial support for the research work.

TABLE OF CONTENTS

TABLE OF CONTENTS (continued)

TABLE OF CONTENTS (continued)

LIST OF FIGURES

LIST OF FIGURES (continued)

LIST OF FIGURES (continued)

LIST OF FIGURES (continued)

LIST OF FIGURES (continued)

LIST OF TABLES

CHAPTER ONE

INTRODUCTION

1.1 GENERAL

Recent developments in the design of high-rise buildings have produced a number of new structural systems which are efficient and economic in the use of materials. The frame tube is one such system. The frame tube can be defined as a structural system that prompts the building to behave as an equivalent hollow tube. At present, of the world's five tallest buildings, four of them are tubular systems. They are the 110-story Sears Tower, the 100-story John Hancock Building, the 83-story Standard Oil Building in Chicago, and the 110-story World Trade Center Towers in New York city. The earliest application of the tubular concept is credited to Fazlur Khan who introduced the system in a 43 story apartment building in Chicago in 1961. Tubular systems are cost-efficient and in most cases, the amount of structural material needed is comparable to the material used in a conventional frame building which is half the size [37]. Until the evolution of the frame tube structures, most high-rise buildings were designed as frame structures consisting of series of rigid joint frames arranged in two perpendicular directions. Lateral loads were resisted by these frames, supplemented, if required, by vertical shear walls or trusses located within the service core of the building. Further improvement in the structural economy is achieved by engaging the exterior frames with core trusses which is accomplished by tying the two systems through belt and outrigger trusses.

The introduction of the tubular system for resisting lateral loads revolutionized the design of high-rise buildings. The system strives to create a wall-like structure around the building exterior. In a frame tube, this is achieved by the use of closely spaced columns with

deep spandrels. The structure can be viewed as a cantilever tube with holes cut out for the windows. Because the perimeter frames resist the entire lateral load, costly interior diagonal bracings or shear walls are kept to a minimum, thus increasing the net leasable area for the building.

The tube system can be constructed of reinforced concrete, structural steel, or a combination of the two. The method of achieving the tubular behavior by using columns on close centers connected by deep spandrel beams is the most popular system because rectangular windows can be accommodated in this design. A different approach which permits larger spacing of columns is called the braced concept. It spans diagonal bracings on the periphery of the building. Yet another approach is to use two or more tubes tied together to form a bundled tube. The frame tube buildings completed in the 1950s and 1960s were mostly rectangular and prismatic in form. Since then, frame tube structures have evolved into nonprismatic and curvilinear shapes.

The majority of the high-rise buildings with tubular systems have been built in strong wind regions such as Chicago and New York. The continuous need for high-rise structures has attracted the interest of many design firms to build such systems in seismic regions. Recently, three high-rise projects in seismic active zones have been completed using the tubular system. All in California, they are the Raymond Kaiser Engineers building in Oakland, the South Tower in Los Angeles and the 345 California Street building in San Francisco. While frame tube structures performed efficiently when subjected to strong wind, their performance when subjected to major earthquake excitations is less certain. The design philosophies for wind and earthquake loadings are different. A structure normally responds within the elastic limit of the material under wind loading that can be expected during its life. The seismic forces specified in the design codes are quite small relative to the actual forces expected during strong seismic shaking. Due to economic considerations, design code allows

structures to be designed for lower seismic forces. In return, part of the energy input in the event of a strong earthquake is expected to be dissipated by means of inelastic deformations.

The purpose of this research is to provide information concerning the efficiency and performance of frame tube structures when subjected to lateral dynamic excitation. More specifically, it is concerned with the dynamic inelastic response of such systems in the event of a strong earthquake.

1.2 LITERATURE SURVEY

As discussed previously, frame tube structures resist lateral loads by means of closely spaced columns placed around the perimeter of the building and connected by deep spandrel beams. Simply stated, the columns and beams form four planar frames which are connected at four corner columns.

To understand the elastic and inelastic behavior of frame tube structures to lateral loads, one needs first to study the response of planar frames (2-D Plane frame), then to study the response when these frames are connected at their edges (frame tube). The study of the elastic response of frame structures will not be reviewed. Such a study can be performed either approximately using the 'Cantilever method' [44] or the 'Portal method' [38], or exactly using a plane frame program. The inelastic response of frame structures deserves special consideration and is reviewed in detail. Then, the elastic response of frame tube structures is reviewed. Finally, the inelastic response of frame tube structures is discussed when reviewing the inelastic response of three dimensional structures.

1.2.1 Inelastic Response of Planar Frames

The majority of seismic response of frame structures is carried out in 2-D space. These planar analyses simplify the problem by assuming that it was sufficient to

independently analyze the structure along its principal axes of resistance subjected to ground motion acting one direction at a time. With this planar modelling, further simplifying assumptions are necessary to carry out such a response. Among these assumptions are the following: (i) yielding may take place only in concentrated plastic hinges at the element ends; (ii) the force deformation relationship is of the bilinear type, and (iii) the strain hardening is approximated by considering the element to consist of elastic and elasto-plastic components in parallel.

Using these assumptions, an early study of the inelastic earthquake response of tall buildings is reviewed by Clough, Benuska and Wilson [10]. Based on the study on a twenty story moment resisting frame, they concluded that the strong column weak beam design is an effective approach to the earthquake resistant design of tall buildings.

A general purpose computer program for the dynamic analysis of inelastic plane structures that is suitable for practical and commercial use (DRAIN-2D) was developed by Powell and Kanaan [21], and has been recently updated by Powell and Allahabadi (DRAIN2-DX) [34]. One of the best features of the computer program is its 'modularity', or structuring the program as a base program to which a number of auxiliary programs for new structural elements or new constitutive laws can be added. The base program reads and prints the structure and loading data, carries out a variety of bookkeeping operations, assembles the structure stiffness and loading, and determines the response of the structure. All stiffness and state calculations associated with elements are carried out within the auxiliary program and information returned to the base program. With this adaptability, the program has a long term objective of providing the structural engineering field a powerfull tool for further understanding of the inelastic response of plane structures.

Within the framework of the planar response, other factors are considered. Andreaus and D'Asdia [3] proposed a method to evaluate the displacement of elasto-plastic

frames when the actual spread of plastic zones is included in the analysis. For their two story frame, very small deviation from the zero length plastic hinge was observed. Hilmy [19] described a Lagrangian formulation in conjunction with force-space for nonlinear analysis of steel frames. The concise formulation of the tangent stiffness provided an effective and reasonably fast nonlinear analysis.

Many researchers have addressed the concept of a mechanism that would insulate the super structure from the earthquake input at the base [9,15,25]. The ultimate step in this direction would put the building on a roller bearing system so that no horizontal forces could be transmitted into the structure when the ground beneath it moves. Practical factors such as problems with utility connections rule out this solution, but a similar alternative of introducing easily deformable soft columns in the first story provides effective protection to the structure.

1.2.2 Elastic Response of Frame Tube Structures

The elastic response of frame tube structures can be performed exactly using a three dimensional frame program as described by Wilson [7,48]. Such an analysis tends to be expensive due to the large number of members and joints encountered in the structure. Thus, effort has been made to adopt simplified model of the structure but requires substantially less computer time to solve. In all these models, the 3-D frame tube was replaced with a set of parallel frames. Coull [12] introduced vertical shear transfer members and Khan [22] described shear hinges to connect the parallel frames. Powell [21] constrained the vertical displacement along the frame edges to be identical. The analysis was then carried out using a standard plane frame program.

1.2.3 Inelastic Response of Three Dimensional Structures

While many investigations have been conducted on the inelastic response of plane frames, the progress in the elasto-plastic dynamic response analysis of three dimensional structures has been slow because of the complicated interactions of bending moments and shears in two directions along with axial forces and torques. .

An early attempt on the dynamic analysis of inelastic three dimensional structures was carried out by Nigam [30]. In his study, the concept of yield surface is used. The yield surface was expressed in terms of the generalized forces acting on the element. By assuming a flow rule that controls the growth of the plastic deformations, the tangent stiffness relating the incremental forces and incremental displacements is formulated. Powell and Riahi [35] extended Nigam's work, and formulated the tangent stifness in matrix form for a three dimensional beam column element oriented arbitrarily in space. Analysis was made possible by the implementation of this element into his general purpose computer program for the three dimensional analysis of nonlinear structural response (ANSR) [26]. However, the large amount of computer time commonly required for large structures limits its use.

Other investigators addressed more refined problems of inelastic analysis of three dimensional space frames. Uzidger [43] describes a numerical method for such analysis where the force displacement at the ends of the members are represented by an equation corresponding to the inverse of the Ramberg-Osgood representation. The tangent stiffness matrix is formulated by taking into account the P-delta effect. Farhoomand [14] considered the plastic deformation over a finite length by replacing a small portion of each yielding member by an elasto-plastic segment with lumped flexibility.

The inelastic analysis of frame tube structures can be carried out by ANSR [26] or the method described by Uzidger [43] or Farhoomand [14]. The computational effort, however, prohibits such an analysis. To date, no published work on the inelastic analysis of frame tube

structures has been reported. However, the planar model described by Coull [12], Khan [22], and Powell [21] can be extended to carry out such an analysis. A more elaborate discussion on the planar model for the inelastic analysis of frame tube structure is described in chapter two.

1.3 SCOPE AND OBJECTIVES

The following objectives are set for the present investigation:

(1) To develop a simplified procedure capable of computing both elastic and inelastic responses of frame tube structures subjected to lateral loading.

(2) To identify the parameters governing the behavior of frame tube structures.

(3) To investigate, and understand, the dynamic inelastic behavior of frame tube structures.

(4) To provide the designer with guidelines on improving the dynamic inelastic response, and

(5) to provide guidelines to account for the bidirectionality of the ground excitation.

The scope of the present study is confined to structures with the following characteristics:

(1) The structure consists of an assembly of four planar perimeter frames which interact through four common corner columns. The floor diaphragms are considered rigid in their own planes.

(2) Frame tube structures with rectangular, or square plan, are considered. Triangular, frame tube having reentrant corners, or bundled tube are not considered.

(3) The planar perimeter frames are idealized as a finite number nodes connected by a finite number of deformable elements. The nodes are considered as points.

(4) The perimeter frames possess stiffness only within their plane. The out-of-plane stiffness is assumed to be small and therefore neglected.

(5) Cores or walls within the perimeter frames are assumed to resist gravity loads only. Therefore, they are not considered to participate to resist lateral loads.

(6) The common columns at the corner of the rectangular frame tube system have identical properties about both principal axes.

(7) Shear deformations in the beams and columns are neglected.

(8) Material nonlinearity is of the bilinear type with yielding taking place in concentrated plastic hinges of zero length at the element ends. In this study, the post elastic stiffness is taken to be 1% of the initial stiffness.

To accomplish the stated objectives, the study is organized as follows. In chapter two, a simplified model will be developed to represent frame tube structures under lateral loadings. In chapter three, the static and dynamic lateral behavior of frame tube structures when loaded within the elastic limit and loaded into the inelastic limit are discussed. The parameters governing the behavior of such structures will be identified. In chapter four, the static and dynamic behavior of frame tube structures with different distributed beam strengths are investigated. In chapter five, the response when the frame tube is subjected to a bidirectional ground excitation is discussed. Finally, the conclusions of this study are summarized in chapter six. It is the intention of this study to clarify the dynamic inelastic response of frame tube structures, and to provide the designer with an understanding of the behavior of such systems when subjected to earthquake ground motions.

CHAPTER TWO

PLANAR MODEL OF FRAME TUBE STRUCTURES

2.1 INTRODUCTION

In its simplest form, a frame tube lateral load resisting system can be considered as a structural system consisting of four planar frames arranged orthogonal to each other and located at the perimeter of the building. These orthogonal frames are connected at the corner columns. In other words, each corner column is a common column to two orthogonal frames. Because of the vertical compatability that is enforced at the corner columns, not only the two frames parallel but also the two frames perpendicular to the load direction will be mobilized to resist the lateral loading. To reduce the shear lag effect, the planar frames are usually designed with closely spaced columns interconnected by stiff spandrel beams.

Since both frames parallel and perpendicular to the direction of loading are providing resistance to the lateral load, the analysis of frame tube structures is three dimensional in nature. Several methods have been proposed for the analysis of three dimensional buildings in general [11,20,46,47]. The concept of these methods relies on treating the structure as an assemblage of plane frames linked by the rigid floor diaphragms. This technique greatly reduced the computational effort and led to commercial software such as the DRAIN-TABS program [20] which is widely used in the engineering profession. However, these softwares do not enforce vertical and rotational displacement compatability at the joints of members common to the orthogonal frames. Therefore, they are not suitable for the analysis of frame tube structures. Other computer programs for the three dimensional analysis of structures are available to carry out such a study [26,35], however, the computational effort will be very large. As a result, there is a need to have a simplified model

capable of predicting the behavior of frame tube system without using the three dimensional frame programs.

Recognizing the rigid diaphragm action provided by the floors and the low out-of-plane stiffness as compared to the in-plane stiffness of the frames, several simplified models exist to analyze the elastic behavior of frame tube structures using a two dimensional analysis. In all these models, the three dimensional frame tube system was replaced by a set of parallel frames connected either by vertical shear transfer members [12], shear hinges [22], restraints capable of transfering only vertical shear forces [24] or by constraining the vertical displacement along the frame edges to be identical [21].

The purpose of this chapter is to introduce a more elaborate planar model for frame tube structures in order that the elastic and inelastic responses of such structures subjected to lateral loading can be calculated without large computational effort. The proposed model herein is similar in concept to the model introduced by Coull & Subedi [12] and by Khan [22]. The frame tube system is replaced by a set of connected plane frames. The inelastic behavior that can occur in these frames are modelled by plastic hinges at the end of frame members similar to the model used in the DRAIN-2D [21] inelastic plane frame program. A complete three dimensional beam column element is developed to represent the common column joining the two orthogonal frames. Inelastic actions at this common column element are also taken to be concentrated at its ends. By means of examples, it is shown that the proposed simplified model leads to accurate results both in the elastic and inelastic ranges, and also leads to significant reduction in computational effort. Therefore, it is believed that the proposed model is a viable tool for the inelastic study of frame tube systems subjected to lateral loading.

2.2 METHOD OF ANALYSIS

Consider a frame tube structure in its simplest form subjected to lateral loading along its principal axis as shown in fig. 2.1. The frame tube consists of four moment resisting frames, two frames are parallel to the load direction (longitudinal frames AabB & CcdD) and two frames are normal to the load direction (transversal frames AadD & BbcC). The longitudinal frames and the transversal frames are connected by the corner columns. The overturning from the lateral loading is resisted by two actions. First, it was partially resisted by the frame actions from the longitudinal frames AabB & CcdD. The deformation of these frames causes two corner columns in tension and two other corner columns in compression. The axial deformation of these columns in turn causes tension and compression in the columns of the two transversal frames AadD & BbcC. These tensile and compressive forces in the columns in the transversal frames form resisting couples to resist the overturning moment. This part of the overturning moment resistance is commonly referred to as the tube action. It is the combination of the frame action of the longitudinal frames and the tube action from the transversal frames which resist the external moment.

To analyze a frame tube system subjected to lateral loading, each node in the frames has two translational and one rotational degrees of freedom in the plane of the frame. The out-of-plane degrees of freedom tend to be restrained by the high rigidity of the floor slabs and are neglected. However, the corner columns, being a common element to two orthogonal frames, has predominant degrees of freedom in both orthogonal directions.

Consider a typical element EF along the corner column Bb of fig. 2.1. Its degrees of freedom are shown in fig. 2.2. The degrees of freedom r_2, r_3 & r_5 correspond to deformation in the X, Y & θ directions of plane AabB, and r_1, r_3 & r_4 correspond to deformation in the X, Y &θ directions of plane BbcC.

If frame BbcC is rotated outward by 90 degrees around column line Bb, frames AabB & BbcC will lie in the same plane, and all degrees of freedom of the corner column can conveniently be represented in one plane as shown in fig. 2.3. Care should be taken in interpreting the degrees of freedom shown in fig. 2.3. r_2, r_3, r_5 represent the displacement in the plane of frame AabB and r_1, r_3, r_4 represent the displacement in the plane of the rotated frame BbcC. A node can have a maximum of three degrees of freedom in a plane frame analysis. Therefore, if one assign r_2, r_3 and r_5 degrees of freedom to the principal node, it is necessary to introduce a dummy node to pick up the remaining two degrees of freedom, r_1 and r_4 as shown in fig. 2.4. The dummy node is restrained to have the same vertical displacement as the principal node to satisfy vertical compatibility. On the basis of these degrees of freedom, the formulation of a corner column element is presented next.

2.3 CORNER COLUMN ELEMENT FORMULATION

2.3.1 General Characteristics

An element along the corner column (referred to as a 3-D beam column element) posseses an axial and two flexural stiffnesses about its two principal axes. The axial-extension and moment-rotation relationships are assumed to be bilinear as shown in fig. 2.5. This bilinear relationship is approximated by considering the element to consist of elastic and elastic-perfectly-plastic components in parallel (fig. 2.6). The elastic-perfectly-plastic component may develop a concentrated plastic hinge with zero length at one or both ends. The forces at each potential hinge interact according to the yield function

$$\phi(M_1, M_2, P) = 0 \qquad (2.1)$$

Where M_1 is the moment effect from the longitudinal frame, M_2 is the moment effect from the transversal frame and, P is the axial force.

A commonly used yield function is the elliptic yield function (fig. 2.7) given by

$$\Phi = \left(\frac{M_1}{M_{01}}\right)^2 + \left(\frac{M_2}{M_{02}}\right)^2 + \left(\frac{P}{P_0}\right)^2 - 1 = 0 \qquad (2.2)$$

in which the subscript 0 denotes the fully plastic value when only the stress resultant concerned is acting on the cross section.

2.3.2 Corner Column Displacement and Deformation

The 3-D beam column element has five degrees of freedom at each end or a total of ten displacement degrees of freedom (fig. 2.3). These ten degrees of freedom permit five modes of deformation (axial extension and two flexural deformation at each end) and five rigid body modes. The five modes of deformation can normally be represented by five independent degrees of freedom. However, when the element yields, plastic hinge at one or both ends would form necessitating that the axial mode be represented by two independent degrees of freedom acting at the two ends of the element as shown in fig. 2.8. The transformation matrix relating the deformation and displacement degrees of freedom is

$$\underline{v} = [A]\,\underline{r} \qquad (2.3)$$

where $\underline{v}^T = [v_1, v_2, v_3, v_4, v_5, v_6]$

$\underline{r}^T = [r_1, r_2, r_3, r_4, r_5, r_6, r_7, r_8, r_9, r_{10}]$

$$[A] = \begin{bmatrix} 0 & 0 & 1 & 0 & 0 & 0 & 0 & 0 & 0 & 0 \\ 0 & -1/L & 0 & 0 & 1 & 0 & 1/L & 0 & 0 & 0 \\ -1/L & 0 & 0 & 1 & 0 & 1/L & 0 & 0 & 0 & 0 \\ 0 & 0 & 0 & 0 & 0 & 0 & 0 & 1 & 0 & 0 \\ 0 & -1/L & 0 & 0 & 0 & 0 & 1/L & 0 & 0 & 1 \\ -1/L & 0 & 0 & 0 & 0 & 1/L & 0 & 0 & 1 & 0 \end{bmatrix}$$

and L is the length of the member.

2.3.3 Corner Column Stiffness for Elastic Component

The elastic stiffness matrix of the 3-D beam column element to relate the element end forces shown in fig. 2.9 and element end deformation shown in fig. 2.8 can be written in the form as follows.

$$[K_e] = \begin{bmatrix} k_a & 0 & 0 & -k_a & 0 & 0 \\ 0 & 4k_1 & 0 & 0 & 2k_1 & 0 \\ 0 & 0 & 4k_2 & 0 & 0 & 2k_2 \\ -k_a & 0 & 0 & k_a & 0 & 0 \\ 0 & 2k_1 & 0 & 0 & 4k_1 & 0 \\ 0 & 0 & 2k_2 & 0 & 0 & 4k_2 \end{bmatrix} \quad (2.4\text{-a})$$

in which k_a = axial stiffness (EA/L),

k_1 = bending stiffness in the longitudinal frame direction (EI_1/L), and

k_2 = bending stiffness in the transversal frame direction (EI_2/L).

2.3.4 Tangent Stiffness for Elastic Plastic Component

The tangent stiffness matrix when the element is in the inelastic range was first derived by Nigam [30] based on the normality of the plastic increment of deformation to the yield surface. Powell [35] presented the tangent stiffness in matrix form and is given by

$$dS = [K_e - (K_e \phi_{,S})(\phi_{,S}^T K_e \phi_{,S})^{-1}(\phi_{,S}^T K_e)]dv \quad (2.4\text{-b})$$

in which K_e is the elastic stiffness matrix, and

$\phi_{,s}$ is the gradient matrix of the yield function.

The complete derivation of the tangent stiffness matrix is presented in Appendix A.

The stiffness matrix in terms of the ten displacement degrees of freedom is then obtained from

$$K_d = [A]^T K[A] \quad (2.5)$$

where [A] is the displacement transformation matrix relating the deformation and displacement degrees of freedom, and K is the elastic or tangent stiffness matrix in terms of the deformation degrees of freedom.

2.3.5 Corner Column Implementation

The three dimensional beam column element just described is implemented into DRAIN-2D [21] (general purpose computer program for dynamic analysis of inelastic plane structures). DRAIN-2D consists of a number of base subroutines which read and print the structure and loading data, carry out a variety of bookeeping operations, assemble the structure stiffness and loading, and determine the displacement response of the structure. The base program is then combined with element subroutines to produce a complete program. All data reading and printing operations and all stiffness and state calculations associated with elements are carried out within the element subroutines, and information returned to the base program. Subroutines for the three dimensional beam column element are developed and added to the program. The structure and loading data are consistent with DRAIN-2D user's guide [21]. The format for the input data associated with the three dimensional beam column element is presented in Appendix B. In implementing the 3-D beam column element, the following assumptions have been made:

(a) The element must be vertical,

(b) The dummy node must have the same y-coordinate as its principal node, and

(c) The number assigned to the dummy node should be higher than that of the principal node by one.

2.4 ACCURACY OF THE PLANAR MODEL

To perform an analysis of the frame tube system under lateral loading, one can "cut open" the tube resulting in four plane frames connected by the common columns. By cutting along Aa and rotating the frames, the planar model of the tube is shown in fig. 2.10. Both the elastic and inelastic behavior of the frames can be modelled using the DRAIN-2D [21] computer code, with the common columns represented by the three dimensional beam column element just described.

A frame tube system having thirty storey with uniform storey height of 3.6 m, and each perimeter frame consists of four bays with bay width of 3 m, is taken as an example structure to illustrate the use of the proposed procedure. The accuracy of the proposed model is evaluated by comparing the results with the results obtained from a complete three dimensional analysis using ANSR computer code [26].

2.4.1 Example 1: Loading Along a Principal Structural Axis

First, consider a uniformly distributed static lateral loading of intensity W, applied along a principal structural axis of the building. Due to symmetry, only half of the tube need to be analyzed in this example. The planar model for the half tube can be obtained by rotating frames 11Aa & 22Bb by 90 degrees around their corresponding corner columns and by making use of the three dimensional beam column element along the intersection of the two orthogonal frames. A planar model of the half tube is shown in fig. 2.11 . Since horizontal displacement orthogonal to the direction of loading are zero due to symmetry, horizontal degrees of freedom of all nodes in frames 11Aa & 22Bb should be restrained. Due to the rigid diaphragm action of the floor slabs, the lateral loads can be applied to any node in the longitudinal frame at story levels. First, the structure was subjected to a reference load level W_0 and the resulting beam moment are averaged over five story intervals. These averaged

values are then set to be the beam capacities of the structure. To simulate strong column weak beam design philosophy commonly used in seismic design, interior column moment capacities are set equal to forty percent higher than the adjoining beam capacities. Corner column moment capacities are set equal to the adjoining beam capacities. The axial capacity of the colunm is assumed very large so that yielding in axial tension or compression will not occur. The member properties of the frame tube are summarized in tables 2.1 & 2.2.

The uniform lateral load is then increased monotonically forcing the structure to go beyond its elastic limit. Let R be the ratio of applied loading to the design load intensity W_0. A plot of R vs roof displacement is shown in fig. 2.12 where the roof displacement is normalized by the total height of the structure. The load-top deflection curves based on the proposed scheme and the ANSR 3-D analysis are almost identical. The lateral displacements, beam moments next to the corner column and corner column axial force obtained from the 3-D model and the planar model are compared in fig. 2.13, 2.14 & 2.15. For R = 1 (elastic response), the deflections agree within 0.7%, the beam moments agree within 0.8% and the axial forces agree within 1%. These degrees of accuracies are similar to those reported by Coull & Subedi when they used a planar model to study the elastic responses of a frame tube system [12]. When the frame tube was loaded into the inelastic range (at R=1.2), the deflections based on the 2-D and 3-D models agree within 12%, and the axial forces in the corner column agree within 2.5% . The slope discontinuities or "kinks" observed in the lateral displacement curve is due to the yielding occurring in the columns. The measure of flexural plastic deformation is represented by the plastic hinge rotation. Comparison of the plastic hinge rotation is shown in fig. 2.14-b where the same distribution pattern is predicted by the two models.

In addition to the static analysis, a dynamic analysis is carried by subjecting the frame tube system to the 1940 ElCentro N-S component along its principal structural axis. Minor modification of the member capacities were made and the modification were sum-

marized in table 2.3. The masses used correspond to the full dead load of 4.8 KN/m^2 lumped at each story level. The periods of the three dimensional and planar models are 2.35 and 2.45 sec respectively. A higher period is predicted using the planar model because this model does not include the out-of-plane stiffness. The level of excitation is chosen such that the dynamic elastic base shear would have been equal to four times the design base shear. Subjected to such an excitation, the structure is excited well into the inelastic range. The comparison of maximum lateral displacements, corner column axial forces and plastic hinge rotations are shown in fig. 2.16. In this case, the deflections agree within 19%, the axial forces in the corner column agree within 10%. The maximum plastic hinge rotations along the height of the structure follow the same pattern as shown in fig. 2.16-c .

Furthermore, the comparison of the distribution of the plastic hinges throughout the longitudinal frame is shown in fig. 2.17 where the hinges predicted by the two models are represented by solid circles, the hinges predicted by the 2-D model and not predicted by the 3-D model are represented by solid triangles, and finally, the hinges predicted by the 3-D model and not predicted by the 2-D model are represented by open circles. From fig. 2.17, almost all the hinges in the beams are predicted by the two models except for the top two stories in which the plastic hinge rotation is very small (fig. 16-c) indicating that the beams in these stories are either on the verge of yielding in one model or just above yielding in the other model. The same argument applies to the hinges in the columns whose capacities are selected such that the yielding is delayed or kept minimal (strong column weak beam concept).

2.4.2 Example 2: Static Loading at an Angle ψ to a Principal Structural Axis

In this case, the load can be decomposed into two components W_1 and W_2, with W_1 acting along the direction of frame (AabB & CcdD) and W_2 acting along the direction of frame (BbcC & AadD). The planar model used is shown in fig. 2.10 where plane AabB is fixed while

the others are rotated around their corresponding corner column until all the frames lie in the same plane. Also shown in fig. 2.10 are the three dimensional beam column elements used at column line Aa, Bb, Cc and Dd, and the load direction on the frames properly oriented. In this example, the ratio W_1 / W_2 was fixed to 3.33. First, the tube was subjected to a reference load W_{01} only and the resulting largest beam moment in the structure was set to be the beam capacities. The column moment capacities are set equal to forty percent higher that the beam capacities. The axial capacity of the columns are assumed to be very large to avoid axial yielding of the columns. The member properties for this example are given in tables 2.4 & 2.5.

The lateral loading W_1 and W_2 are increased monotonically, forcing the tube to go beyond its elastic limit. If R is the ratio of the intensity of the lateral load W_1 and W_{01}, a plot of R versus roof deflection is shown in fig. 2.18. The lateral deflections and the corner column axial forces corresponding to $R = 1$ (elastic response) and $R = 1.3$ are compared in fig. 2.19 & 2.20. For $R = 1$ (elastic), the deflections computed using the two computer models agree within 2% and the axial forces agree within 4%. In the inelastic range, the top deflection agree within 13% and the axial forces agree within 5%.

2.5 COMPUTATIONAL EFFICIENCY ESTIMATES FOR INCORE SOLUTIONS

One way to measure computational efficiency is in terms of the number of arithmetical operations, since computer time is directly proportional to the number of operations. The number of operations for solving a system of n equations(equilibrium equations) using the most widely used technique (Gauss elimination) is proportional to n^3 [39]. However, proper numbering of the nodes in the structure yields a banded matrix (i.e. $K_{ij}=0$ for $j>i+mk$ where mk is the half bandwidth of the system) requiring about $1/2nmk^2$ operations for solution [45]. Therefore, computer time is proportional to nmk^2. In this section, the computational efficiency of using the proposed model for inelastic analysis of frame tube structures is compared to a

complete 3-D model.The number of degrees of freedom as well as the half bandwidth for each of the two models are calculated next.

Let ns be the number of stories and nb the number of bays per frame under consideration. If the nodes are numbered sequentially in one particular floor until all the nodes are numbered before proceed to the next floor, the maximum difference between any two connected nodes will be equal to the number of nodes in one floor. Therefore, the maximum half bandwidth will be approximately equal to the number of degrees of freedom in one floor.

Assuming that all frames panels have the same number of bays, the number of nodes per floor for the three dimensional model is 4nb.

The total number of nodes for the three dimensional model excluding the fixed nodes at ground level are

$$\text{node})_{3D} = (4nb)(ns) \tag{2.6}$$

The number of nodes per floor for the planar model is equal to the number of nodes per floor of the three dimensional model plus the number of dummy nodes along the four corner columns, namely, 4nb+4. The total number of nodes excluding the ground level nodes is then given by

$$\text{node})_{2D} = (4nb+4)(ns) \tag{2.7}$$

The number of degrees of freedom per node for the three dimensional model is six. Therefore, the half bandwidth

$$\text{mk})_{3D} = (4nb)(6) = 24nb \tag{2.8}$$

and the total number of degrees of freedom

$$N_{3D} = (24nb)(ns) \tag{2.9}$$

The number of degrees of freedom per node for the planar model is three. The vertical degree of freedom of the dummy node is constrained to the vertical degrees of freedom to its adjacent node. This will reduce the number of degrees of freedom by 4 per story. Therefore, the half bandwidth

$$mk)_{2D} = (4nb + 4)(3) - 4 = 12nb + 8 \tag{2.10}$$

and the total number of degrees of freedom

$$N_{2D} = (12nb+8)ns \tag{2.11}$$

The ratio of the arithmetic operation is then

$$C = ((24nb) / (12nb+8))^3 \tag{2.12}$$

A commonly used assumption in analyzing multi story buildings is the rigid diaphragm assumption. If this assumption is considered, the number of degrees of freedom can be reduced. For the three dimensional model, a master node at the center of mass of each floor is specified. Each master node has only three degrees of freedom which are the displacements of the rigid diaphragm horizontally as a rigid body.If a node is connected to a diaphragm, three degrees of freedom will be obtained from the master node thus reducing the degrees of freedom per node to three. Therefore, the number of degrees of freedoms per story will be three times the number of nodes per story plus the freedoms of the master node. As a result, the half bandwidth is

$$mk)^*_{3D} = (4nb)(3) + 3 \tag{2.13}$$

and the total number of degrees of freedom

$$N^*_{3D} = (12nb+3)(ns) \tag{2.14}$$

For the two dimensional model, the rigid diaphragm assumption reduces the degrees of freedom by (4nb) per floor. Therefore, the half bandwidth

$$mk)^*_{2D} = (12nb + 8) - 4nb = 8nb + 8 \tag{2.15}$$

and the total number of degrees of freedom

$$N^*_{2D} = (8nb+8)(ns) \tag{2.16}$$

The ratio of the arithmetic operation is then

$$C^* = ((12nb+3) / (8nb+8))^3 \tag{2.17}$$

The two ratios given in equation 2.12 and equation 2.17 are plotted in fig. 2.21. The calculated computer time involved with the planar model is about one third of that for the

three dimensional model if the rigid diaphragm assumption is used in both models. However, much larger reduction in computer time can be achieved in the 2-D modelling if the rigid floor assumption is not involved. It is interesting to note that the ratio does not depend on the number of stories in the structure but depends on the number of bays. The ratio of CPU time experienced during this study agreed with the ratios given in fig. 2.21.

2.6 CONCLUSION

A planar model has been proposed to analyze the inelastic behavior of frame tube structures. This proposed model reduces the 3-D frame tube system into sets of plane frames, interconnected by 3-D beam column elements. The DRAIN-2D computer code was employed to model the inelastic behavior of the frames, and plastic hinges are built into the 3-D beam column elements to allow for inelastic behavior of the corner columns. The model was used to obtain the lateral displacement along the height of the structure, corner column axial force, and plastic hinge rotation in the beams for frame tube structures under both static and dynamic lateral loadings. Based on the results and discussion presented in the chapter, the following conclusions can be drawn;

1. The proposed model for frame tube structure gives good accuracy for each of the static and dynamic loading cases when compared with the results based on a three dimensional model.

2. The computer time involved with the planar model is at least one third that for the three dimensional model.

Story No	Beam Inertia m^4x10^{-3}	Column Inertia m^4x10^{-3}	Column Area m^2
1-5	2.5	1.87	.038
6-10	2.25	1.68	.034
11-15	2	1.5	.031
16-20	1.75	1.31	.027
21-25	1.5	1.12	.023
26-30	1.25	.94	.019

E = 207000 MPa

Table 2.1 Member Properties (ψ = 0) static

Story No	Beam Capacity kN-m	Int. Col. Capacity kN-m	Ex. Col. Capacity kN-m
1-5	286	401	286
6-10	241	337	241
11-15	191	267	191
16-20	141	197	141
21-25	90	126	90
26-30	43	60	43

Table 2.2 Member Properties (ψ = 0) static

Story No	Beam Capacity KN-m	Int. Col Capacity KN-m	Corner Col Capacity KN-m
1-5	270	378	270
6-10	239	335	239
11-15	212	297	212
16-20	176	247	176
21-25	129	181	181
26-30	66	92	92

Table 2.3 Member Capacities (Dynamic Analysis)

Story No	Beam Inertia m^4x10^{-3}	Column Inertia m^4x10^{-3}	Column Area m^2
1-30	2.5	1.87	.083

E = 207000 MPa

Table 2.4 Member Properties (ψ different than zero)

Story No	Beam Capacity kN-m	Int. Col. Capacity kN-m	Ex. Col. Capacity kN-m
1-30	271	380	380

Table 2.5 Member Capacities (ψ different than zero)

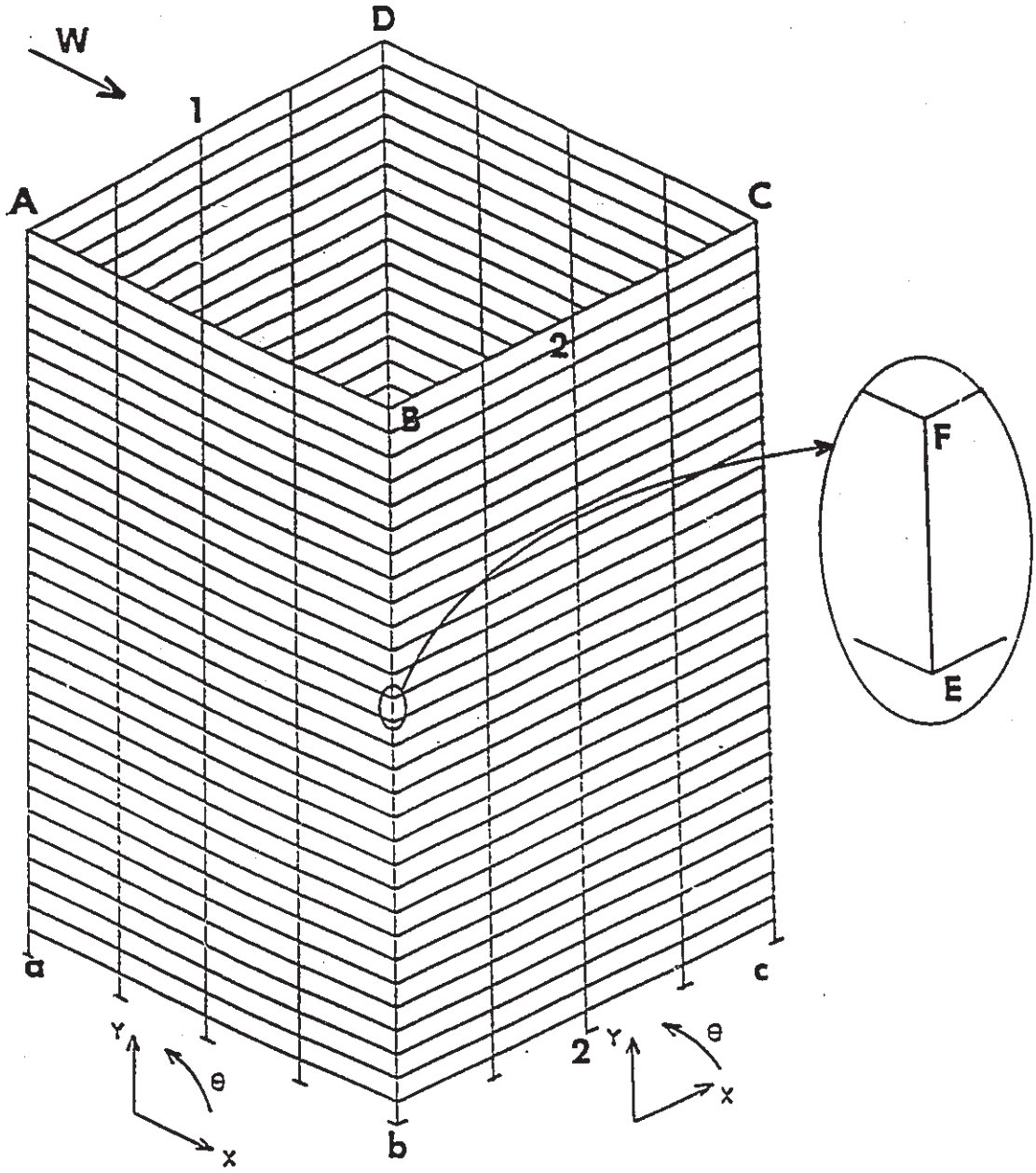

Fig (2.1) Frame Tube Stucture

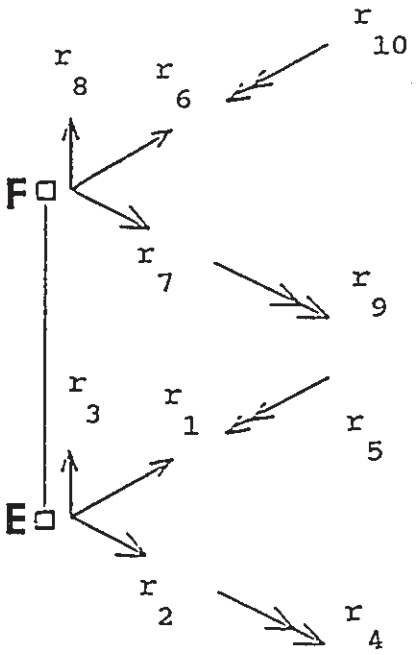

Fig (2.2) Corner Column Degrees of Freedom

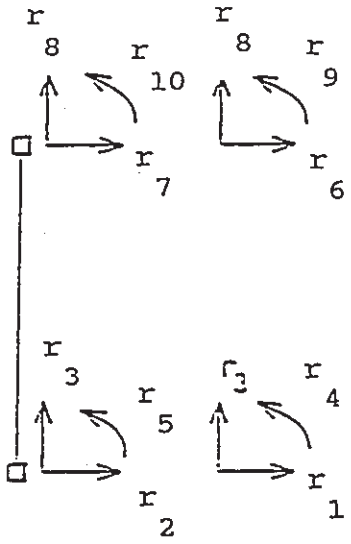

Fig (2.3) Planar Representation of Corner Column DOF

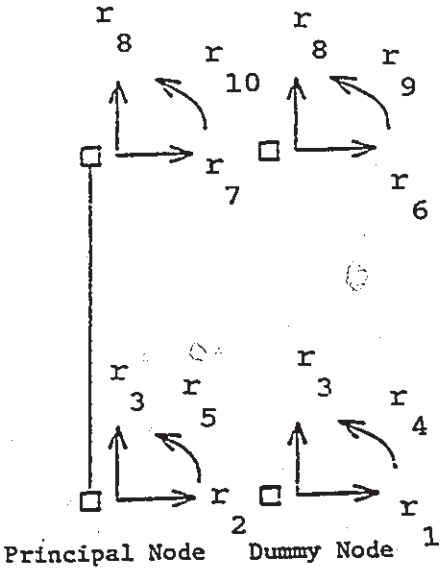

Fig (2.4) Planar Representation of Corner Column Element

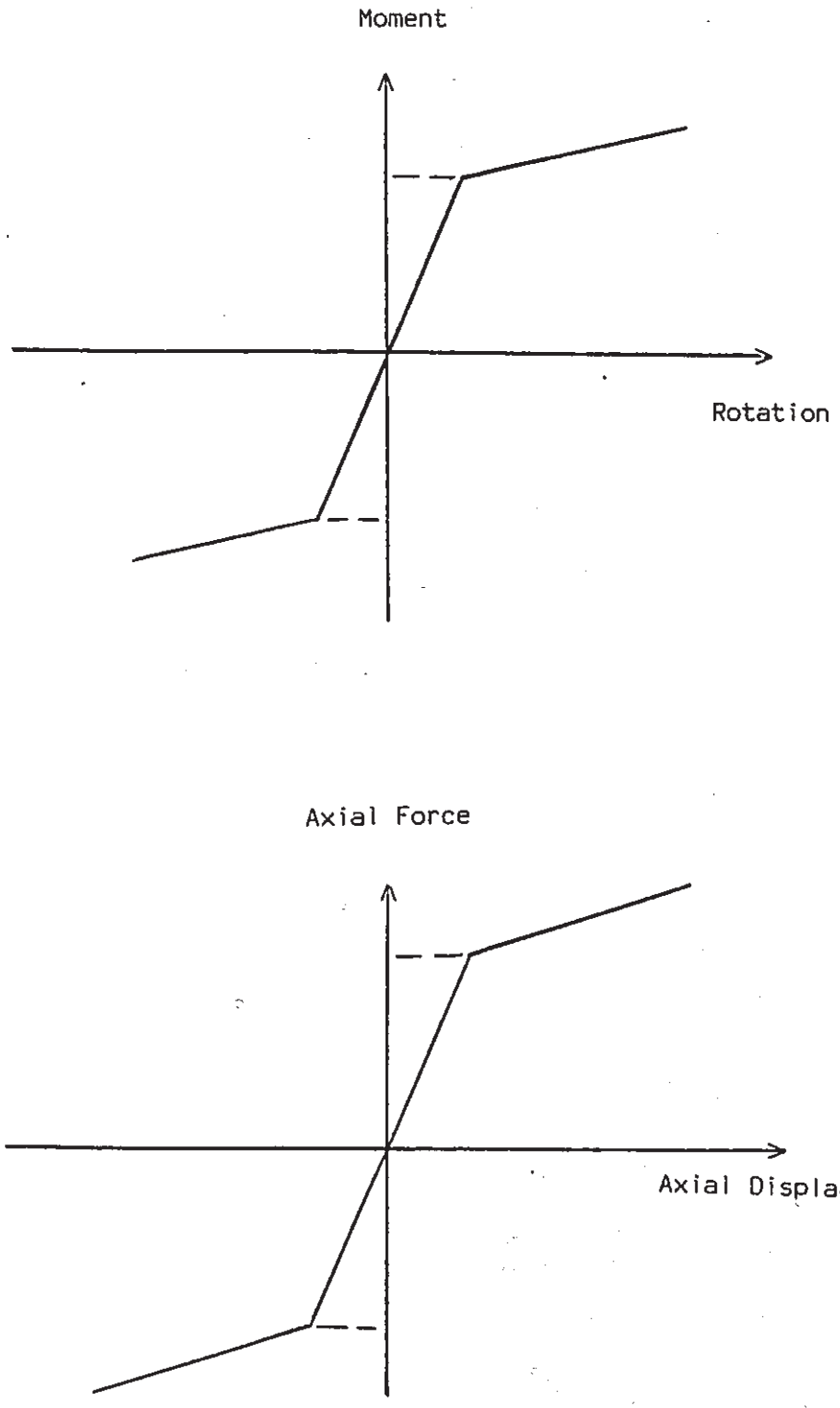

Fig (2.5) Moment-Rotation, and Axial Force-Axial Extension Relationships

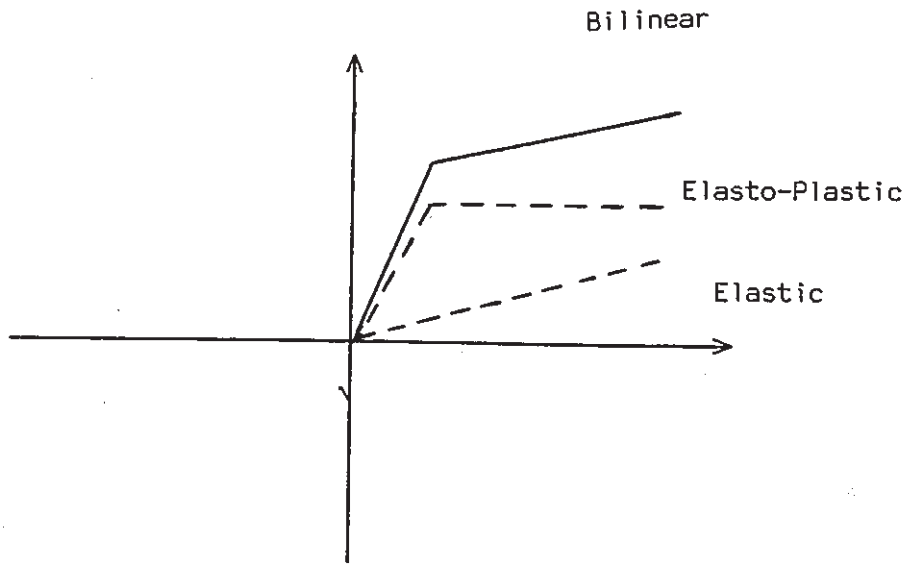

Fig (2.6) Elastic and Elasto-Plastic Components

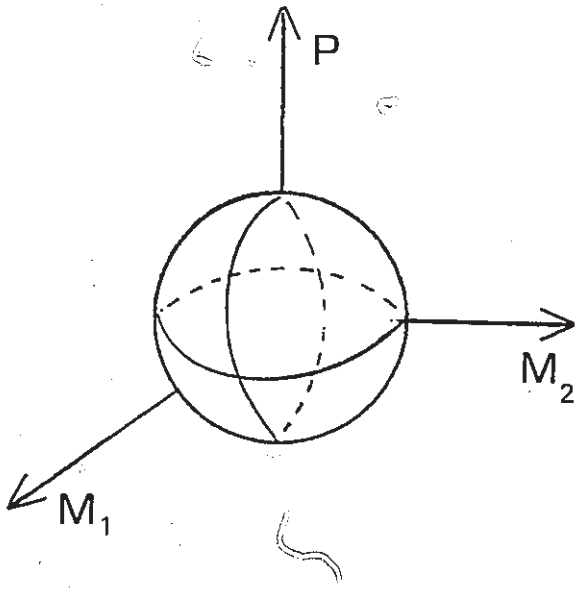

Fig (2.7) Yield Surface

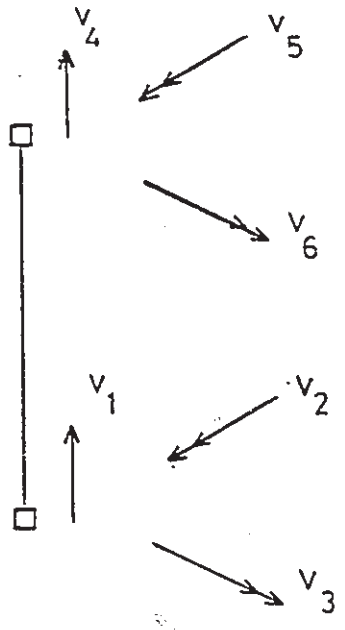

Fig (2.8) Element End Deformation

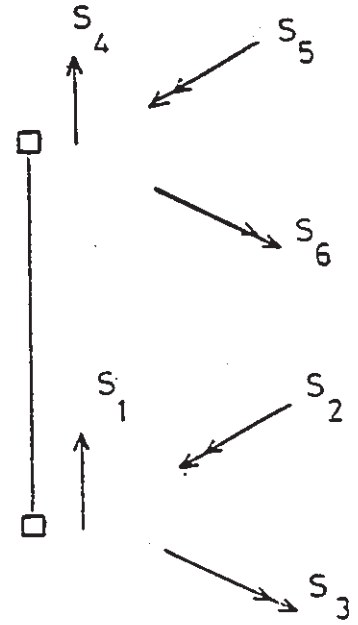

Fig (2.9) Element End Forces

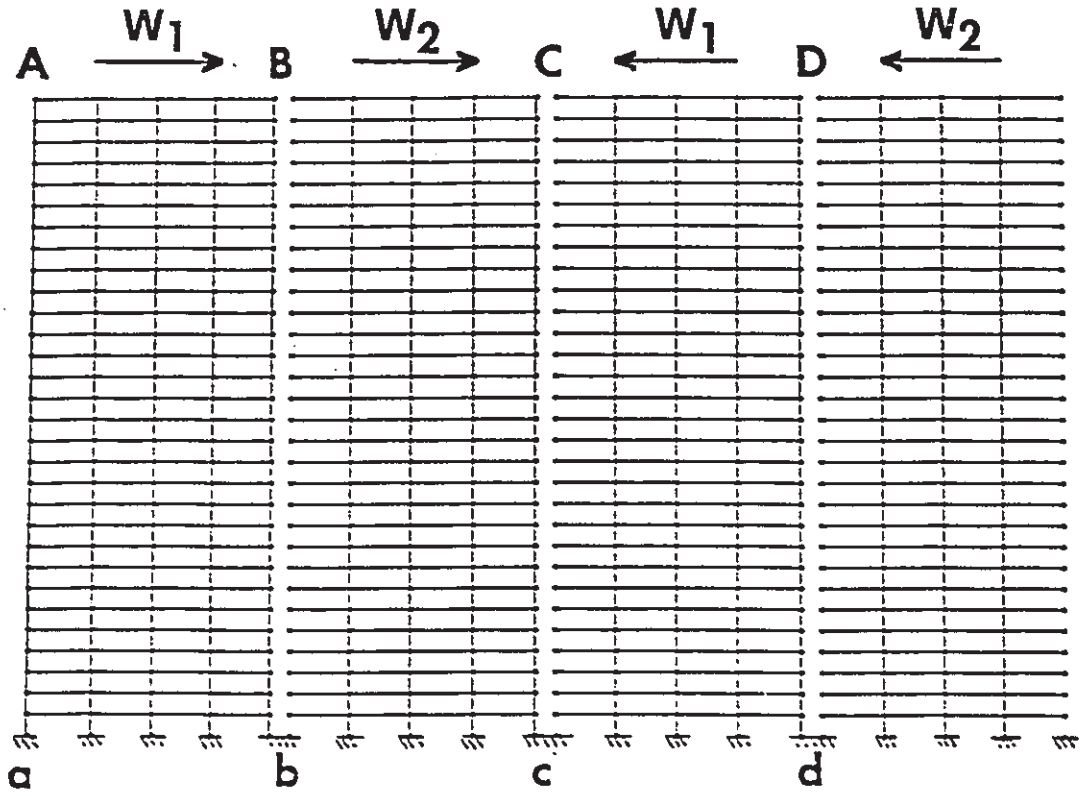

Fig (2.10) Planar Model of Frame Tube Structure

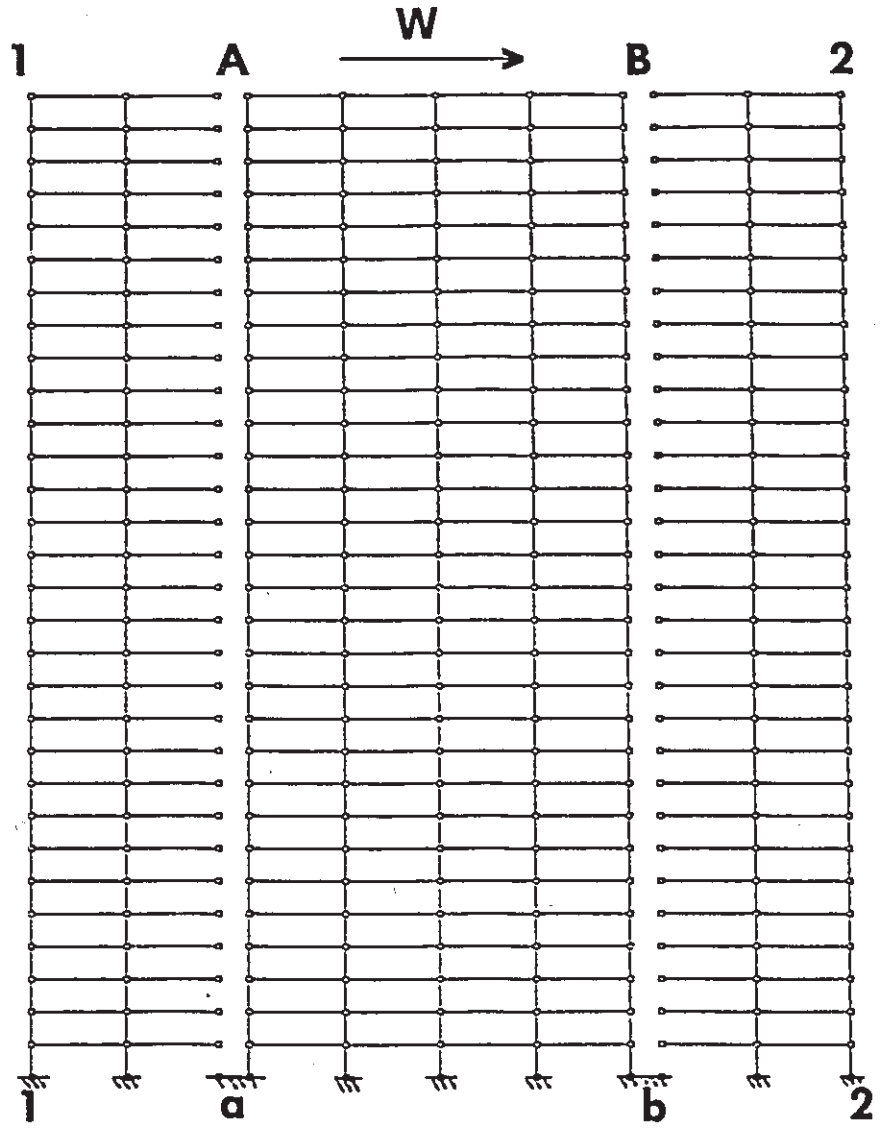

Fig (2.11) Planar Model of Half Tube

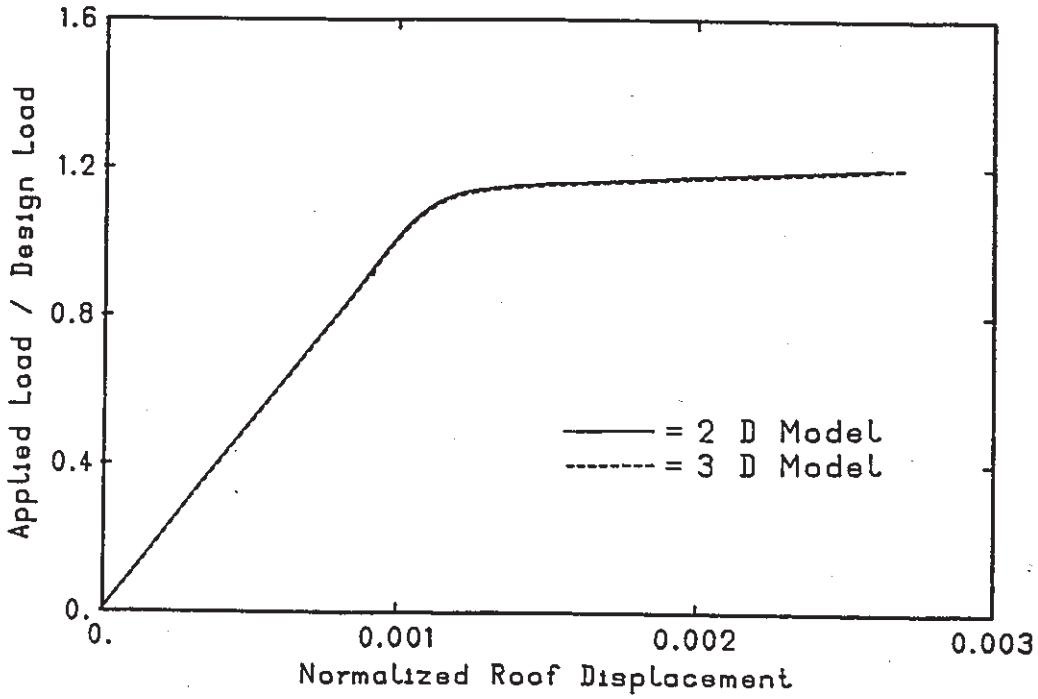

Fig (2.12) Load Displacement Curve, Unidirectional Loading

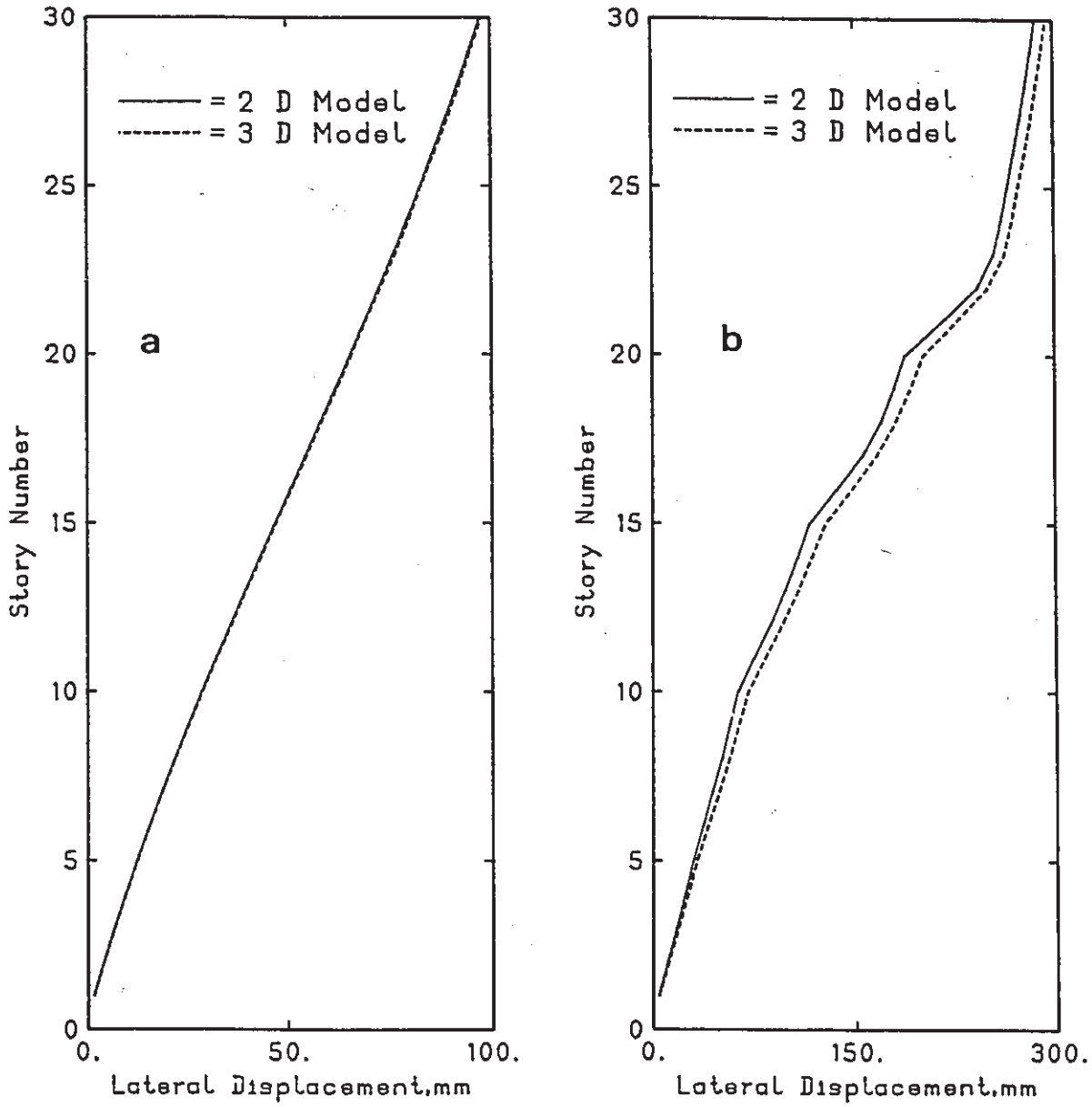

Fig (2.13) Comparison of Lateral Displacement, Unidirectional Loading; a- Elastic, b- Inelastic

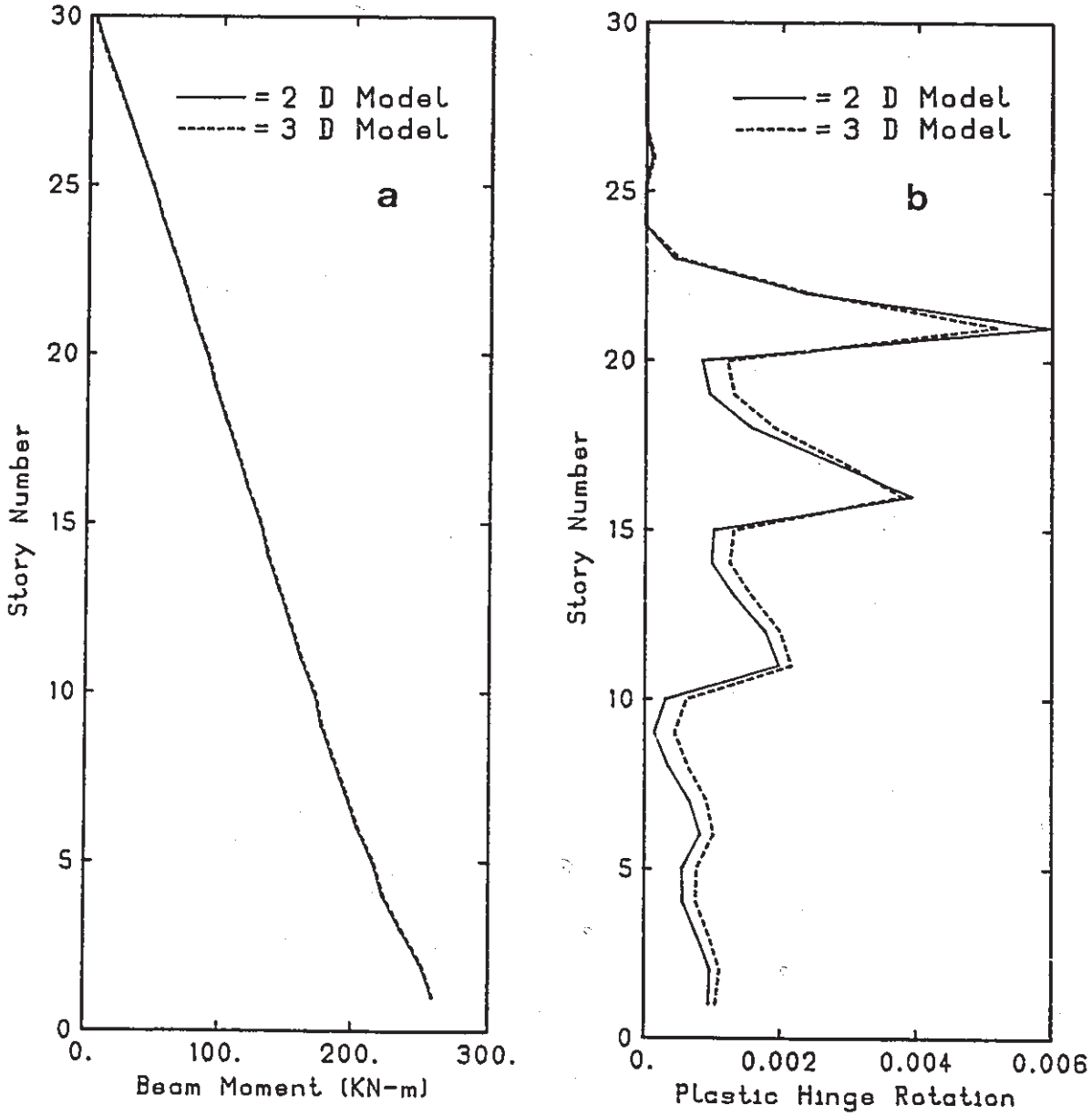

Fig (2.14) Comparison of: a- Beam Moment, b- Plasic Hinge Rotation, Unidirectional Loading

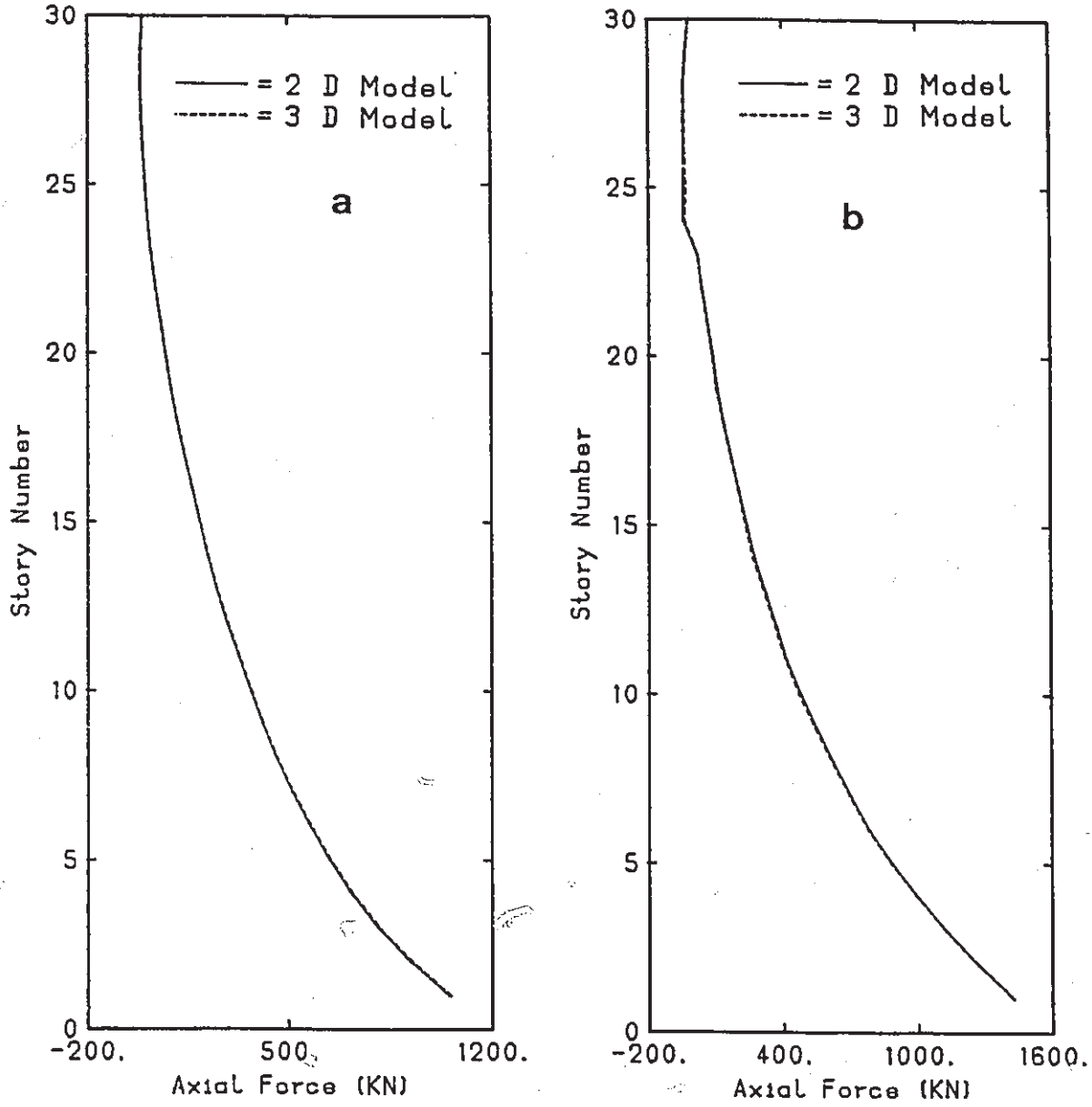

Fig (2.15) Comparison of Axial Force, Unidirectional Loading; a- Elastic, b- Inelastic

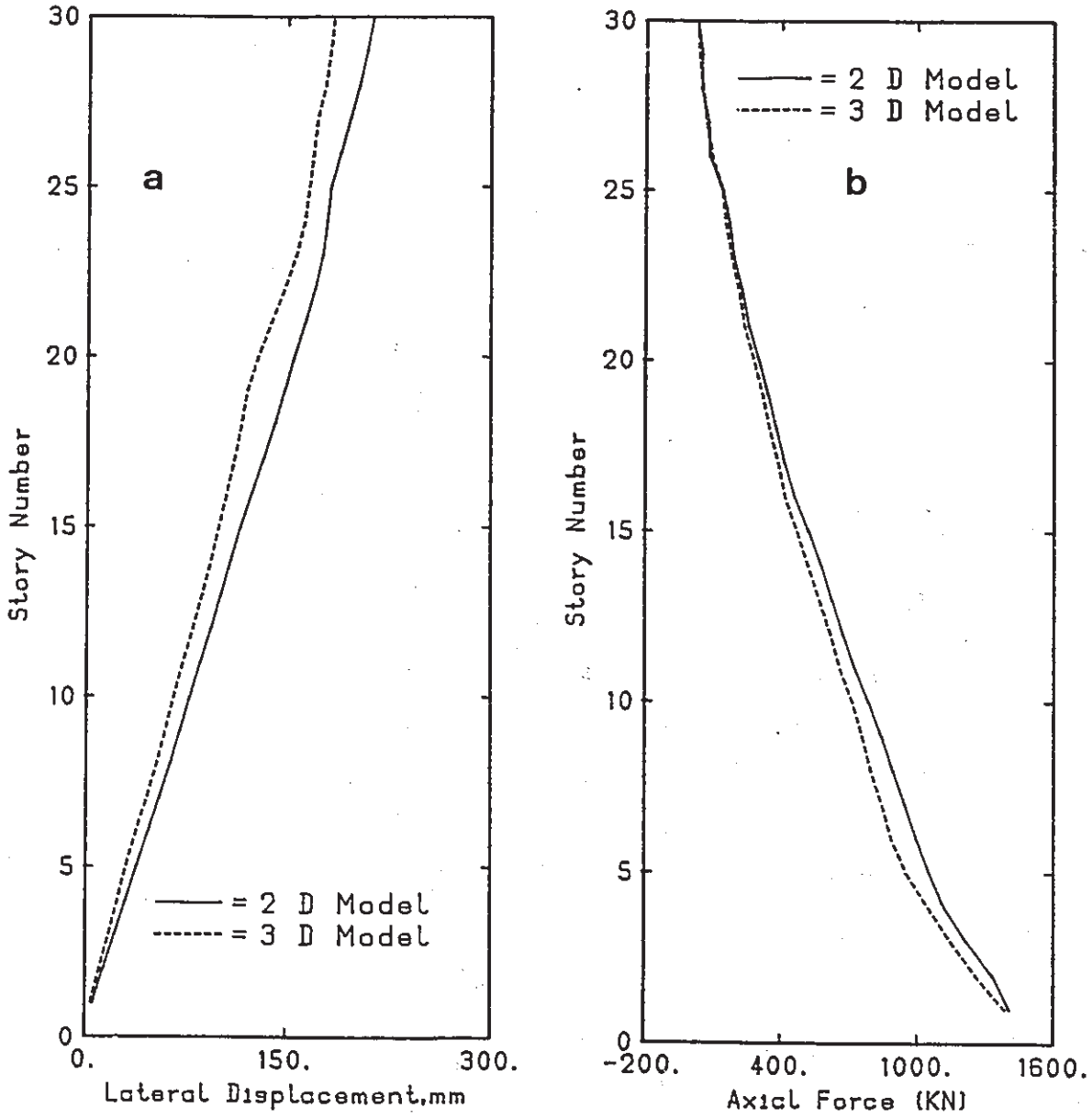

Fig (2.16) Comparison of: a- Lateral Displacement,
b- Axial Force, Dynamic

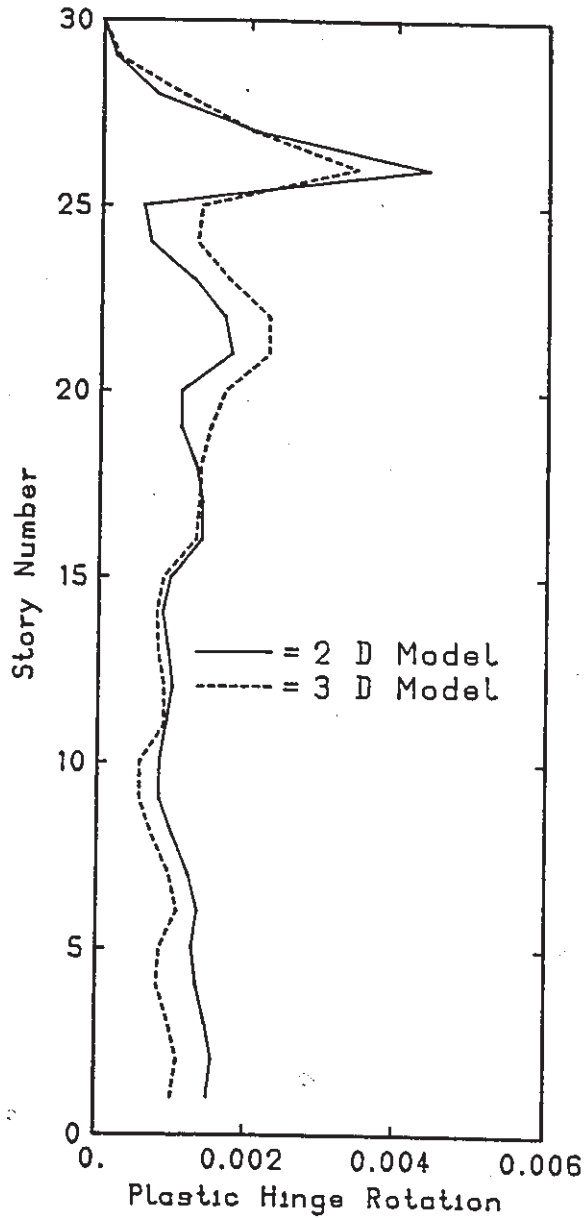

Fig (2.16c) Comparison of Plastic Hinge Rotation, Dynamic

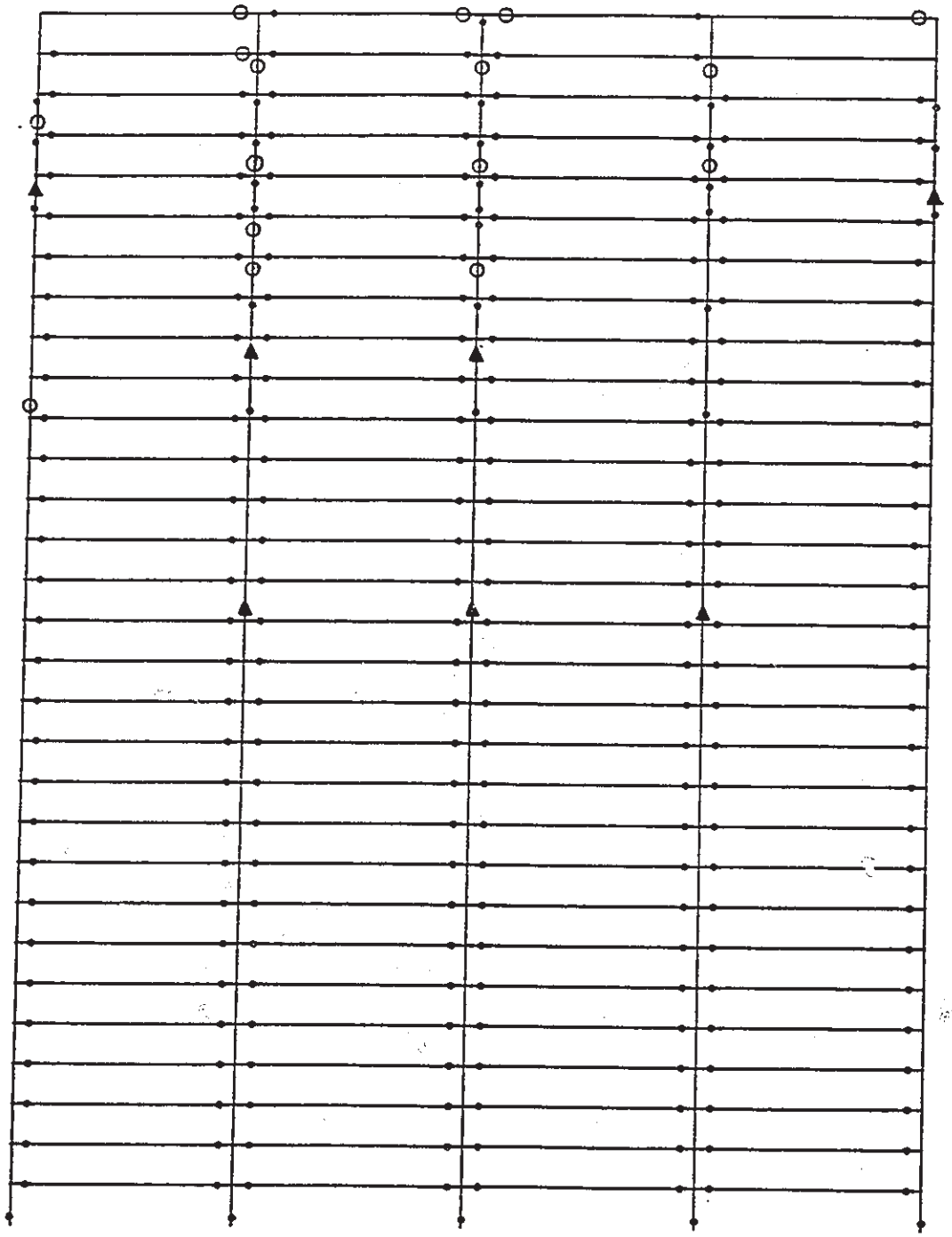

● 2D & 3D Model
▲ 2D Model
o 3D Model

Fig (2.17) Comparison of the Distribution of Plastic Hinges, Dynamic

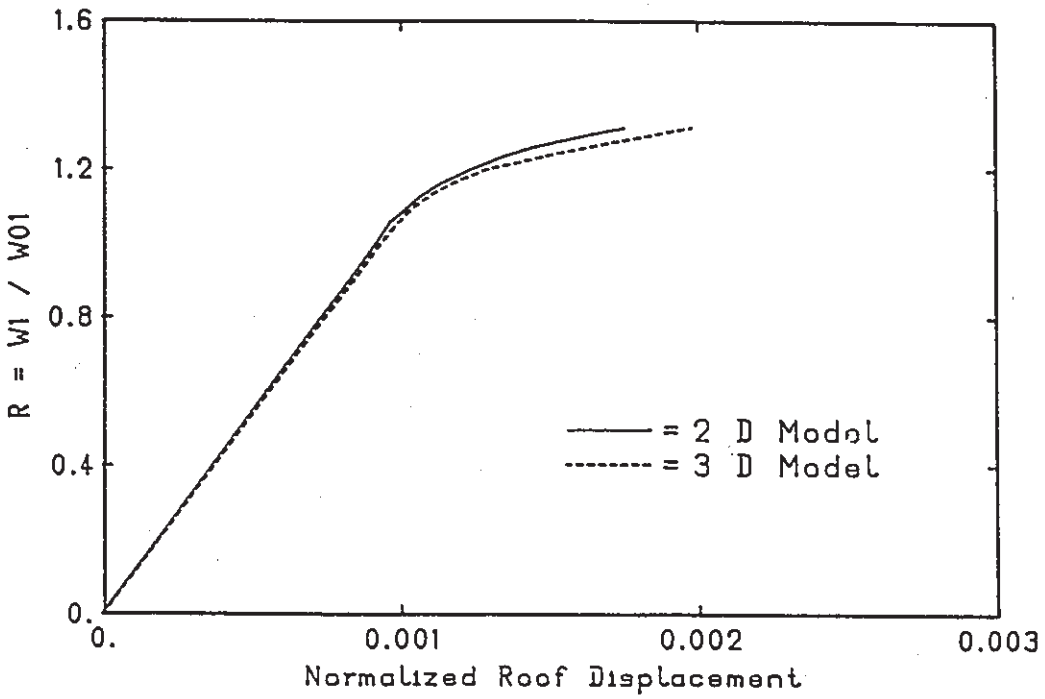

Fig (2.18) Load Displacement Curve, Load at Arbitrary Orientation

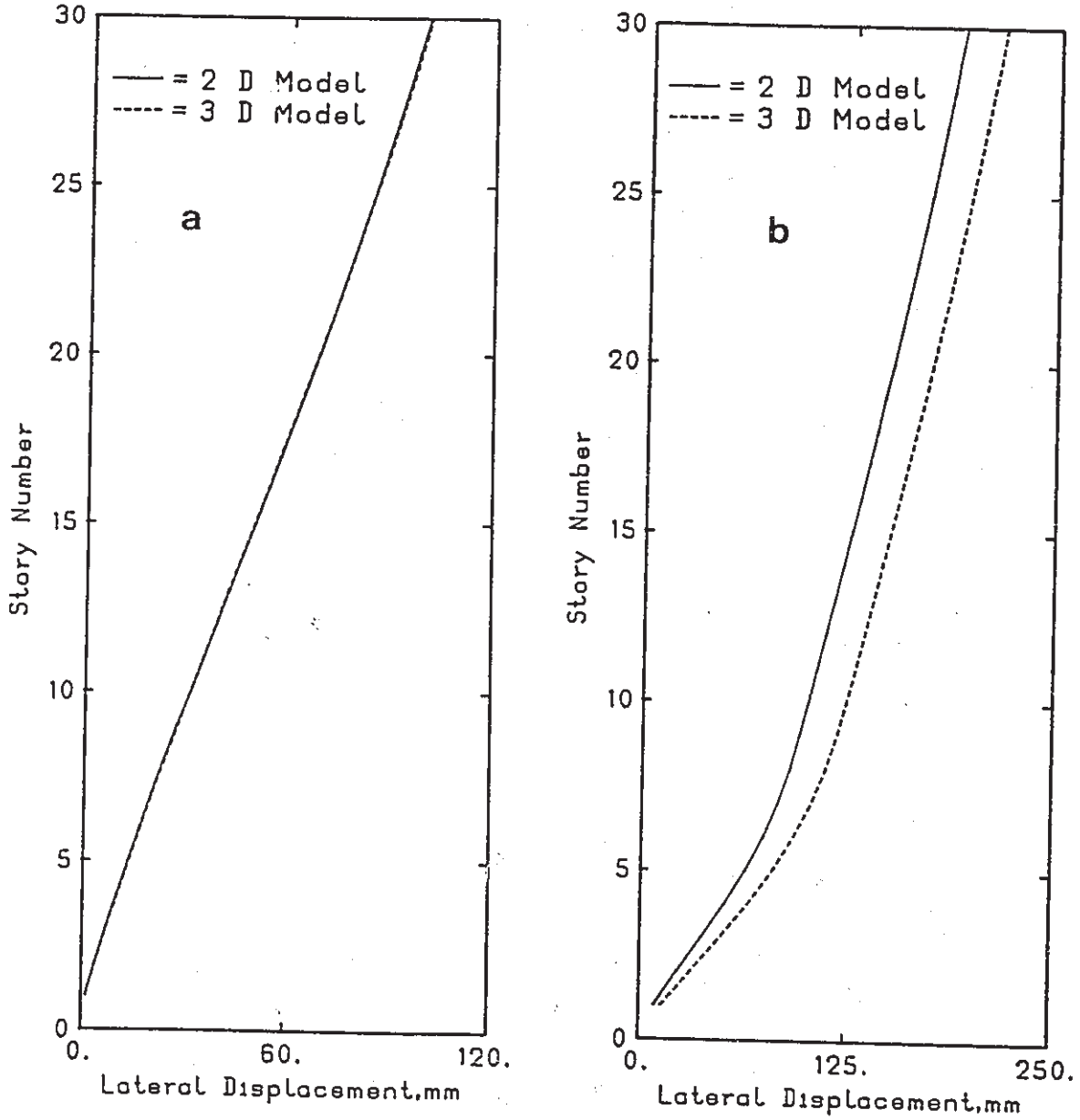

Fig (2.19) Comparison of the Lateral Displacement, Load at Arbitrary Orientation; a- Elastic, b- Inelastic

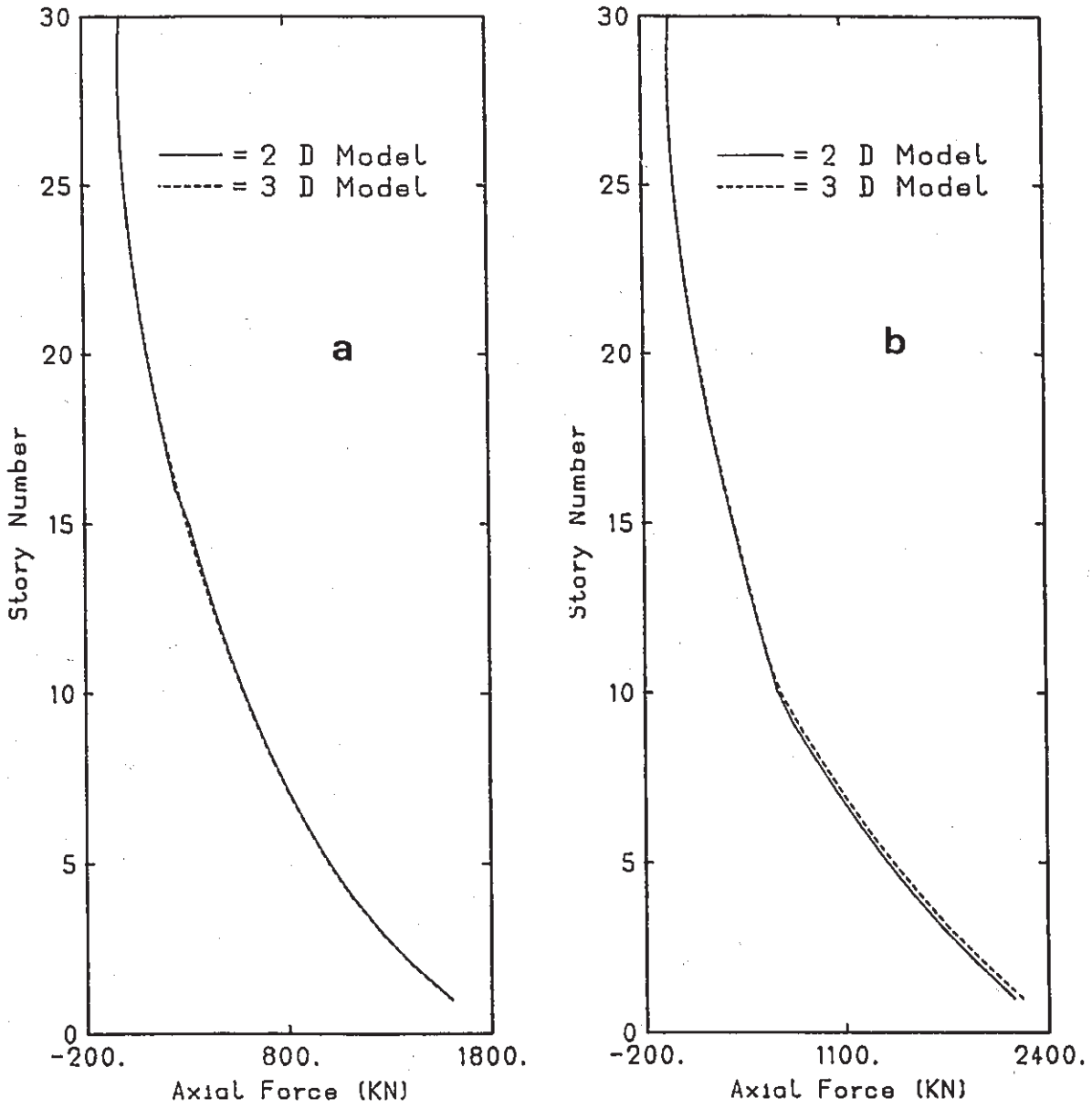

Fig (2.20) Comparison of Axial Force, Load at Arbitrary Orientation; a- Elastic, b- Inelastic

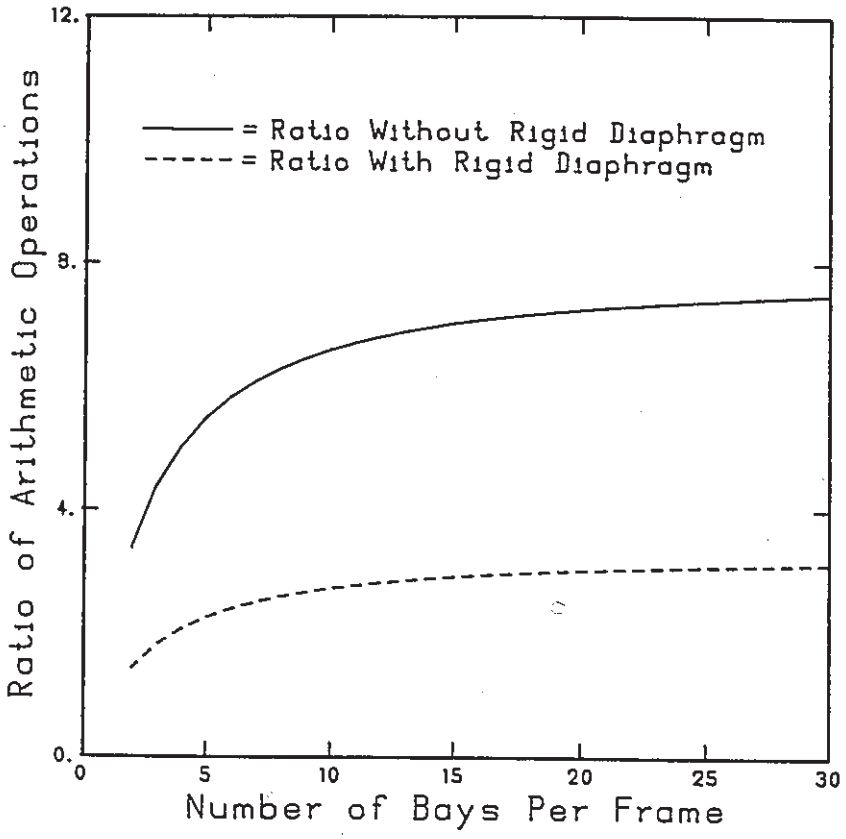

Fig (2.21) Ratio of Arithmetic Operations

CHAPTER THREE

STATIC AND DYNAMIC BEHAVIOR OF FRAME TUBE STRUCTURES UNDER LATERAL LOADS

3.1 INTRODUCTION

The frame tube structural system offers considerably improved efficiency over the traditional moment resisting frame system to provide the necessary stiffness under lateral loadings. In its simplest form, the frame tube consists of closely spaced columns along the perimeter of the building connected at each floor level by deep spandrel beams; thereby, creating the effect of a hollow tube perforated by openings for the windows. While the structure has a tube like appearance, the behavior is much more complex than that of a plain tube due to the openings and the flexibility of the beams and columns.

The objective of this chapter is to study the behavior of frame tube structures subjected to lateral loads along one principal structural axis. First, a parametric study is performed on a typical frame tube to identify the parameters governing the behavior. Then, based on this study, a frame tube structure was designed. The lateral strength of this structure was according to the seismic provision specified in the NBCC 1985. The static lateral response of the designed frame tube when loaded within the elastic limit and when loaded into the inelastic range is investigated. A response spectrum analysis is then presented to examine the dynamic characteristics and the elastic dynamic response of such system. Finally, the inelastic dynamic response based on the average response to an ensemble of six earthquake records is investigated.

3.2 PARAMETERS IDENTIFICATION

As discussed in the previous chapter, the overturning effect of the lateral load on frame tube structures (fig. 3.1) is resisted by two actions; namely, the frame action of the two frames parallel to the direction of loading (longitudinal frames AabB & CcdD), and the tube action that is produced by the compressive and tensile forces on the columns of the frames which are perpendicular to the direction of loading (transversal frames AadD & BbcC). The shearing effect from the lateral load is resisted by bending and shearing of the columns and beams in the longitudinal frames. The portion of the total overturning moment resisted by the tube action may be higher, or lower, than that resisted by the frame action. This distribution of the total overturning moment between the frame and the tube action depends on the member properties of the perimeter frames in the frame tube system. In a well-proportioned frame tube, the overturning moment is primarily resisted by the tube action, while in a poorly-proportioned frame tube, little tube action exists and no benefit can be obtained from the transversal frames. The necessary conditions for good tube action is to ensure all the columns in one transversal frame to be in compression, while the columns in the other transversal frame are in tension. This can be achieved if the axial shortening or lengthening of the corner columns can be distributed to the other columns by the spandrel beams in the transversal frames.

The key parameters involved in characterizing the frame tube behavior are: (a) The axial stiffness of the columns EA_c/h, (b) The bending stiffness of the columns EI_c/h, and (c) The bending stiffness of the beams EI_b/L, where E, A_c, I_c, I_b, h & L are Young's modulus, area of the column, moment of inertia of the column, moment of inertia of the beam, column height and beam length, respectively. In addition, a fourth parameter that plays an important role in distributing the axial force between the columns of both the transversal and longitudinal frames is the shear stiffness of the beams namely, $12EI_b/L^3$.

The above four parameters can be grouped into two nondimensional parameters. By forming the ratio of the beam shear stiffness to the column axial stiffness, we obtain the "spandrel shear stiffness factor". Taking the ratio of the beam bending stiffness to the column bending stiffness, we obtain the "stiffness ratio". Mathematically, these nondimensional parameters are defined as:

$$\text{The spandrel shear stiffness factor} = 12\, I_b\, h / A_c\, L^3 \tag{3.1}$$

$$\text{The stiffness ratio} = I_b\, h / I_c\, L \tag{3.2}$$

3.2.1 Static Behavior of Frame Tube Structures under Lateral Loads

A series of elastic analyses were made for a uniform thirty story four bays by four bays frame tube structure shown in fig. 3.1. The center to center spacing between the columns is 3 m with a story height of 3.6 m. The structure was subjected to an inverted triangular lateral load distribution that corresponds to the seismic lateral load distribution as specified in the NBCC 1985. The base shear of this loading is obtained by using the base shear expression of the NBCC 1985, namely,

$$V = v\,S\,K\,I\,F\,W \tag{3.3}$$

where $v = .4$, $S = .22/\sqrt{T}$, $T = 3$ sec, $K = .7$, $I = 1$, $F = 1$, and $W = 20736$ KN. These values resulted in a base shear of 737 KN.

The member properties are taken to be uniform along the height of the structure. A number of structural models having such a configuration are considered. They represent the cases of small, intermediate, and large values of the stiffness ratio and spandrel shear stiffness factor, respectively. For the different examples considered, the member properties are listed in table 3.1. The axial force in the columns of the first story and the lateral displacement along the height of the structure are taken to be the response parameters of interest.

Column Axial Force

Fig. 3.2 shows the axial force variation in the first-floor columns as a function of the stiffness ratio and spandrel shear stiffness factor. Columns 1, 2 and 3 are the columns of the longitudinal frame while columns 4 and 5 are the columns of the transversal frame. For the frame tube, the longitudinal and transversal frames are orthogonal to each other. However, to display the effect of variation of the stiffness ratio and the spandrel shear stiffness factor on the column axial force, it is convenient to represent the two frames in one plane.

A large value of the spandrel shear stiffness factor leads to a linear variation of axial force in the columns of the longitudinal frame, and the axial force in the columns of the transversal frames is almost uniform as shown in fig. 3.2-a. Fig. 3.2-b shows the results when the spandrel shear stiffness factor has an intermediate value. When the stiffness ratio has a small or intermediate value, the axial force also varies linearly in the columns of the longitudinal frame and uniform in the columns of the transversal frame. However, with a large stiffness ratio, the shear lag phenomenon can be observed with the axial force at the edge considerably higher than what a linear distribution of axial force would predict. Finally, fig. 3.2-c shows the results when the spandrel shear stiffness factor is small. The shear lag effect is widespread for all values of the stiffness ratio.

In summary, therefore, to insure tube action, the spandrel shear stiffness factor needs to be large. In practice, the large spandrel shear stiffness factor can be achieved by using stiff beams in shear. The shear stiffness of the beams can be increased effectively by the use of deep spandrel beams and closely-spaced columns.

The present study shows that the tube action is effective if the spandrel shear stiffness factor is greater than, or equal to, 0.1 and the stiffness ratio is less than, or equal to, 1.6.

Lateral Displacement

Fig. 3.3 shows the lateral displacement variation along the height of the frame tube as a function of the stiffness ratio and spandrel shear stiffness factor. To simplify the comparison of their shapes, all curves are normalized to have a unit displacement at the top story.

For a large value of the spandrel shear stiffness factor, the frame tube deflects like a cantilever independent of the stiffness ratio as shown in fig. 3.3-a. Fig. 3.3-b shows the results when the spandrel shear stiffness factor has an intermediate value. When the stiffness ratio has a small or intermediate value, the frame tube also deflects like a cantilever. However, with a large stiffness ratio, the frame tube deflects like a shear beam. Finally, fig.3.3-c shows the results when the spandrel shear stiffness factor is small. The frame tube deflects like a shear beam for all values of the stiffness ratio.

The frame tube deflects like a cantilever column when the spandrel shear stiffness factor is greater than or equal to, 0.1 and the stiffness ratio is less than 1.6. These same conditions are necessary for the tube action to take place in the frame tube.

3.3 DESCRIPTION OF THE ANALYTICAL MODEL FOR THE STATIC AND DYNAMIC ANALYSIS OF FRAME TUBE STRUCTURES

Based on the parametric study in section 3.2, a thirty story frame tube is designed such that substantial tube action will take place. This frame tube has four bays on each side, (fig. 3.4), and all four frame panels are identical. The center to center spacing between the columns is 3 m with a uniform story height of 3.6 m. The stiffness properties as well as the sizes of beams and columns are presented in table 3.2 and in Appendix C. It should be noted that the determination of member stiffnesses is an iterative process. The member stiffnesses presented in table 3.2 limit the maximum interstory drift to .4 percent of story height. This

interstory drift is based on the NBCC 1985 statement 4.1.9.2.2. To achieve an optimum design, the stiffnesses of the beams and columns are varied along the height of the structure, while the stiffness ratio and the spandrel shear stiffness factor are unchanged. The change occurs every five stories and the change between two adjacent stories is kept relatively small. This variation is intended to ensure smooth transition in member stiffness along the height of the structure.

The design gravity loadings consist of 4.8 KN/m^2 dead load. The story masses are uniform along the height of the frame tube and correspond to the design dead load. These masses are lumped at story levels, and are used in determining the lateral seismic design forces and the fundamental period.

The total lateral seismic design force V is calculated according to

$$V = v S K I F W \tag{3.4}$$

In which

v = zonal velocity ratio,

S = seismic response factor,

K = structural behavior coefficient,

I = importance factor,

F = foundation factor, and

W = total weight of the structure.

The zonal velocity ratio v is defined as the ratio of the zonal peak ground velocity to a velocity of 1 m/s. The frame tube is assumed to be located in regions with high seismicity and v is taken to be 0.4. The structural behavior K represents the energy dissipation capacities of the different types of structural systems due to inelastic deformation and damping. The frame tube is assumed to behave as a moment-resisting frame and K is taken to be 0.7. The period dependence of the seismic response factor S is given as $S = 0.22/\sqrt{T}$ for $T > 0.5$ sec. The

fundamental period of the frame tube, determined from a dynamic vibration analysis, is 2.45 sec. For ordinary buildings, the importance factor is taken as 1.0. The frame tube is assumed to be located on rock, or stiff soil sites, consistent with the local soil conditions for the selected earthquake accelerograms used later as input ground motions. Accordingly, the foundation factor is assigned a value of 1.0. The total weight of the frame tube is computed from the design dead load and is 20736 KN. Finally, the resulting design base shear is 815 KN.

The computed design base shear is distributed along the height of the frame tube based on the following distribution formula as suggested by the NBCC 1985.

$$F_x = \frac{(V - F_t) w_x h_x}{\Sigma w_i h_i} \tag{3.5-a}$$

in which

w_i, w_x = that portion of W assigned to level i or x respectively,

h_i, h_x = the height above the base to level i or x respectively,

n = total number of stories,

F_x = lateral force at level x,

F_t = that portion of V concentrated at the top of the frame in addition to F_n.

F_t is given by

$$F_t \quad \begin{array}{l} = 0.004\, V\, (h_n/D_s)^2 <= 0.15\, V \\ = 0.0 \text{ if } h_n/D_s <= 3 \end{array} \tag{3.5-b}$$

in which

h_n = the total height of the frame above the base,

D_s = the dimension of the frame in the direction parallel to the applied lateral seismic forces.

The portion F_t of the design base shear is concentrated at the top of the frame tube in an attempt to accommodate higher mode effects on the force distribution. The distribution of the lateral seismic design forces is presented in table 3.3.

In the present investigation, attention is focused on the behavior of frame tube structures under lateral loads. For this purpose, it is assumed that the seismic loading governed the design strength, and the yield capacities of the beams are taken to be the beam moments of the longitudinal frames when the frame tube is subjected to the design lateral load. These beam capacities are taken to be constant over intervals of five stories and they are obtained by averaging the beam moments of the longitudinal frames over the five stories.

The various types of loads specified in the NBCC 1985 are nominal loads. In a limit state design, the strength of a structure, or member, must be at least equal to the required strength calculated from the factored loads. For this reason, the design lateral load is factored by 1.5 and accordingly, the beam capacities are also increased by 1.5. The actual values of the beam capacities are presented in table 3.4. Throughout the rest of this chapter, the design lateral load and the design base shear will be the factored lateral load and the factored base shear.

The column flexural capacity is set equal to ten times the adjoining beam capacity and the axial capacity is assigned a relatively large number. This column capacity is selected only for numerical purposes so that the inelastic action is restricted to the beams. A detailed discussion on the selection of the column capacity, to be used in subsequent chapters, is examined in section 3.5.

3.4 EFFECT OF TUBE ACTION ON THE BEHAVIOR OF FRAME TUBE STRUCTURES

To quantify the effects of the tube action on the behavior of the frame tube, a frame structure as shown in fig. 3.5 (referred as the associate frame system), is also analyzed in conjunction with the frame tube. The configuration of the frame structure is the same as the frame tube. In each of its perimeter frame, the center to center spacing between the columns is 3 m with uniform story height of 3.6 m. Each frame panel has its own edge column, and is the same size as the corner column in the frame tube. The only difference between the associated frame structure and the frame tube is that the longitudinal and transversal frames in the former are not connected at the corner columns. In other words, no transfer of forces between them can take place. As a result, the associated frame structure resists the lateral load by the frame action alone, utilizing the two frames parallel to the direction of loading. By comparing the behavior of the frame tube and its associated frame, the effects of the tube action will be evaluated.

Although this associated frame system has the same member stiffnesses and story masses as those of the frame tube, its fundamental period is found to be 3.1 sec. The corresponding base shear, computed according to the NBCC 1985, is 725 KN. The beam and column capacities of this frame system are then computed in the same manner as the frame tube. The actual values are given in table 3.5.

3.4.1 Behavior Under Quasi Static Lateral Loading

The static nonlinear analysis of the frame tube is carried incrementally where the external load intensity P is divided into a series of load increments dP applied sequentially to the structure. The external load P was taken to be the design lateral load magnified by a factor $R > 1$. A loading intensity corresponding to $R = 1.5$ was selected to illustrate the discussion

presented in the next section. Similarly, the frame system is analyzed under a lateral loading with intensity equal to 1.5 times its design lateral load. The response paramters of interest in this analysis are the lateral displacement, interstory drift,and the story stiffness.

Lateral Displacement

If R is the ratio of the total applied load, and the design base shear, a plot of R versus the roof displacement for the frame tube, and its associated frame, are shown in fig. 3.6. The roof displacement is normalized by the total height of the structure. The frame tube behaves linearly up to point A, where the first hinge in the beams of the longitudinal frames occurs. At point B, all the beams of the longitudinal frames have yielded. The behavior beyond this point is also linear since no more hinges can be formed. The overall stiffness beyond point B is the result of the contribution of the column stiffness, the post elastic stiffness of the beams of the longitudinal frames, and the elastic stiffness of the beams of transversal frames. In a similar manner, the associated frame system behaves linearly up to point A' and also behaves linearly beyond point B'.

The fact that points A and B, or A' and B', are two distinct points is due to the beam capacities that are set to the average of the design forces demand over five story intervals. If the beam capacities are selected so that the capacity of each beam corresponds exactly to the design force, points A & B will converge to a single point. This point would have an ordinate of unity and an abscissa equal to the normalized roof displacement when the structure is subjected to the design lateral load, and the response is elastic. In a similar manner, points A' and B' would become a single point in the load deflection curve of the associated frame system.

The lateral displacement along the height of the structure is shown in fig. 3.7. Fig. 3.7-a corresponds to an elastic behavior under the design lateral load, while fig. 3.7-b corresponds to R = 1.5. In the elastic range, the lateral displacement along the height of the

frame tube is much smaller than that of the associated frame. When loaded into the inelastic range, however, the lateral displacement is about the same for both the frame tube system and its associated frame. Therefore, one concludes that the tube action is effective only when the behavior is elastic and has the beneficial effects of reducing the lateral displacement of the frame tube system. The tube action, however, becomes ineffective when the frame tube is loaded beyond its elastic limit.

The loss of the tube action, when the frame tube is loaded into the inelastic range, is due to yielding of the beams in the longitudinal frames. When these beams are yielded, any further increase in the external applied loading will result in only a small increase in the corner column axial force. Therefore, the axial forces in the columns in the transversal frames are little changed which leads to the tube action to be ineffective after all the beams in the longitudinal frame that framed into the corner columns become inelastic.

Interstory Drift

The interstory drift along the height of the structure is shown in fig. 3.8. Fig. 3.8-a corresponds to an elastic response, while fig. 3.8-b corresponds to R = 1.5. In the elastic range, the highest drift occurs in the upper portion of the structure as a consequence of the cantilever deflection shape. In the inelastic range with R=1.5, there is substantial increase in story drift and the highest drift is shifted to the lower portion of the structure. The high drift in the bottom portion of the frame tube is a consequence of the shear type of deformation in which the structure exhibited as a result of the inelastic behavior.

Story Stiffness

Heidebrecht and Smith [17] define the story stiffness in planar frames of the shear type of deformation as the ratio of the story shear force and the corresponding interstory drift.

By assuming points of contraflexure at midheight of beams and columns, they calculated the story stiffness in terms of member stiffness, frame configuration and the rigidity of the joints. This definition of story stiffness is applicable only to frames of the shear type of deformation in which the axial deformation in the columns is negligible.

For frame tube structures in which substantial column axial deformation takes place, the above definition needs to be modified so that the effect of axial deformation is included. In this thesis, the story stiffness is measured as the ratio of story shear force, and interstory drift, calculated when the complete frame tube structure is subjected to the design lateral loading.

To evaluate the effect of the tube action on the story stiffness, the story shear versus story drift, at the fifth story for the frame tube and its associated frame, is plotted in fig. 3.9. The story shear is normalized by the design story shear, and the story drift is presented as a percentage of story height. Fig. 3.9 indicates that in the elastic range, the frame tube story stiffness is larger than the associated frame story stiffness. In the inelastic range, the two curves are parallel indicating that the story stiffnesses for the frame tube and its associated frame are the same. Similar behavior on the story shear versus story drift takes place at other floors as indicated by the plots for the eleventh and twenty first story, shown in fig. 3.10- a& b.

One important parameter that is relevant to the inelastic dynamic behavior is the ratio of story stiffness (R.S.S.) defined as

$$\text{R.S.S.} = \frac{K_p}{K_e} \tag{3.6}$$

where K_p is the post elastic story stiffness, and

K_e is the elastic story stiffness.

In preparation to understand the dynamic inelastic behavior, it is useful to observe that the ratio of story stiffness is smaller for the frame tube than for the associated frame as shown in table 3.6.

3.4.2 Elastic Response Spectrum Analysis

The frame tube and its associated frame are analyzed using a common method of dynamic structural analysis, namely, the response spectrum techinque. The Newmark and Hall response spectrum, shown in fig. 3.11, is used as the input spectrum. This spectrum is constructed by well known procedures and corresponds to a maximum ground acceleration, maximum ground velocity and maximum ground displacement of 1 g, 122 cm/sec and 91 cm, respectively. Amplification factors selected from [29] for 84.1 percentile response, and five percent damping ratio are 2.67, 2.32 and 2.04 for acceleration, velocity and displacement, respectively.

The first five modal periods of the frame tube, and its associated frame, are listed in table 3.7. In addition, the first five vibrational mode shapes for both systems are plotted in fig. 3.12. It is apparent that the modal periods, as well as the mode shapes of the frame tube and frame are different. These differences are attributed to the tube action. The effects of this tube action on story shears and on the modal contribution of higher modes are discussed next.

Story Shears

The story shears of the frame tube, and its associated frame, for the first five modes are shown in fig. 3.13. In a lumped mass system, the shear remains constant in each story with discontinuities at each floor. However, such a plot would not be convenient in displaying the differences between the frame tube and the frame responses. Therefore, the alternative presentation with the shear varying linearly over the story height is adopted. The tube action

leads to higher story shears in the frame tube in the first mode but lower story shears in the second mode.

The story shear considering the contribution of all five modes using the square root of the sum squares (SRSS) combination rule is shown in fig. 3.14. The percent increase in story shear of the frame tube over the story shear of the associated frame defined as,

$$P_s = \frac{V_t - V_f}{V_f} \times 100 \tag{3.7}$$

where,

V_t is the frame tube story shear due to all five modes, and

V_f is the frame story shear due to all five modes,

quantifies the effect of tube action on story shear distribution. By plotting P_s (fig. 3.15), it is clear that the tube action leads to a significant increase in story shears in the middle portion of the structure while the increase of story shear in the upper and lower portion of the frame tube is less significant.

Modal Contribution of Higher Modes to Story Shears

The percent increase in story shears, considering the contribution of all five modes over the story shears due to the first mode only, defined by

$$P_m = \frac{V_{all} - V_1}{V_1} \times 100 \tag{3.8}$$

where V_{all} is the story shear due to all five modes using SRSS, and

V_1 is the story shear due to the first mode only,

is a measure of the contribution of higher modes to the story shears. Fig. 3.16 shows P_m for the frame tube and the associated frame. The contribution of higher modes to story shears is significant in the upper portion of the structure, and to a less extent in the bottom portion of

the structure for the frame tube and frame. However, the contribution of higher modes is almost negligible in the middle portion of the structure.

Modal Contribution of Higher Modes to Base Shear

It is useful to examine the effect of tube action on the modal contribution of higher modes to the base shear. This is summarized in table 3.8. By comparing the ratios of the higher modal base shear to the fundamental base shear for the frame tube and the frame, the tube action leads to a reduction of the contribution of higher modes to the base shear.

In summary, the elastic response spectrum analysis shows that:

(1) The tube action leads to a significant increase in story shears only in the middle portion of the frame tube.

(2) The modal contribution of higher modes to story shears is significant in the top portion of the frame tube, and to a less extent, in the lower portion of the frame tube. However, negligible contribution of higher modes occurred in the middle portion of the frame tube.

(3) The tube action leads to a reduction of the contribution of higher modes to the base shear.

3.4.3 Elastic and Inelastic Time History Analysis

Ground Motions

The ground motions considered consist of six actual earthquake records. The specifics of these records are shown in table 3.9. All earthquake excitations belong to the class of records having a peak horizontal acceleration to peak horizontal velocity ratio of nearly one, when the acceleration is expressed in units of g, and velocity expressed in meter/sec.

The elastic response spectrum for five percent damping for each of the six ground motions is computed using the computer program SPEC [27], where each record is scaled to

have a peak acceleration of one g. The mean of the six response spectra is presented in fig. 3.17, together with the mean plus standard deviation as a measure of dispersion. The Newmark and Hall response spectrum used in section 3.4.2 is also included in fig, 3.17.

Analysis Strategy

To compute the seismic base shear, the NBCC 1985 assigns different numerical values for the coefficient K, depending on the structure's capability to absorb energy. Since the purpose of this study is to investigate the inelastic behavior of frame tube structures, a value of .7 is selected for K when computing the design base shear (section 3.3).

To introduce equivalence among the responses of the frame tube, and its associated frame system, to different earthquake ground motions, each record is scaled so that: (1) The frame tube elastic base shear obtained from a time history dynamic analysis, under the action of a particular earthquake, is the same as the frame tube design base shear. (2) The associated frame elastic base shear obtained from a time history dynamic analysis, under the action of the same earthquake, is the same as the associated frame design base shear.

The dynamic elastic base shear, as well as the design base shear, are different for the frame tube and the associated frame system. Therefore, different scaling factors are used for the frame tube and the associated frame even for the same earthquake record. The scaling factors for the different earthquake records are presented in table 3.10. In order to interpret these factors correctly, the tabulated values should be multiplied by the original intensity of the earthquake record to yield the scaled record. This scaled record intensity is referred to as excitation level one. On this basis, for example, an earthquake intensity about 22 percent of 1940 ElCentro record would correspond to excitation level one as shown in table 3.10.

When the structure (either the frame tube or the associated frame system) is subjected to earthquakes corresponding to excitation level one, the structure behaves

essentially elastically. To investigate the inelastic behavior of the structures, the intensity of the earthquake records are magnified by factors of 2, 4 & 8. These magnified records are referred to as excitation levels 2, 4 & 8. Excitation levels 2, 4 & 8 would result in base shears that are 2, 4 & 8 times the design base shear, if the structure responds elastically.

Method of Analysis

The structural analysis program DRAIN-2D [21], supplemented with the three dimensional beam column element described in chapter two, is used to carry out the dynamic analysis. The frame tube is modelled in two dimensional space as described in chapter two. The equations of motions are integrated numerically with a constant acceleration within the time step. This method has the advantage of being stable for all periods and time steps. In any analysis, greater accuracy can be expected as the integration time step is reduced. To minimize computational effort, however, it is important to select as long a time step as possible. After several preliminary trials, a time step of 0.005 second was adopted as the best compromise between accuracy and economy.

To minimize the dependency on any particular ground motion record, the mean and the coefficient of variation (COV) of the response quantities are calculated and presented in this study. The COV is the ratio of the standard deviation estimate to the mean value. Mean values are used to show trends, and COV should reflect the sensitivity of the response quantity measured.

3.4.3.1 Elastic Response

The response parameters of interest in this analysis are the story shears and the interstory drifts.

Story Shears

The ensemble average of the story shear distribution, along the height of the structure, are presented in dimensionless form in fig. 3.18, where the response is purely elastic corresponding to excitation level one. The normalized base shear with a unit value is expected since it follows the definition of excitation level one; namely, the dynamic elastic base shear is the same as the design base shear.

When comparing the story shears of the frame tube and the frame, the tube action has its greatest effect in the middle portion of the structure causing higher shear forces to develop in the frame tube. This observation agrees with earlier findings on the effect of tube action on story shear based on elastic spectrum analysis (section 3.4.2, fig. 3.15).

The normalized design story shear envelop according to the NBCC 1985 and the ensemble average of the story shear along the height of the frame tube are plotted and compared in fig. 3.19. The difference between the ensemble average and the design values is due mainly to the effects of higher modes which cannot be accounted for simply by a concentrated force F_t at the top of the structure. The design story shears are smaller than those corresponding to the ensemble average in the top portion of the structure.

Interstory Drift

The ensemble average of the story drift along the height of the structure is shown in fig. 3.20, where the story drift is presented as a percentage of story height. The interstory drift in the frame tube is smaller than that in the frame, specifically in the upper portion of the structure. Therefore, the tube action has the beneficial effects of reducing the story drift in the frame tube.

3.4.3.2 Inelastic Response

The response parameters of interest in this analysis are the story shears, interstory drifts,and ductility ratio.

Story Shears

The ensemble average of the story shear distribution for the frame tube and the frame corresponding to excitation levels 4 & 8 is plotted in fig. 3.21. The increase in story shears from excitation level four to excitation level eight defined as

$$dV = V_8 - V_4 \tag{3.9}$$

where V_8 is the story shear corresponding to excitation level 8 and

V_4 is the story shear corresponding to excitation level 4,

is plotted in fig. 3.22 for the frame tube and the associated frame system. The increase in story shear is higher in the lower portion than in the upper portion of the frame tube structure. On the other hand, the increase in story shears beyond level four is almost uniform along the height of the associated frame system. The consequences of this observation are further discussed later in this chapter.

Dispersion of Results

Before investigating the dynamic inelastic response of frame tube structures, it is interesting to look at the dispersion of the results. Fig. 3.23 shows the coefficient of variation (COV) associated with the mean responses of story shears along the height the frame tube, and its associated frame. Fig. 3.23-a corresponds to an elastic response, and fig. 3.23-b corresponds to an inelastic response with excitation level eight. For an elastic response, the frame shows larger scatter than the frame tube, especially in the upper two third of the structure as shown in fig. 3.23-a. The zero value of the COV at the base is expected because all records are

normalized to have the same base shear. When the response is inelastic, the scatter of the frame tube and frame are similar as shown in fig. 3.23-b

In addition to the comparison between the frame tube and frame scatters, one can observe that the dispersion of story shears decreases when the behavior is in the inelastic range.

Interstory Drift

The ensemble average of the interstory drift along the height of the structure for excitation levels 1, 2, 4 & 8 are shown in fig. 3.24. As the excitation level increases, the interstory drift in the frame tube and frame increases. However, the increase in story drift is not proportional to the increase in the excitation level due to the inelastic behavior. In other words, the drift corresponding to excitation level eight is not eight times the drift corresponding to excitation level one. In addition, the increase in drift as the excitation level increases is not uniform along the height of the structure and is different for the frame tube and the associated frame system.

Since the point of interest is to evaluate the effect of the tube action when the frame tube is excited well into the inelastic range, the drift for the frame tube, and its associated frame, corresponding to excitation level eight, is compared in fig. 3.25. An interesting and disturbing effect is that the drift in the frame tube is much larger than the drift in the frame in the lower portion of the structure. The same trend of story drift distribution is given for an individual earthquake. This is displayed in fig. 3.26 where the 1940 ElCentro N-S record is used as input.

Inelastic Behavioral Characteristics of Frame Tube Structures

Examination of fig. 3.25, indicates that: (1) For the frame tube, the drift in the bottom stories is higher than the drift in the upper stories, and (2) for the frame system, the drift in the upper stories is higher than the drift in the bottom stories.

The large drift in the frame tube near the bottom, with much smaller drift near the top, led to the hypothesis that when subjected to very strong shaking, the lower stories may act as a series of soft stories, thereby reducing the shear force transmission to the upper stories. As shown earlier in this chapter, this hypothesis is in agreement with the story shears distribution for excitation levels 4 & 8 shown in fig. 3.21 and 3.22, where the increase in story shears is mainly restricted to the bottom stories of the frame tube.

Because of the assumed bilinear hysteretic deformation characteristics of the members in the study, these soft stories also serve as energy absorbing mechanisms. The story shear versus story drift at the fifth story when the model is subjected to the 1940 ElCentro N-S component shaking is given in fig. 3.27. The larger hysteresis loop for the frame tube as compared to the associated frame system indicates larger energy dissipation.

To substantiate the above hypothesis, a thorough literature review on buildings with a soft story subjected to earthquake excitation has been carried out. The objective is to define the parameters governing the behavior of such buildings, and to compare those parameters with similar parameters for the frame tube and its associated frame.

Response of Buildings with a Soft First Story

One of the essential features of the earthquake loading is that the external loading is applied to the structure through its base. Forces developed at the upper stories are a consequence of the local accelerations which would result from the earthquake motions introduced at the base. Because the forces in the building depend on the story accelerations, their

magnitude is the result of the motion propagated through the building from the base. This propagated motion can be amplified, or reduced, depending on the characteristics of the lower stories where the earthquake input is applied.

To limit the propagation of motion into the upper stories, Fintel and Khan [15] suggested that the first story can act as a soft ductile link which yields at a specified value of horizontal shear force and therefore cannot transmit a greater force than this into the upper stories. Chopra, Clough and Clough [9] presented a more thorough study on the dynamic response of buildings with a soft first story. The basic parameters considered in the yielding first story is the yield force level and the ratio of story stiffness as defined in equation 3.6. Their findings show that the ratio of story stiffness in the first story plays an important role in controlling the forces that can propagate to the upper stories. For a higher ratio of story stiffness, larger shear forces are transmitted to the stories above the first story. However, there is smaller displacement in the ductile link (first story). On the other hand, for a small ratio of story stiffness, smaller shear forces are transmitted to the stories above the first story but there is larger displacement in the ductile link (first story).

Relationship between the Frame Tube and Buildings with a First Soft Story

To relate the findings by Chopra, Clough and Clough [9] to the inelastic behavior of the frame tube and its associated frame system, table 3.6 shows the ratio of story stiffness for the two systems. This table was first introduced in section 3.4.1 along with the definition of story stiffness. The ratio of story stiffness is smaller for the frame tube. As a result, the lower stories in the frame tube can act more like a series of soft ductile links (soft stories) suffering large displacement but allowing lesser force to propagate into the upper stories.

To lend further credibility to the proposed hypothesis, the ratio of story stiffness will be modified, and the effect of this modification on the frame tube behavior is re-investigated. This study is described in the next chapter.

To relate the ratio of story stiffness to the tube action, one can refer to the tube action when the frame tube is under quasi static loading. It was concluded there that when the frame tube is subjected to a static lateral load, the tube action is ineffective beyond the elastic limit and leads to a small ratio of story stiffness. Therefore, one can relate the large story drift in the bottom stories when the frame tube is subjected to a dynamic excitation beyond the elastic limit to the loss of the tube action.

Ductility Ratio

The force deformation curve and the response time histories provide complete information regarding the inelastic response of a structure. However, it is impossible to examine all the details of these curves for every structure considered. As a result, a simple response parameter needs to be defined to characterize the inelastic response and to provide measures of the extent of damage to the structure. For a single degree of freedom, the response parameter generally used to describe the performance of inelastic systems subjected to ground motions, is the maximum displacement ductility ratio defined as

$$\mu = v_{max} / v_y \tag{3.10}$$

where,

v_{max} is the maximum displacement, and

v_y is the yield displacement.

For the moment resisting frames where the inelastic action occurs mainly in the beams undergoing rotational displacements, a new definition for the ductility ratio was initiated [10], namely, the rotational ductility defined by

$$\mu_\theta = 1 + \theta_p / \theta_y \tag{3.11}$$

where,

θ_p is the maximum plastic hinge rotation, and

θ_y is the yield rotation.

In nonlinear analysis of frame structures, the maximum plastic hinge rotation is evaluated at the end of each member during the course of the earthquake. The yield rotation can be presented by

$$\theta_y = M_y L/6EI \tag{3.12}$$

Once these two quantities are known, the rotational ductility at the end of each member can be calculated.

Another parameter that characterizes the overall inelastic response of multi story structures is used in the literature [8,32], namely,the overall displacement ductility of the structure defined as

$$\mu_{ov} = v_{max} / v_y \tag{3.13}$$

Where,

v_{max} is the maximum roof displacement obtained from the dynamic analysis, and

v_y is the roof displacement corresponding to first yield.

In this study, v_y is taken to be the roof displacement when the frame tube is subjected to the static design lateral load and the response is elastic.

It is important to recognize that there is a significant difference between the overall displacement ductility and the rotational ductility. Once yielding has commenced in the structure, the deformations concentrate at the plastic hinge positions. As a result, the required rotational ductility may be greater than the overall displacement ductility. Borges and Ravari [8] report values of the overall displacement ductility between 1.6 and 2.1, with the local

ductility varying between 2.1 and 5.1 for an eight story reinforced concrete building. They also conclude that the overall ductility decreases as the number of stories increases.

The relationship between the rotational ductility and the overall displacement ductility for the frame tube is shown in fig. 3.28. This set of data is obtained from the dynamic inelastic analysis carried out in section 3.4.3.2. Specifically, it corresponds to six earthquake records each having four intensities. For each record with a particular intensity, three values of the rotational ductility are selected. These values correspond to the maximum rotational ductility among all beams in the top one third, in the middle one third, and in the lower one third of the frame tube. From fig. 3.28, the followings can be observed: (1) the rotational ductility is much higher than the overall ductility. (2) The maximum rotational ductility occurs in the bottom of the structure. (3) The maximum overall displacement ductility has approximately a value of three, and corresponds to excitation level eight.

3.5 COLUMN CAPACITY

Up to this point, the static and dynamic analyses were conducted with the assumption that the inelastic deformation is restricted to the beams, while the columns are elastic. Seismic design codes repeatedly emphasize that the formation of plastic hinges in columns should be avoided, if possible. The reason is that column failure have much more serious consequences than beam failure. Column yielding in all columns in a story will lead to a permanent misalignment of the building, and introduces problems of instability. In addition, for the case of frame tube structures, if column hinging cannot be prevented, one should avoid at least column hinging in the corner column where heavy interaction between the two orthogonal frames is taking place.

To avoid column hinging, one common approach is the strong column weak beam concept, where the sum of the moment capacities of the columns above and below the joint is

greater than the sum of the beam capacities framing into the joint. Mathematically, this can be represented as

$$M_{yc} = \gamma M_{yb} \qquad \text{for an interior joint} \qquad (3.14\text{-a})$$

$$M_{yc} = \frac{\gamma}{2} M_{yb} \qquad \text{for an exterior joint} \qquad (3.14\text{-b})$$

where M_{yc} is the column capacity,

M_{yb} is the beam capacity, and

γ is a factor greater than unity.

Typical values of γ range between 1.25 and 2. For this study, attention is focused on the selection of the corner column capacity. To determine the proper value of γ, the flexural capacity demand of the corner column is investigated when the frame tube is subjected to its static design lateral load and then when subjected to a dynamic excitation.

3.5.1 Corner Column Flexural Capacity under Static Loading

The bending moment diagram of the corner column, when the frame tube is loaded into the inelastic range with its design lateral loading 50% exceeding the yield load is plotted in fig. 3.29. At a typical joint (fig. 3.30), the beam moment is resisted by the sum of the column moments; therefore,

$$M_b = M_{c1} + M_{c2} \qquad (3.15)$$

where

M_b is the beam moment,

M_{c1} column moment above the joint, and

M_{c2} column moment below the joint.

or, the greatest column moment is

$$M_{c1} = M_b - M_{c2} \qquad (3.16)$$

At yield, the requirement to prevent corner column hinging would be

$$M_{yc} > M_{yb} - M_{c2} \tag{3.17}$$

It is apparent from fig. 3.29 that the columns in the bottom five stories, as well as in the upper stories, are in single curvature which puts more severe restriction on preventing column hinging, namely,

$$M_{yc} > M_{yb} + M_{c2} \tag{3.18}$$

Hence, to prevent corner column hinging, the corner column capacity should be greater than the adjoining beam capacity. Therefore, if equation 3.14-b is to be used, the value of γ should at least be equal to 2.

The column capacities used in the analytical model, described in section 3.3, were selectected to be ten times the adjoining beam capacities. This corresponds to a γ value of twenty and ten for an exterior and interior joint, respectively. Therefore, according to equation 3.14, no hinging can occur in the columns.

3.5.2 Corner Column Flexural Capacity Under Dynamic Excitation

In order to estimate the corner column flexural capacity as it compares to the adjoining beam capacity, a dynamic inelastic analysis was carried out. The frame tube, as described in section 3.3, is considered with the exception that the interior column capacities are derived from equation 3.14-b with $\gamma = 1.4$ and the corner columns are designed with moment capacity M_{01} and M_{02} such that they remain elastic. If $M_{01} = M_{02} = \beta M_{yb}$, and the yield criteria for hinge formation at the corner column is

$$\left(\frac{M_1}{M_{01}}\right)^2 + \left(\frac{M_2}{M_{02}}\right)^2 + \left(\frac{P}{P_0}\right)^2 = 1 \tag{3.19}$$

where,

M_1 is the moment effect from the longitudinal frame,

M_2 is the moment effect from the transversal frame,

P is the axial force, and

the subscript 0 denotes the fully plastic value when only the stress resultant concerned is acting on the cross section.

Then,

$$\frac{1}{\beta^2}\left[\left(\frac{M_1}{M_{yb}}\right)^2+\left(\frac{M_2}{M_{yb}}\right)^2\right]=\left[1-\left(\frac{P}{P_0}\right)^2\right] \tag{3.20}$$

or solving for beta

$$\beta=\sqrt{\frac{\left(\frac{M_1}{M_{yb}}\right)^2+\left(\frac{M_2}{M_{yb}}\right)^2}{1-\left(\frac{P}{P_0}\right)^2}} \tag{3.21}$$

To estimate the value of beta, the frame tube is subjected to the 1940 ElCentro N-S earthquake with excitation levels 2, 4 & 6. The values of the moments M_1, M_2, and P obtained in this analysis are used to calculate beta. A plot of beta along the height of the structure is shown in fig. 3.31. It is apparent that beta increases as the excitation level increases. In other words, to avoid yield, the flexural capacity demand of the corner column increases as the excitation level increases. At the excitation level four, beta = 1 for the first twenty five stories and beta = 2 for the top five stories would appear to be a proper choice for the corner column flexural capacity to avoid corner column yielding.

The above estimate of beta gives some guidelines for determining the corner column flexural capacity to avoid yield. To further justify the above recommendation, the frame tube, with beta = 1 for the first 25 stories and beta = 2 for the top 5 stories, is subjected to the 1971 E-W San Fernando earthquake record listed in table 3.9. The excitation level selected is four. Fig. 3.32 shows the plastic hinge pattern throughout the longitudinal frame. It is apparent that the above recommendation produced reasonable estimate for the corner column flexural capacity with very few hinges occurring in different locations along the corner column line.

3.6 CONCLUSIONS

The static and dynamic behavior of frame tube structures under lateral loads are examined in this chapter. The main objective of the study is to assess the significance of the tube action. For this purpose, a thirty story four bays by four bays frame tube is taken as a typical frame tube structure for the study. It is first subjected to an inverted lateral load distribution to define the tube parameters so that the tube action will provide resistance to the applied loading in the elastic range. The results of the parametric study showed that in order for the tube action to be effective, the frame tube should deflect like a cantilever column with a linear variation of the axial force in the columns of the longitudinal frames and almost uniform axial force in the columns of the transversal frames. The tube action can be obtained by using relatively stiff beams both in flexure and in shear (S.R. $<=1.6$, S.S.S.F. $>=0.1$).

A thirty story four bays by four bays frame tube with the above specified properties is designed according to the seismic provision specified in the NBCC 1985. To assess the significance of the tube action, a comparison between the behavior of the frame tube and an associated frame system is carried out. From this comparison, the following conclusions can be drawn:

A. Static

(1) The tube action is effective only when the behavior is elastic and provides the beneficial effect of reducing the lateral displacement of the frame tube system.

(2) The tube action becomes ineffective when the frame tube is loaded beyond the elastic limit.

(3) The ratio of story stiffness is smaller for the frame tube than for the associated frame system.

B. Dynamic

Based on the results of the elastic response spectrum analysis, the following can drawn:

(1) The tube action leads to a reduction of the contribution of higher modes to the base shear.

(2) The modal contribution of higher modes to story shears is significant in the top portion of the frame tube and to a less extent in the lower portion of the frame tube. However, negligible contribution of higher modes occurred in the middle portion of the frame tube.

(3) The tube action leads to a significant increase in story shears only in the middle portion of the frame tube.

Based on the results on the dynamic inelastic analysis, the following can be drawn:

(1) The tube action leads to a large interstory drift in the bottom stories when the frame tube is subjected to a dynamic excitation beyond the elastic limit.

(2) The parameter governing the inelastic dynamic response of the frame tube is the ratio of story stiffness.

Finally, the capacity of the corner column required to prevent hinging is examined. It is found that the corner column capacity should at least be equal to the adjoining beam capacity.

Beam Inertia $mm^4\ 10^6$	Column Inertia $mm^4\ 10^6$	Column Area $mm^2\ 10^3$	S.S.S.F.	S.R.
208	15.6	32.3	.01	16
208	15.6	3.23	.1	16
208	15.6	.323	1.	16
208	156	32.3	.01	1.6
208	156	3.23	.1	1.6
208	156	.323	1.	1.6
208	1560	32.3	.01	.16
208	1560	3.23	.1	.16
208	1560	.323	1.	.16

Table 3.1 Member Properties for Different Examples.

Story No	Beam Inertia $cm^4\ 10^6$	Column Inertia $cm^4\ 10^6$	Column Area $cm^2\ 10^2$	Beam Size cm	Int. Col. Size cm
1-5	1.69	1.27	26.3	30.5x87	34.5x76
6-10	1.53	1.14	23.7	28.5x87	31x76
11-15	1.36	1.02	21.1	25x87	27.6x76
16-20	1.19	.891	18.4	25x82.5	24x76
21-25	1.02	.736	15.8	25x78.5	21x76
26-30	.848	.636	13.3	25x74	17.5x76

Modulus of Elasticity E = 30500 MPa

Table 3.2 Member Properties and Sizes for the Frame Tube.

Story No	Seismic Force KN
1	1.49
2	2.98
3	4.47
4	5.96
5	7.44
6	8.93
7	10.42
8	11.9
9	13.4
10	14.9
11	16.4
12	17.9
13	19.4
14	20.8
15	22.3
16	23.8
17	25.3
18	26.8
19	28.3
20	29.8
21	31.2
22	32.8
23	34.3
24	35.7
25	37.2
26	38.7
27	40.2
28	41.7
29	43.2
30	166.94

Table 3.3 Distribution of Design Lateral Forces along the Height of the Frame Tube.

Story No	Beam Capacity KN-m
1-5	270
6-10	239
11-15	212.4
16-20	176.5
21-25	129
26-30	66

Table 3.4 Beam Capacities for Frame Tube

Story No	Beam Capacity KN-m
1-5	255
6-10	225
11-15	200
16-20	167
21-25	122
26-30	62

Table 3.5 Beam Capacities for Associated Frame System

Story No	Ratio of Story Stiffness	
	Frame Tube	Frame
1	.0708	.0736
5	.029	.04
11	.034	.054

Table 3.6 Ratio of Story Stiffness, Uniform Beam Capacities.

Mode	Period (sec) Frame Tube	Frame
1	2.45	3.1
2	.72	.79
3	.38	.39
4	.25	.26
5	.19	.2

Table 3.7 Modal Periods for the Frame Tube and its Associated Frame.

Mode	Modal Weight Frame Tube	Frame	Base Shear Ratio V_i/V_1, i=1,2,...5 Frame Tube	Frame
1	.688W	.6554W	1	1
2	.1576W	.2036W	.747	1.225
3	.0431W	.0572W	.2144	.403
4	.0424W	.0264W	.2114	.1856
5	.0047W	.0148W	.0236	.1044

Table 3.8 Effect of Higher Modes to Base Shear.

Date	Earthquake	Recording Site	Component	Maximum Acc g	Maximum Vel m/s
1952 Jul 21	Kern County	Taft Lincoln School Tunnel	S69E	.179	.177
1940 May 18	Imperial Valey	ElCentro	S00E	.348	.334
1968 Apr 8	Borrego Mountain	San Onofre	N57W	.046	.042
1971 Feb 9	San Fernando	Hollywood Storage	N90E	.211	.211
1971 Aug 2	Japan	HK004	EW	.078	.068
1979 Apr 15	Yugoslavia	Albatros Hotel	N00W	.171	.194

Table 3.9 Information on the Ensemble of Recorded Earthquake Ground Motions.

	Scaling Factors	
Earthquake	Frame Tube	Frame
Taft	.47	.43
ElCentro	.23	.21
San Onofre	2.62	1.25
San Fernando	.33	.4
Japan	1.38	.73
Yugoslavia	.47	.45

Table 3.10 Scaling Factors for the Earthquake Records.

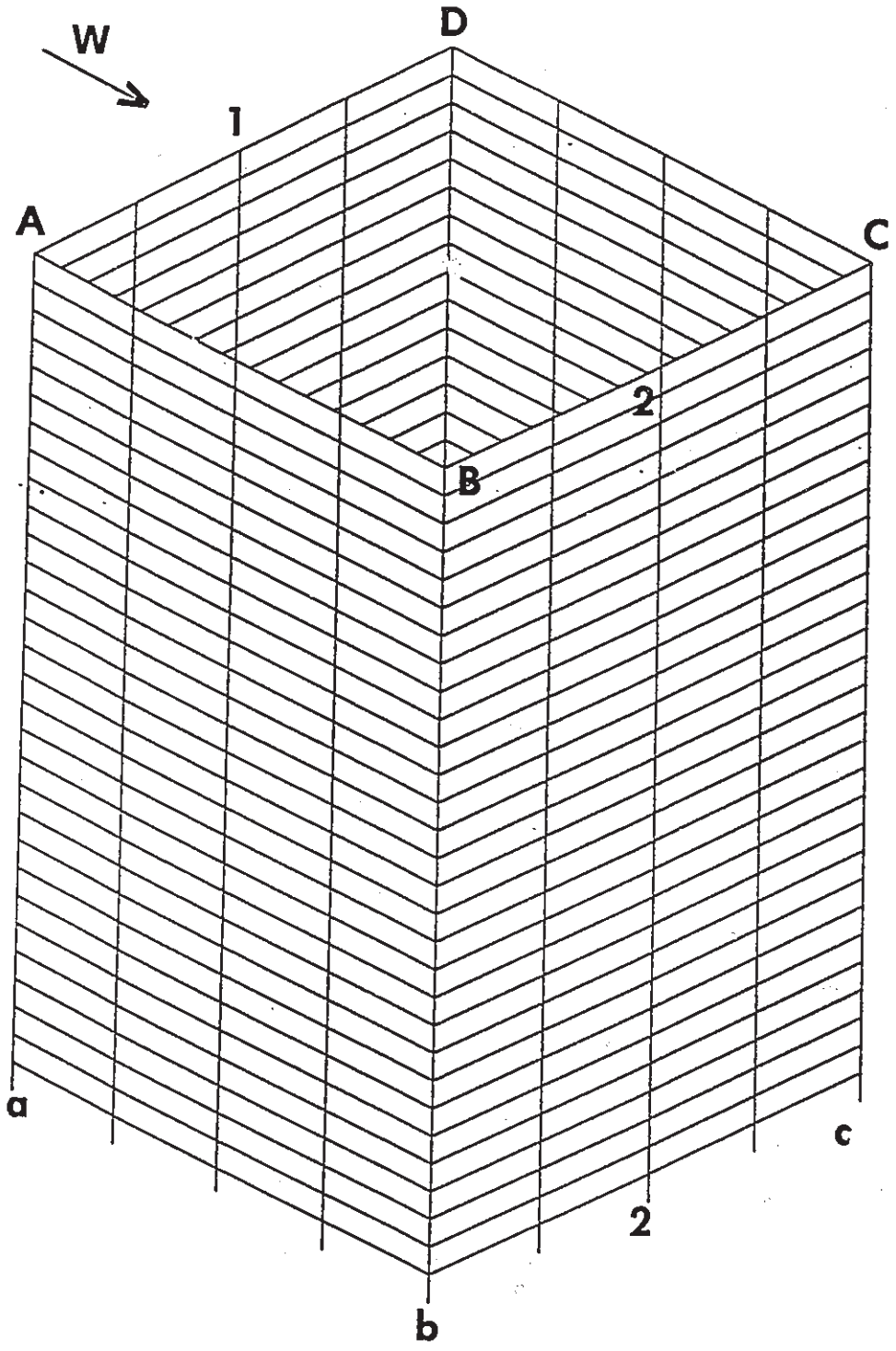

Fig (3.1) Frame Tube Structure

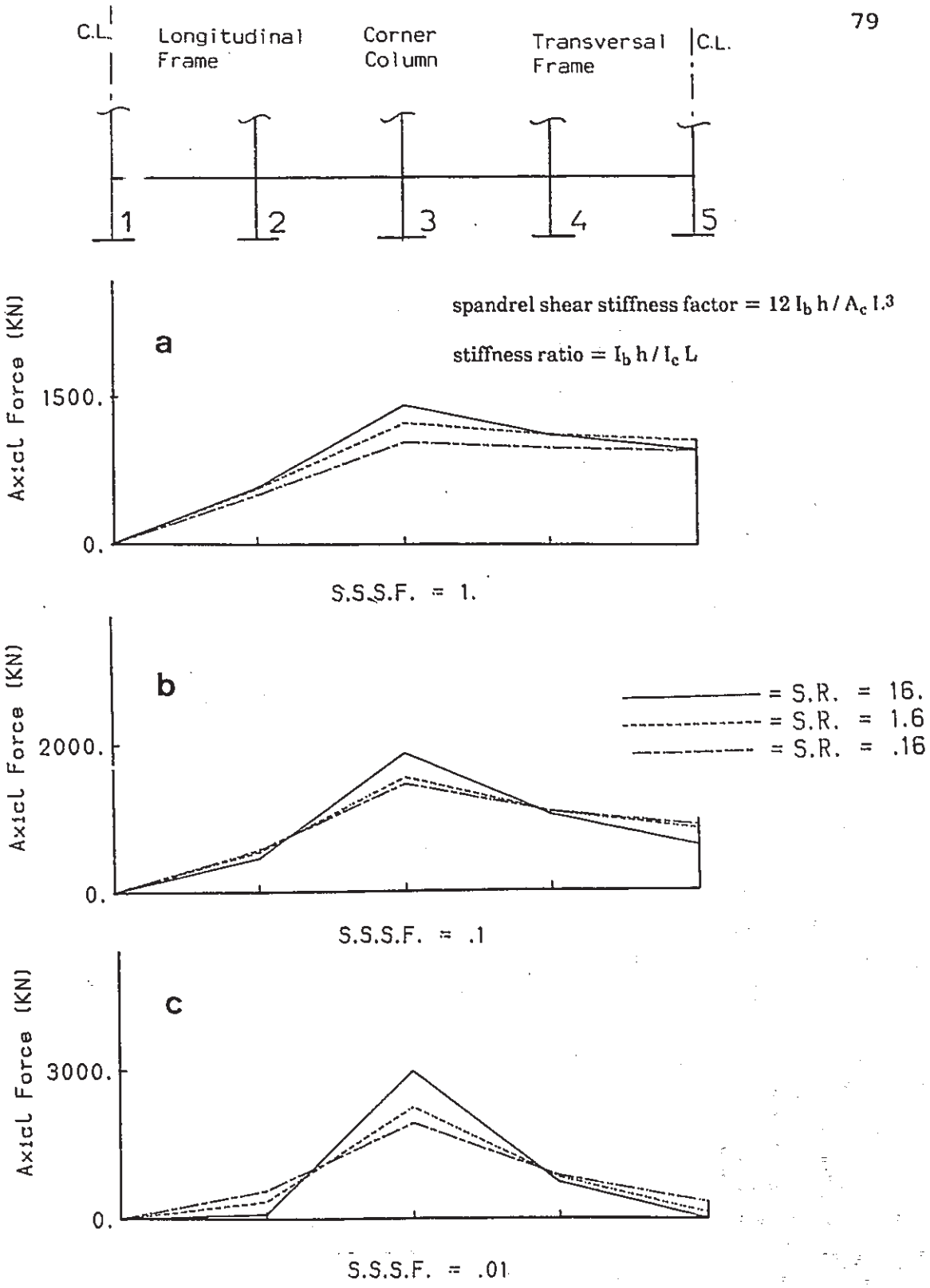

Fig (3.2) Effect of Variation of Stiffness Ratio and Stiffness Factor on Column Axial Force

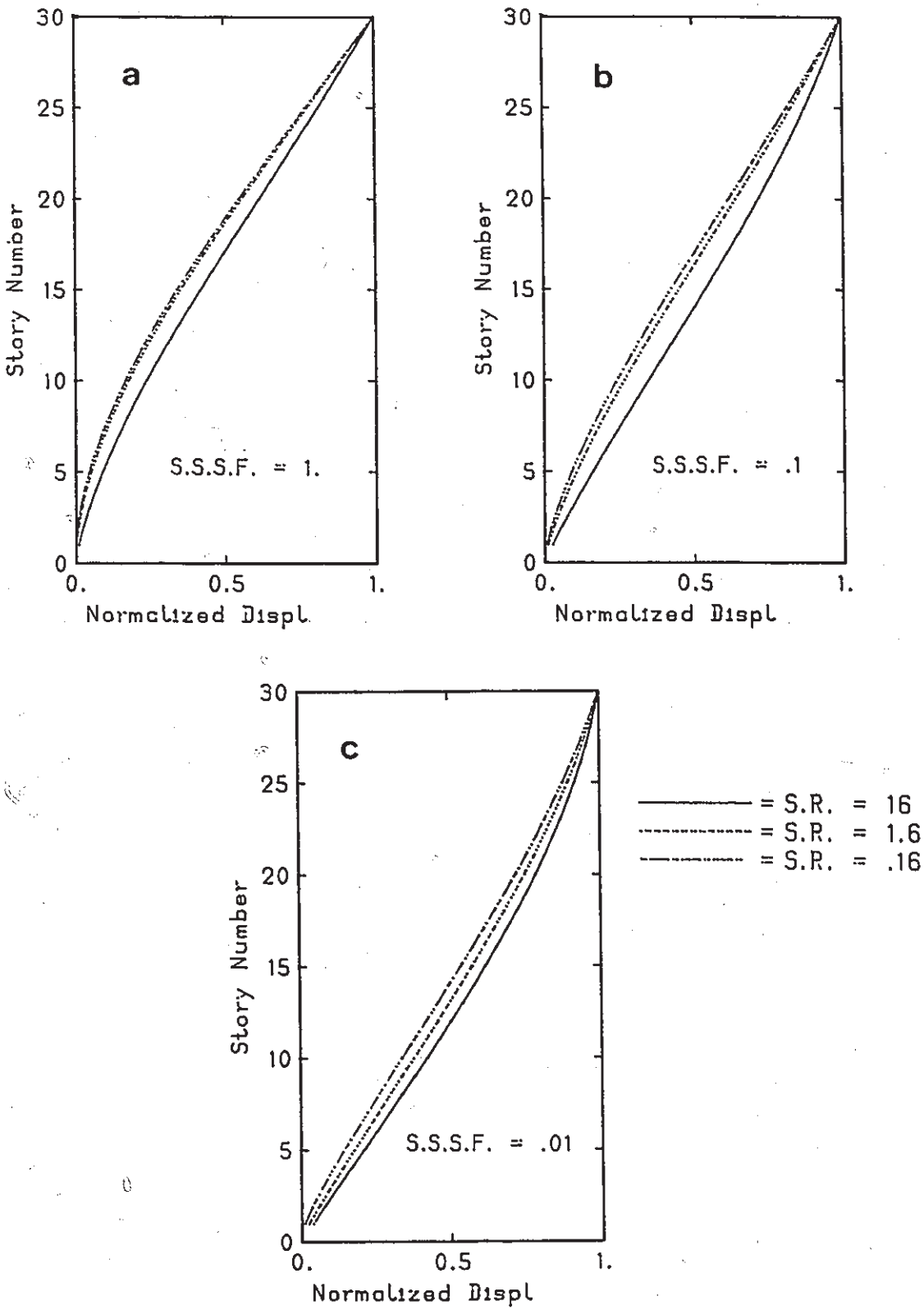

Fig (3.3) Effect of Variation of Stiffness Ratio and Stiffness Factor on the Lateral Displacement

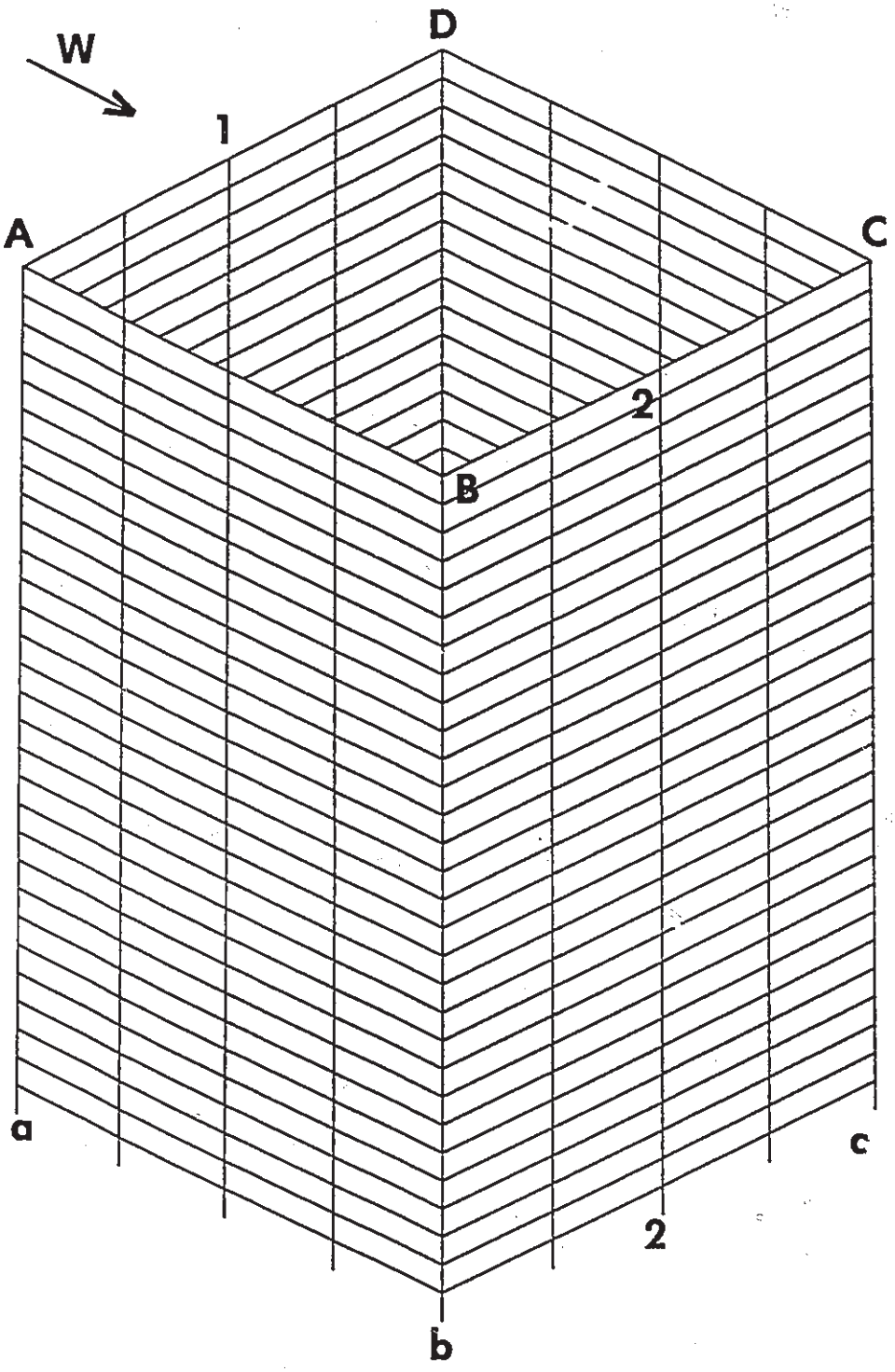

Fig (3.4) Frame Tube Structure

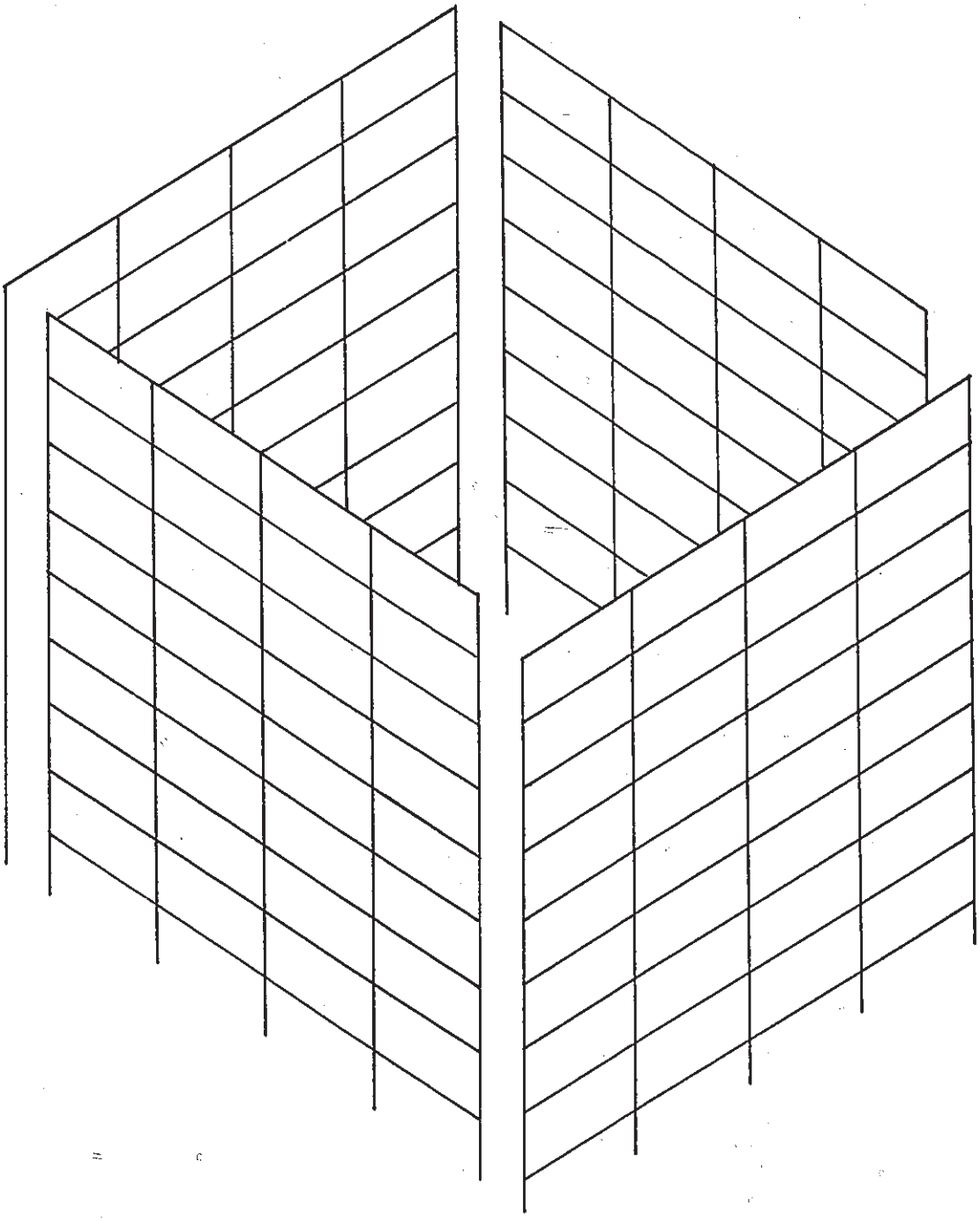

Fig (3.5) Associated Frame System

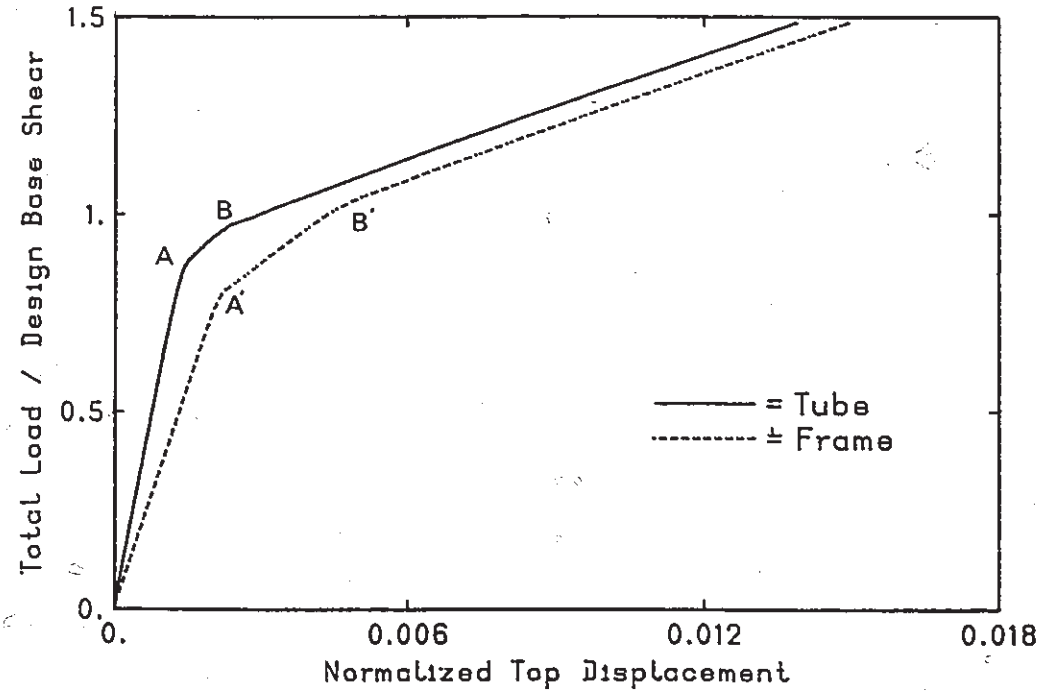

Fig (3.6) Top Story Load Displacement Curve

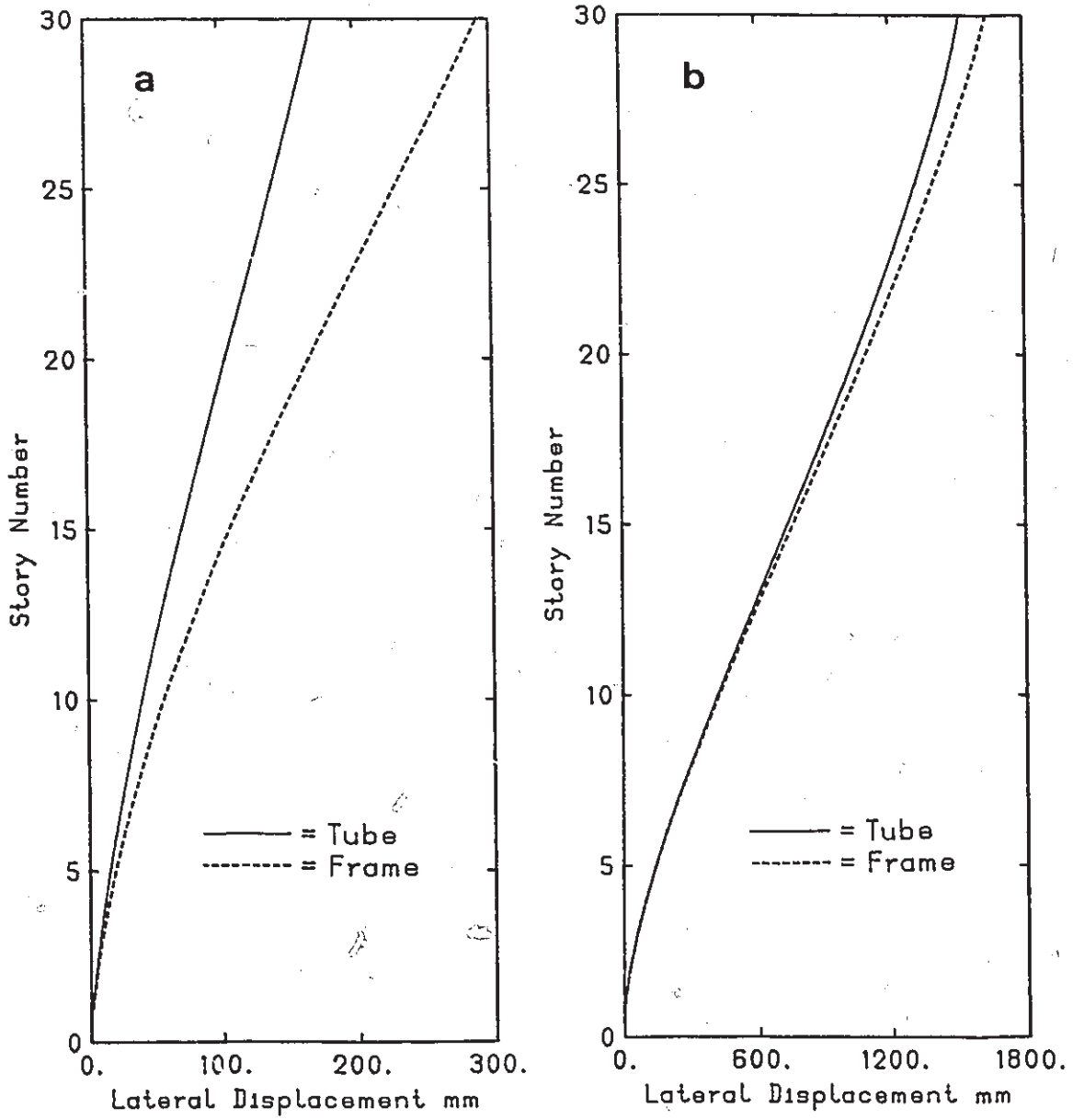

Fig (3.7) Effect of Tube Action on Lateral Displacement;
a- Elastic, b- R= 1.5

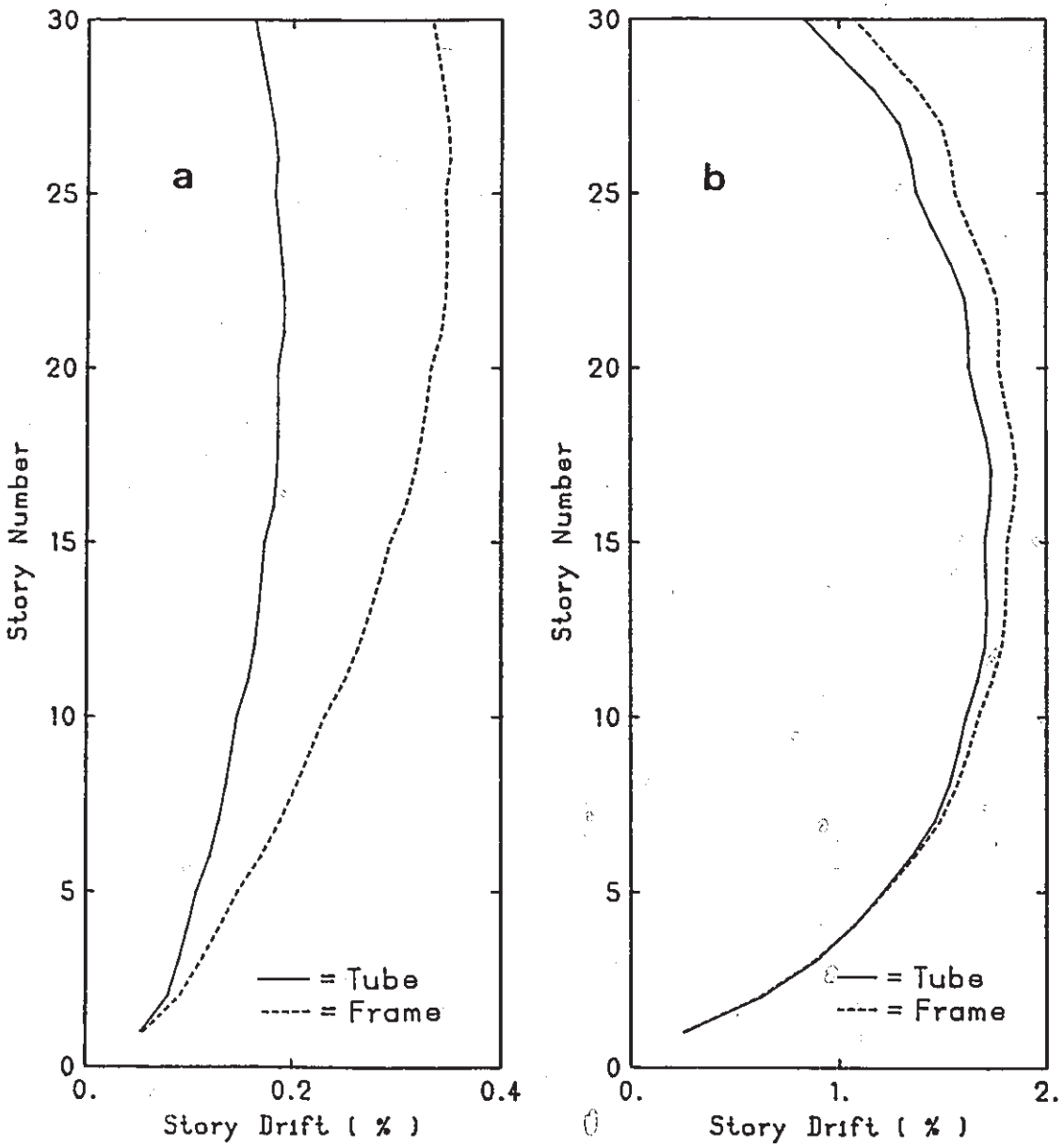

Fig (3.8) Effect of Tube Action on Interstory Drift;
a- Elastic, b- R= 1.5

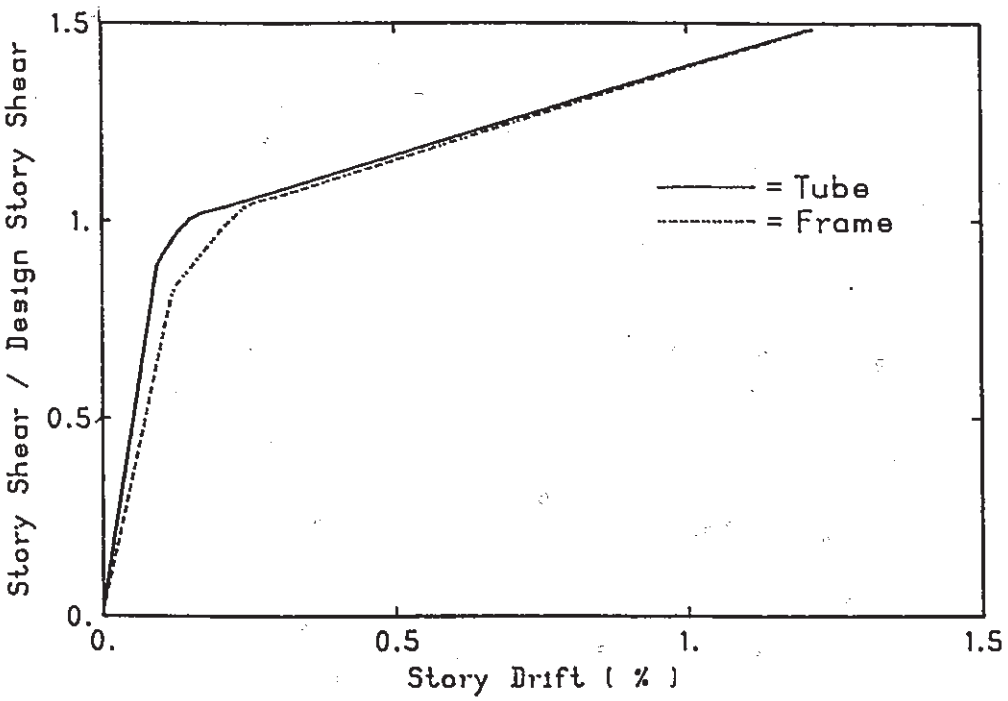

Fig (3.9) Fifth Story Load Deformation Curve

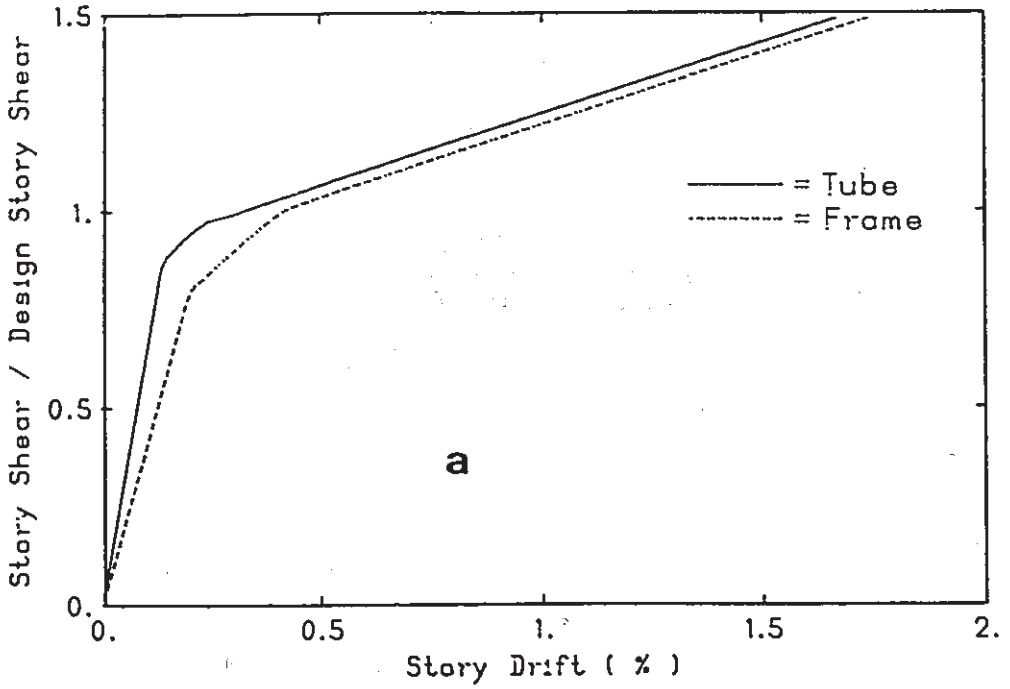

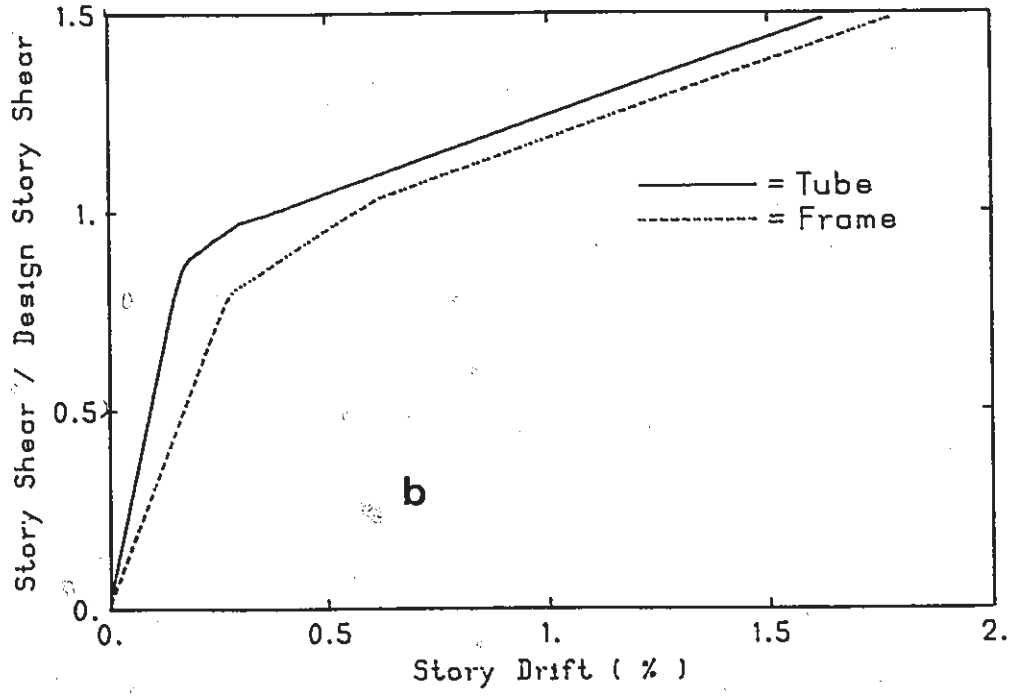

Fig (3.10) Eleventh and Twenty First Story Load Deformation Curve; a- Eleventh, b- Twenty First

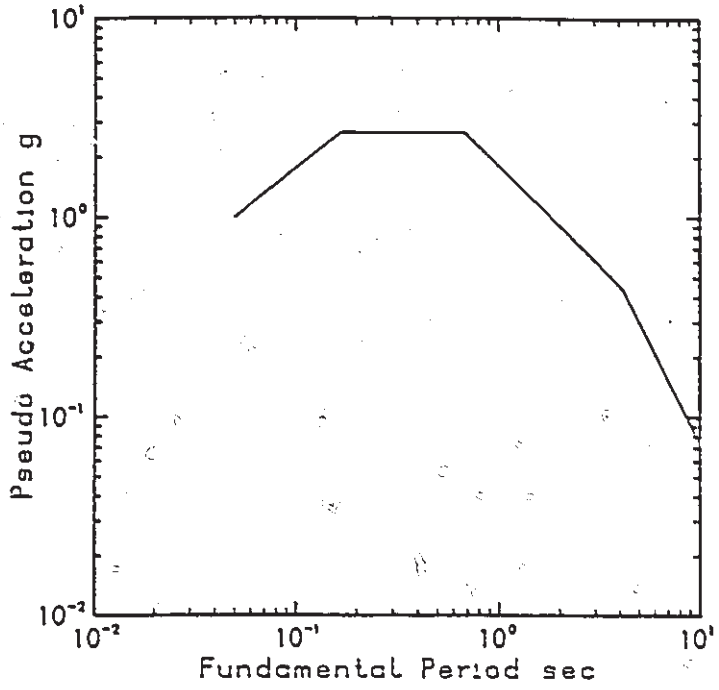

Fig (3.11) Newmark and Hall Spectrum

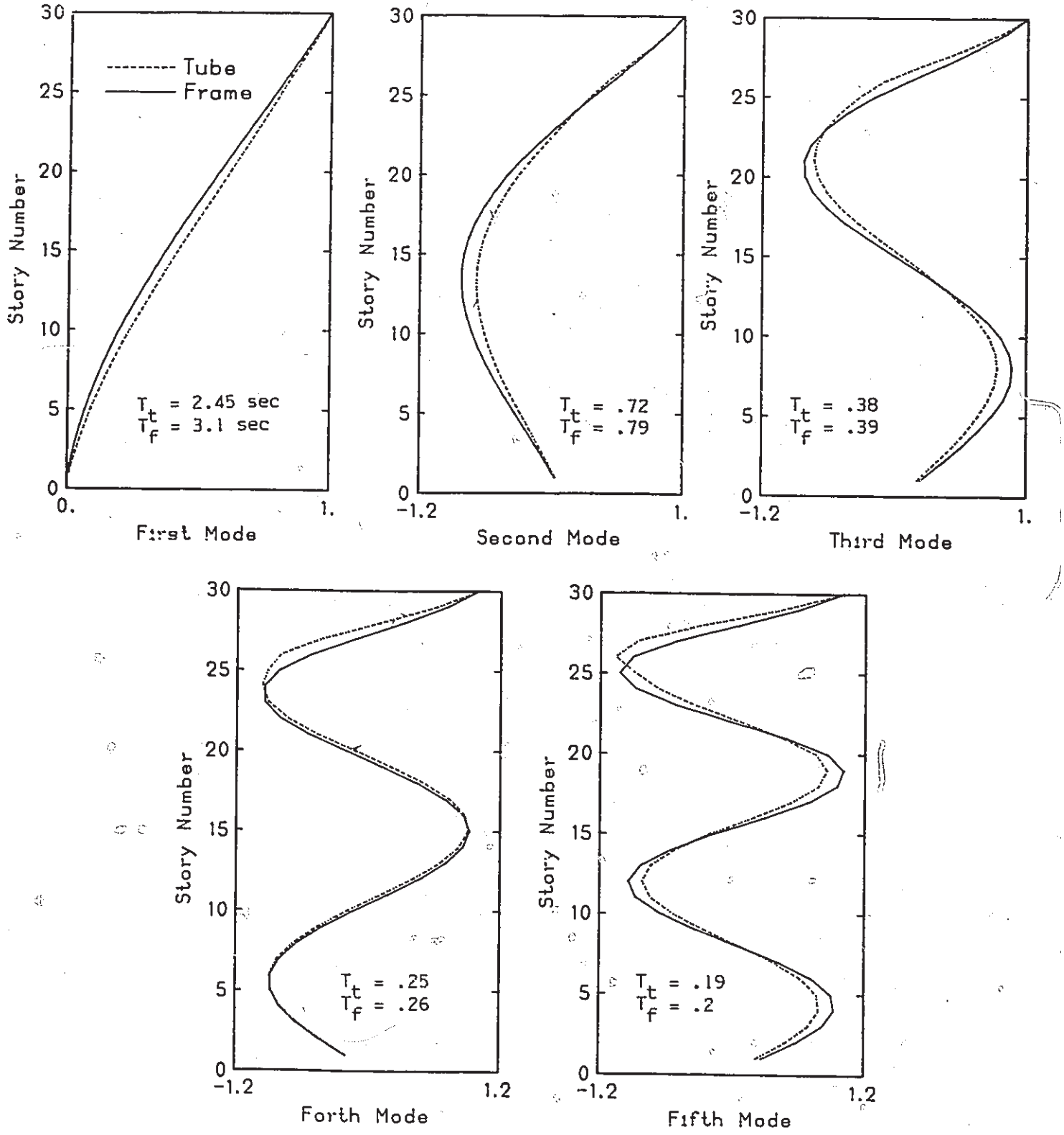

Fig (3.12) Mode Shapes

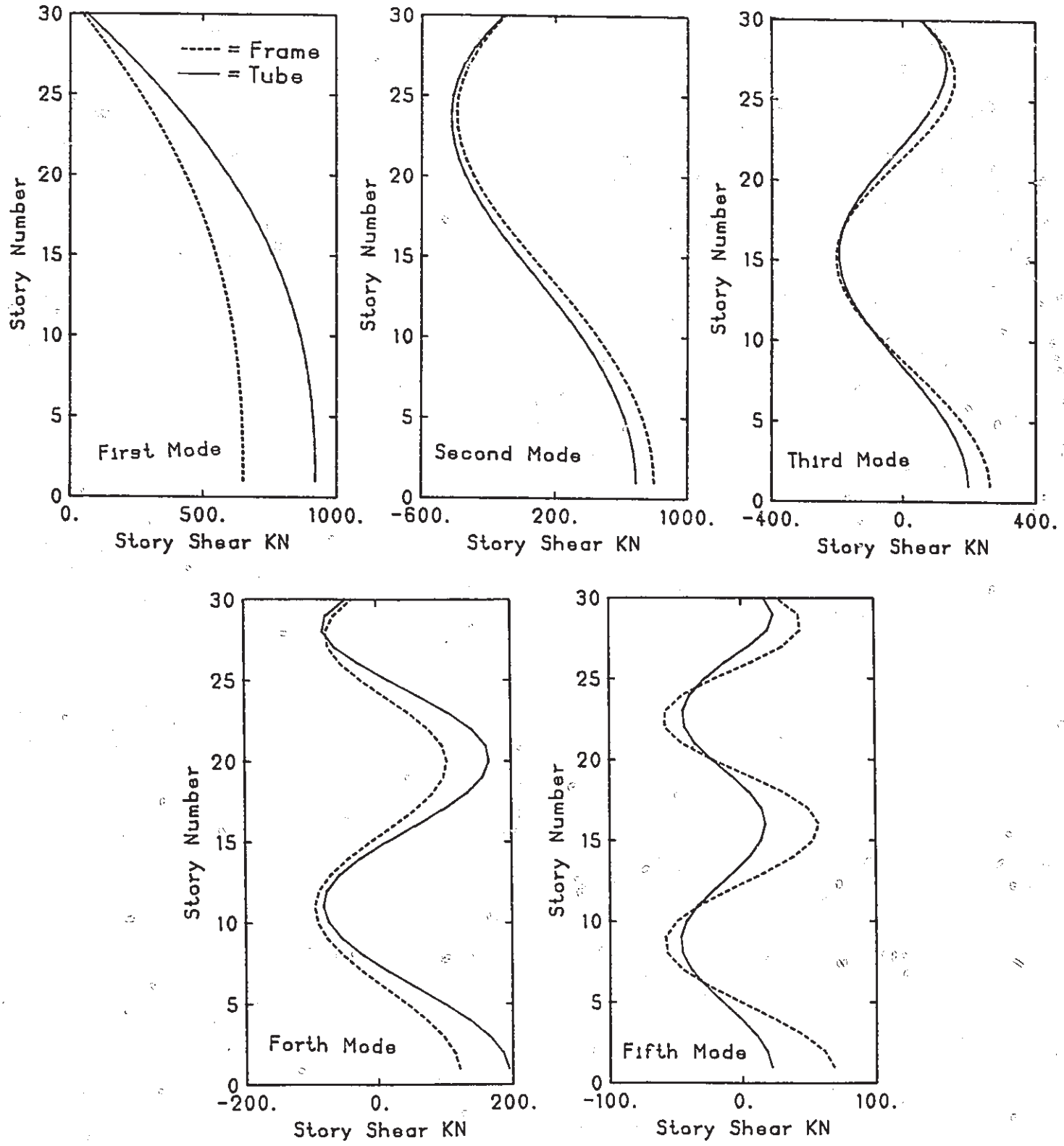

Fig (3.13) Modal Story Shear

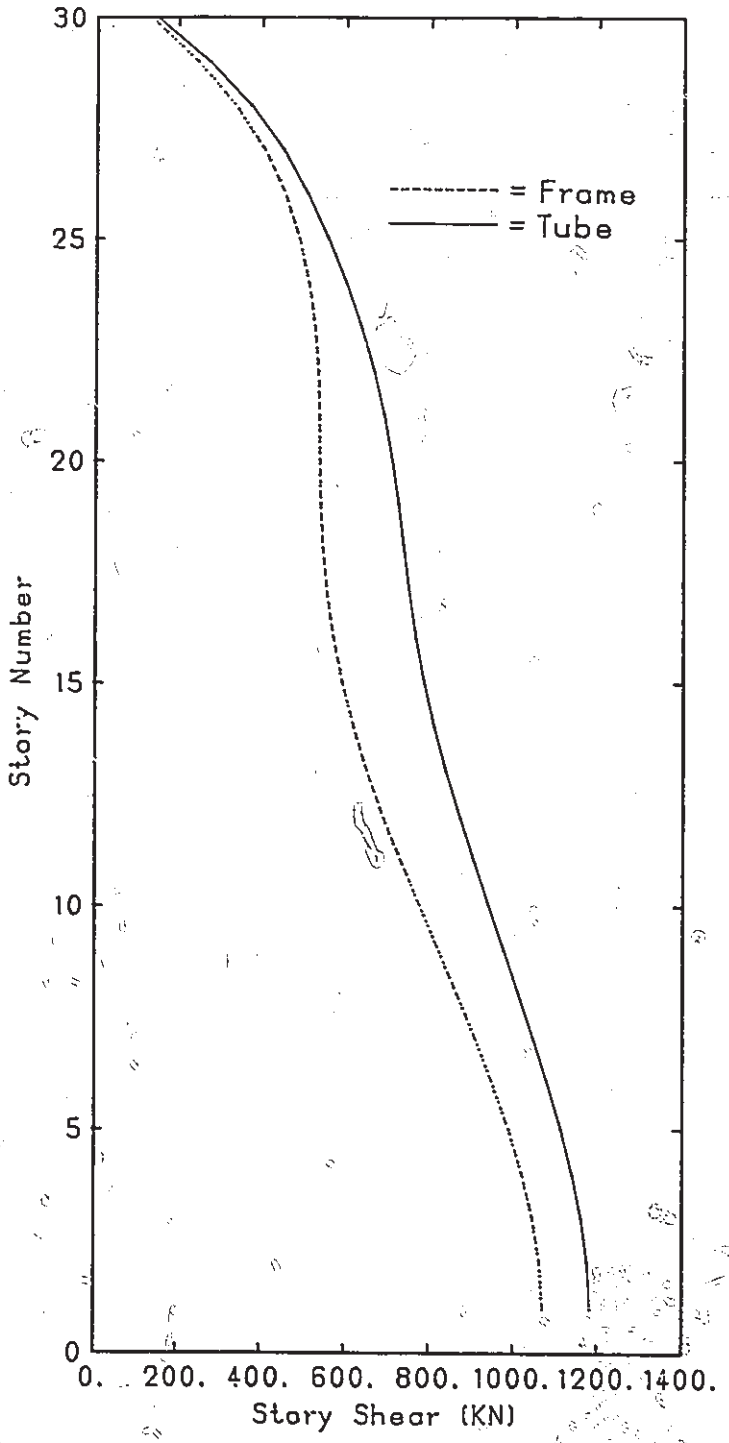

Fig (3.14) Story Shear Due to the Contribution of All Five Modes

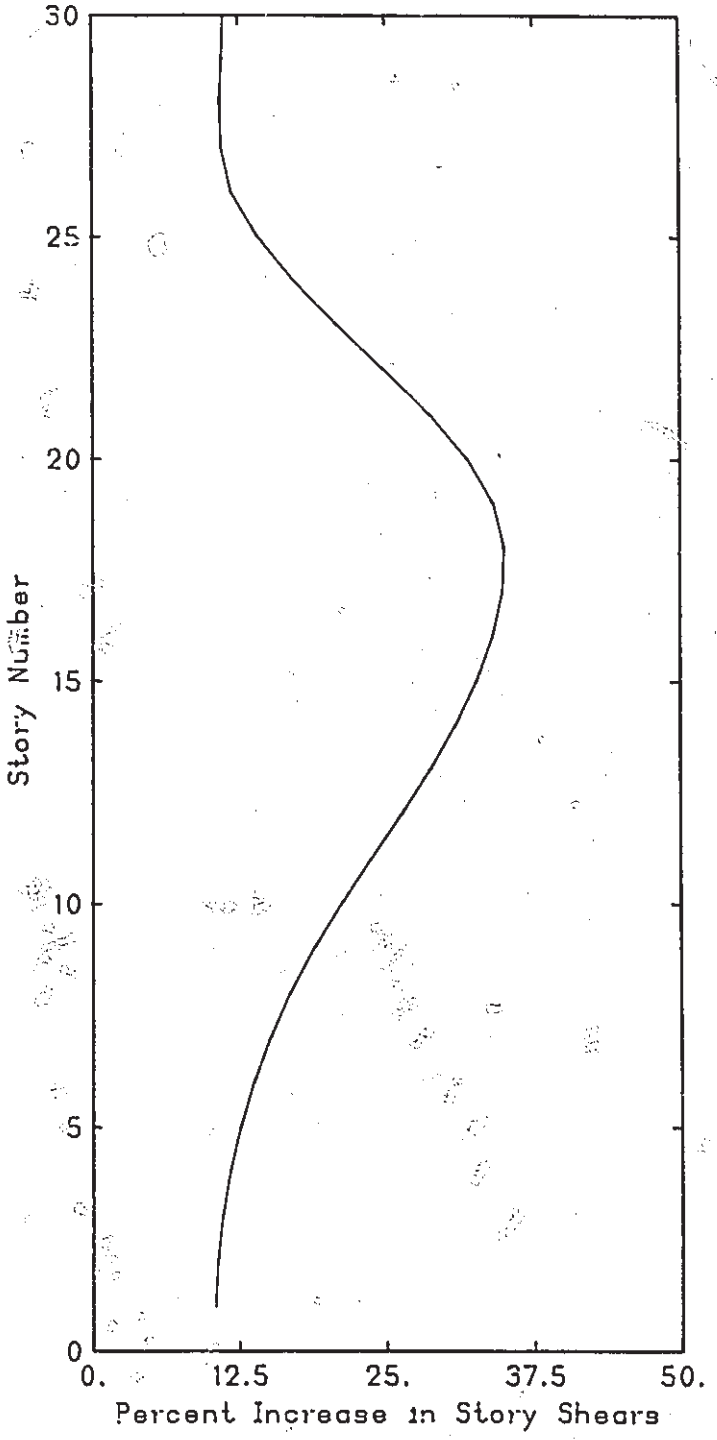

Fig (3.15) Effect of Tube Action on Story Shear Distribution

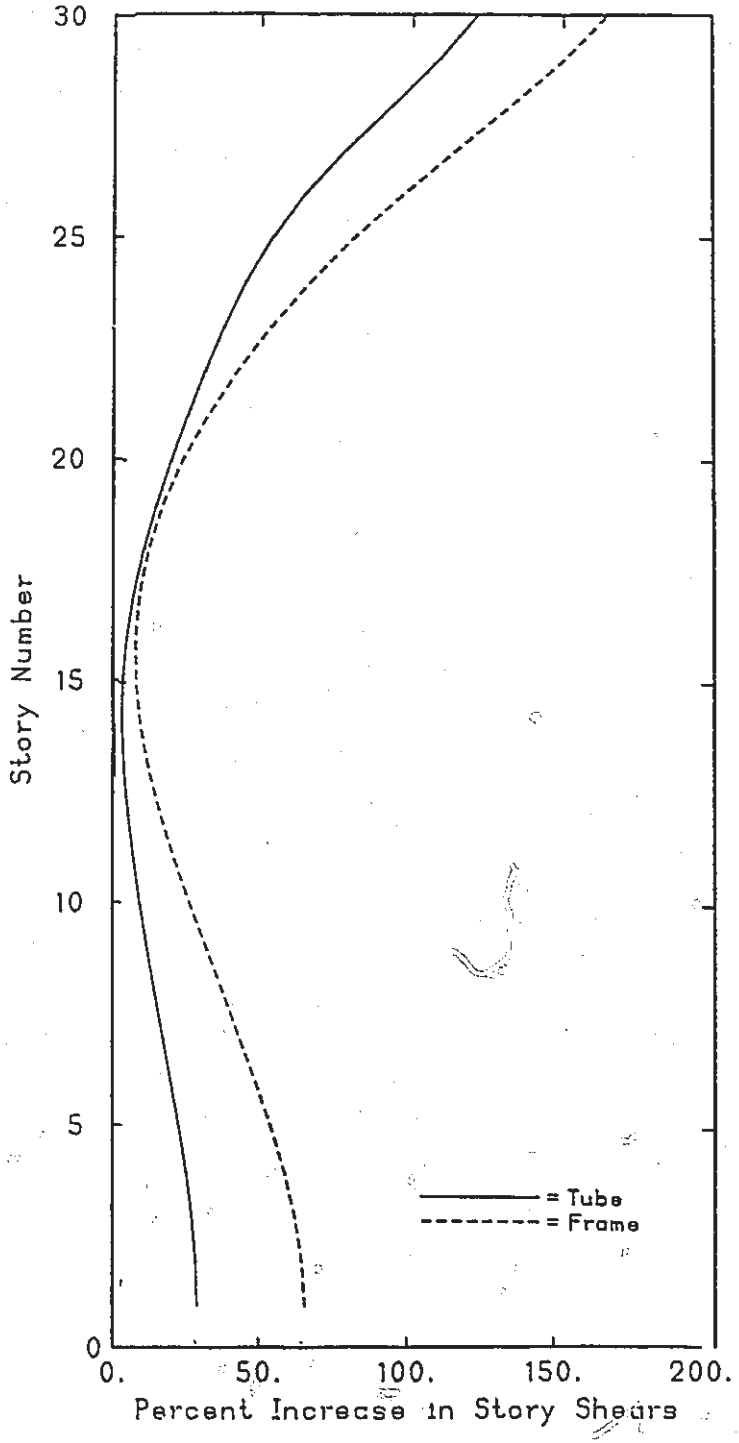

Fig (3.16) Effect of Higher Modes

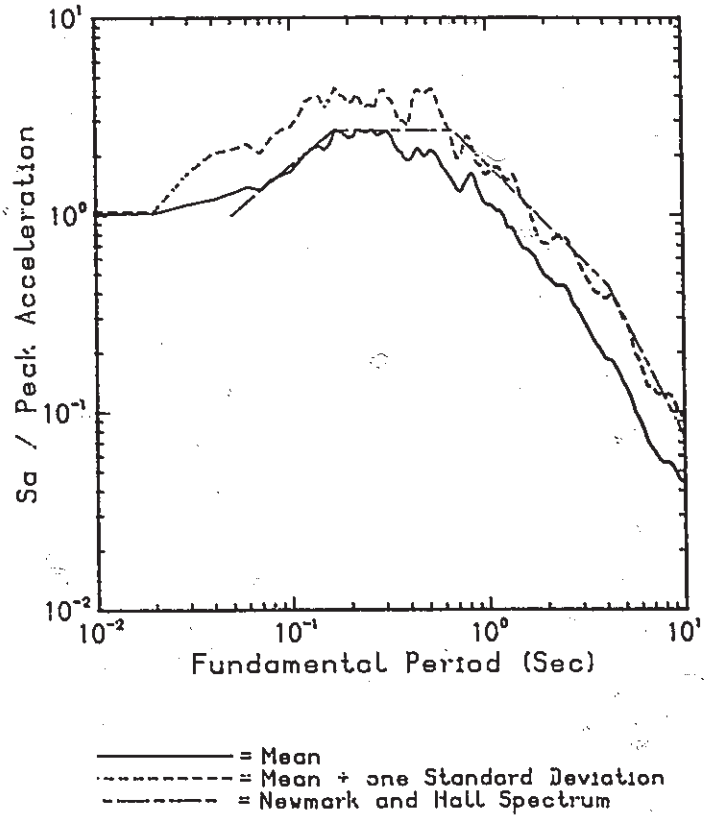

Fig (3.17) Elastic Acceleration Spectrum of the Ensemble of Earthquake and Newmark and Hall Spectrum

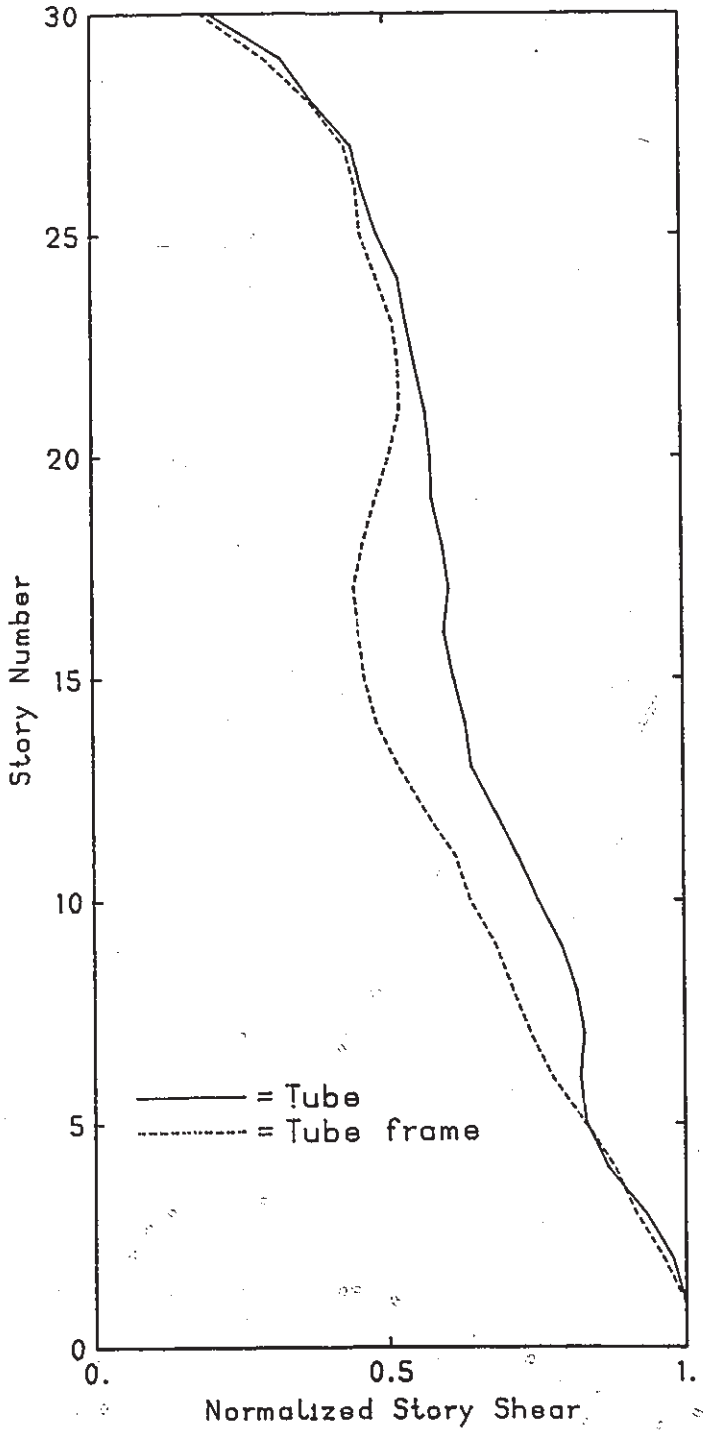

Fig (3.18) Effect of Tube Action on Story Shear Distribution, Elastic

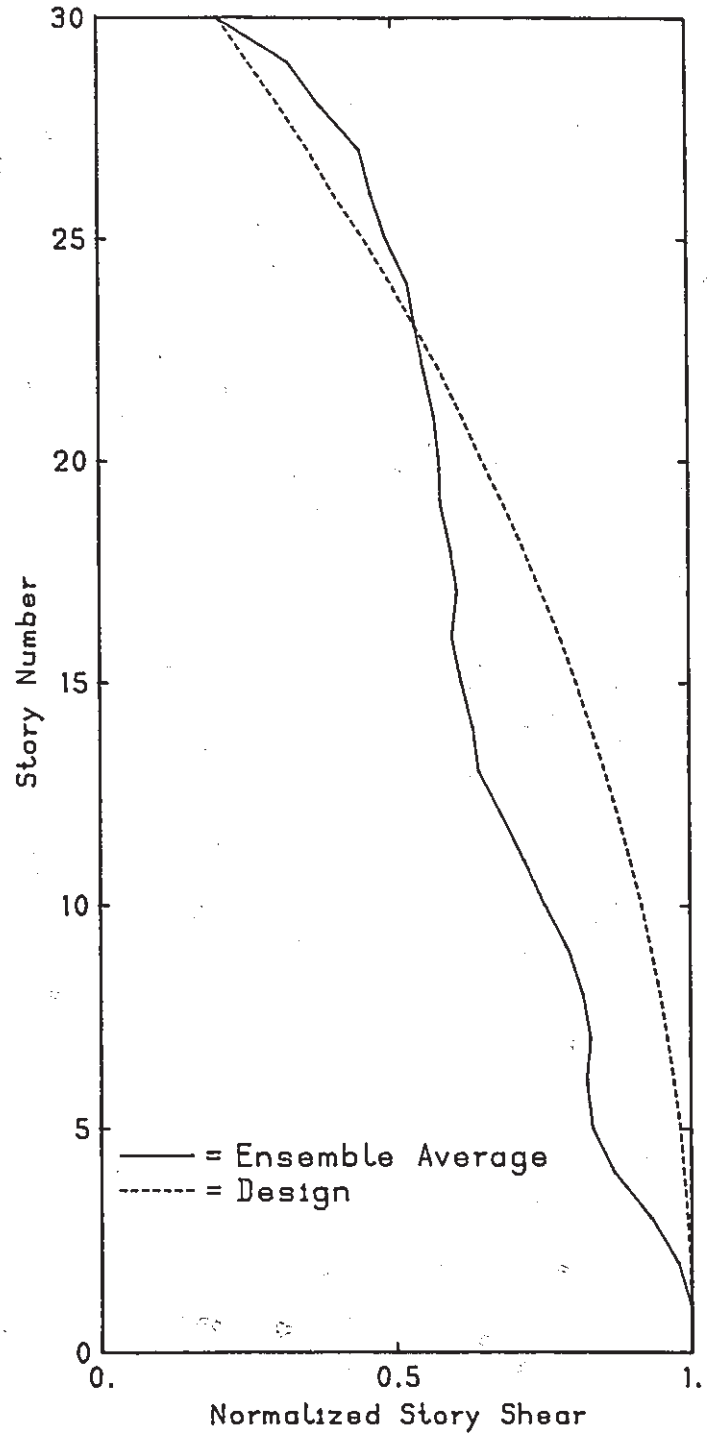

Fig (3.19) Comparison between Design and Average Story Shears

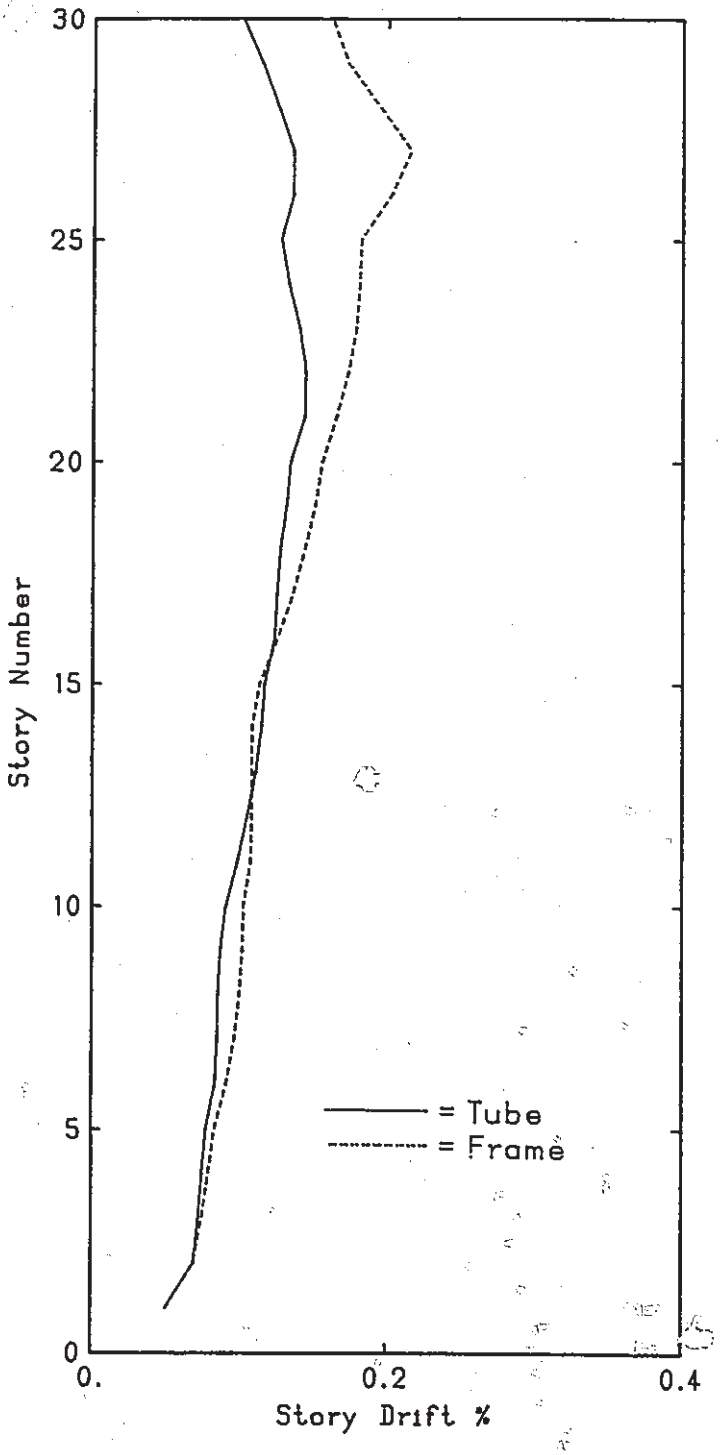

Fig (3.20) Effect of Tube Action on Interstory Drift, Elastic

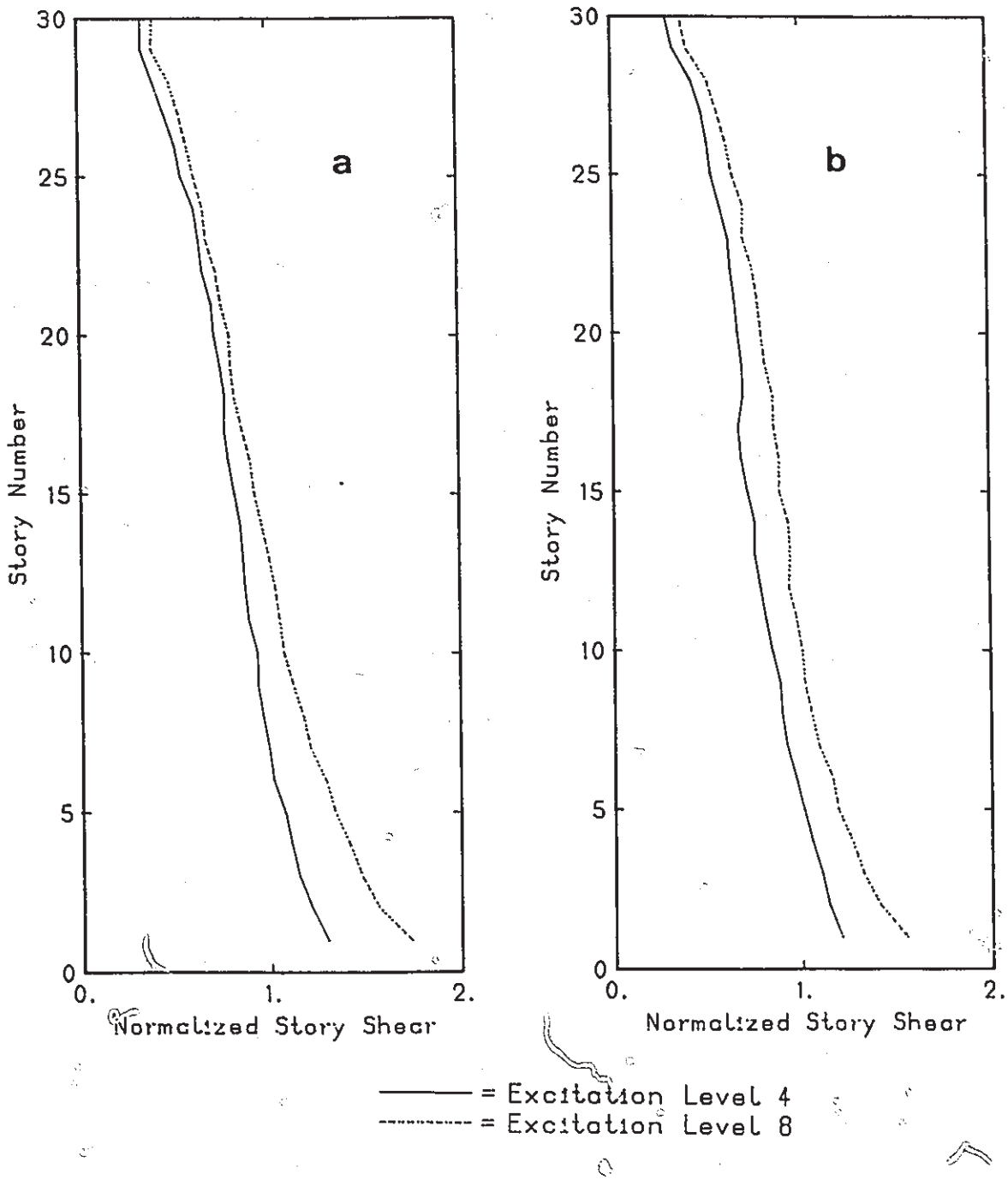

Fig (3.21) Effect of Tube Action on Story Shear, Inelastic Response; a- Frame Tube, b- Frame System

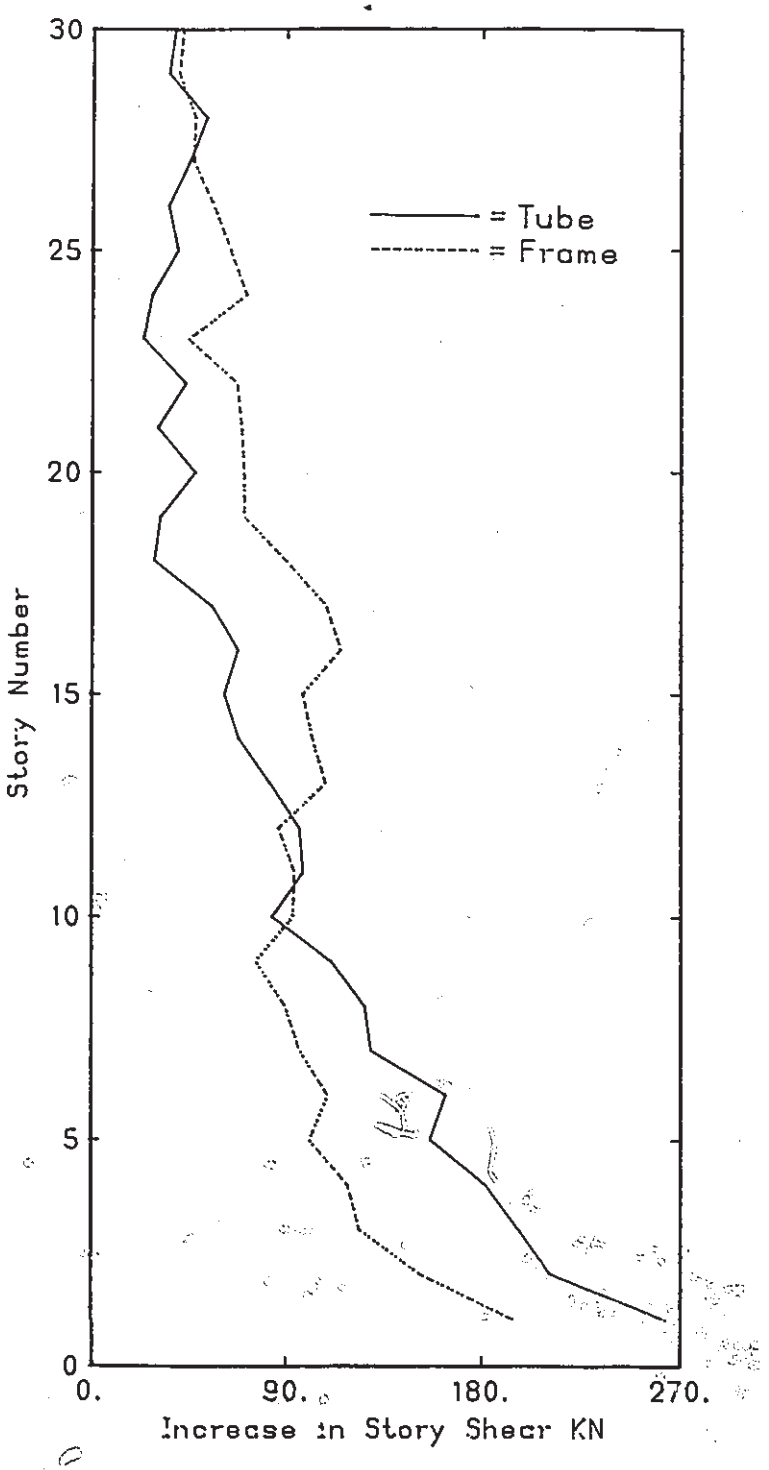

Fig (3.22) Increase in Story Shears from Excitation Level 4 to Excitation Level 8

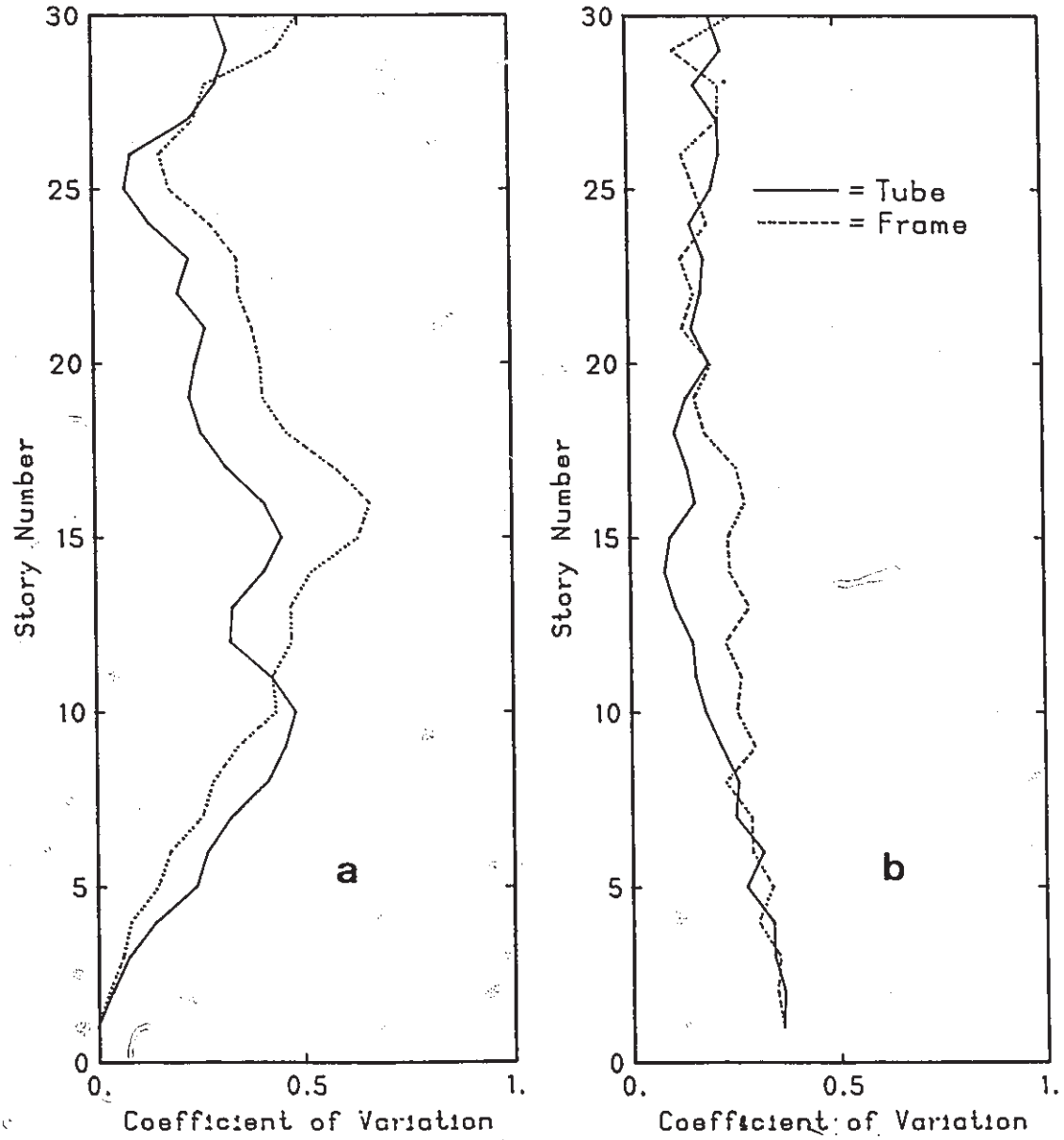

Fig (3.23) Story Shear COV; a- Elastic, b- Inelastic

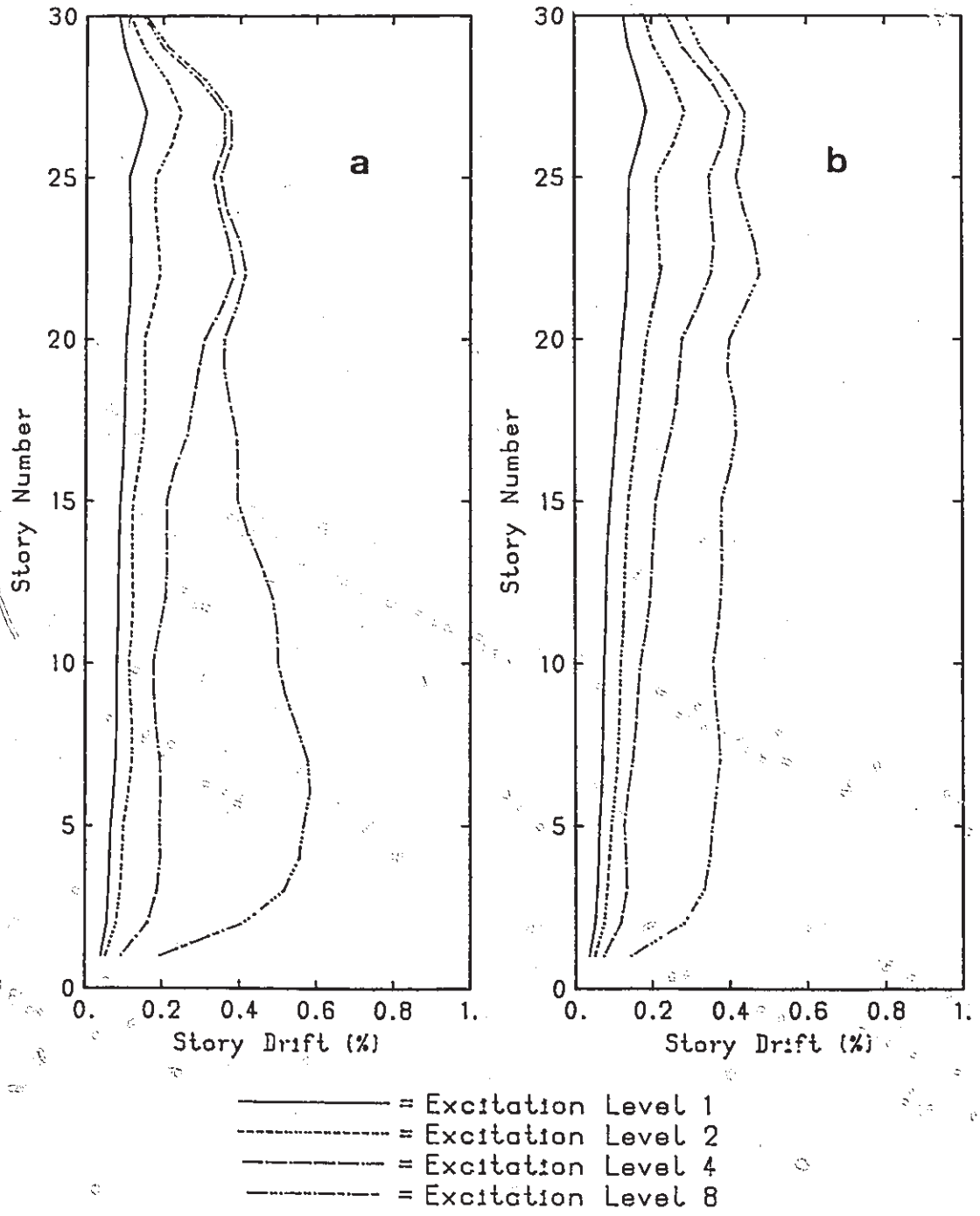

Fig (3.24) Effect of Tube Action on Interstory Drift; a- Frame Tube, b- Frame System

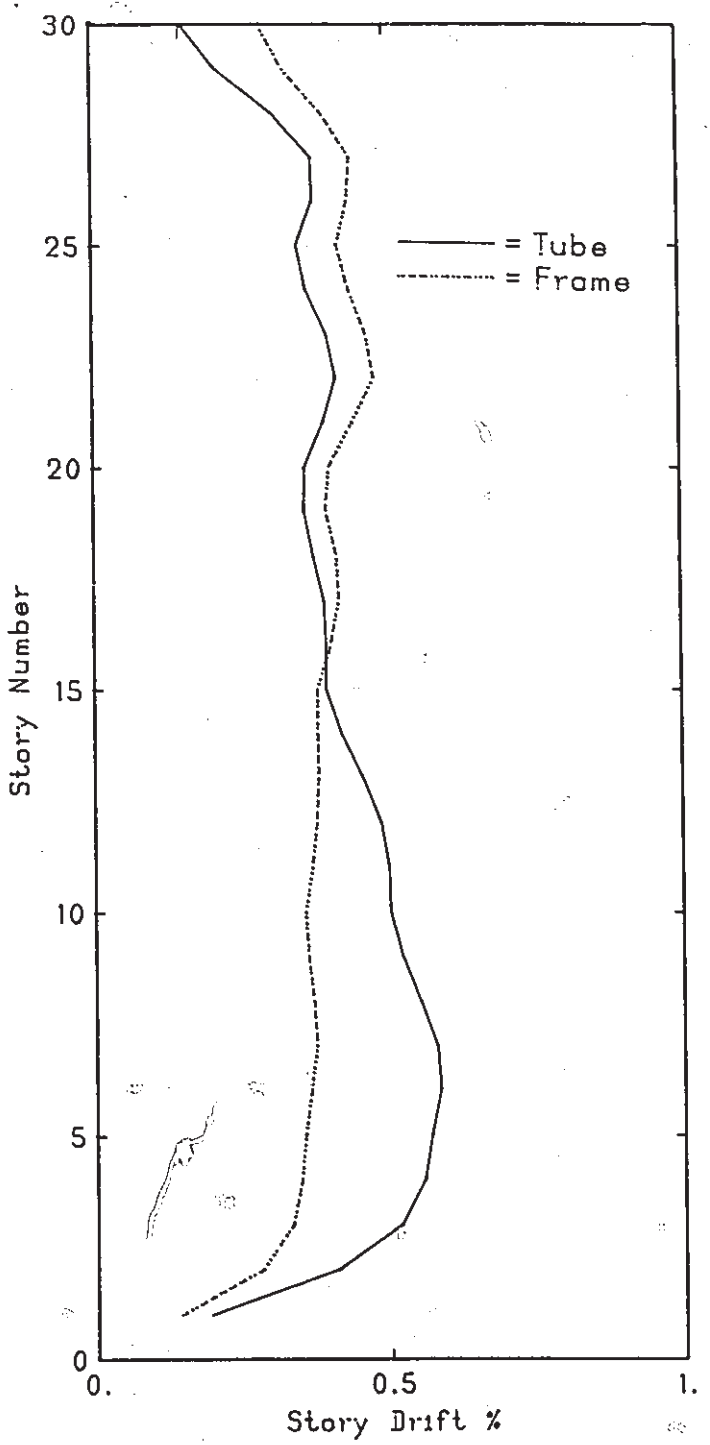

Fig (3.25) Effect of Tube Action on Interstory Drift; Excitation Level 8

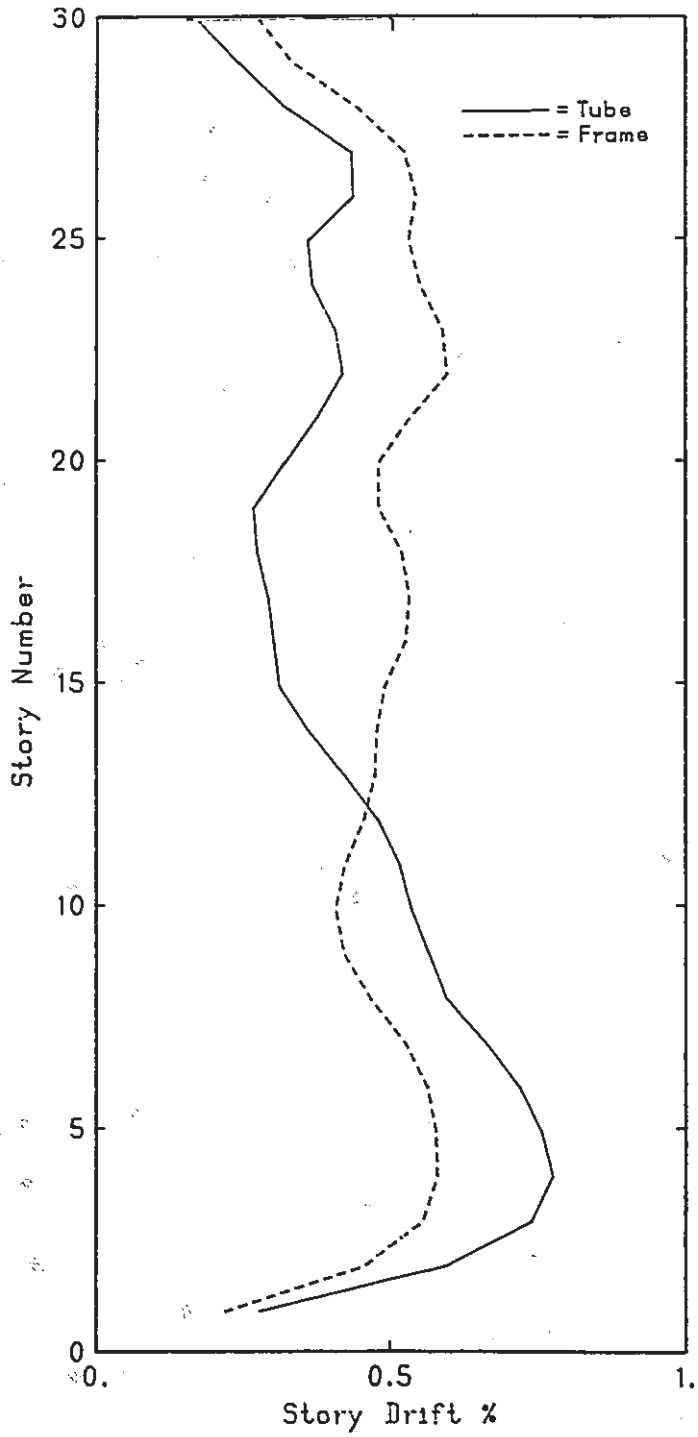

Fig (3.26) Effect of Tube Action on Interstory Drift,
1940 ELCentro N-S Component, Excitation level 8

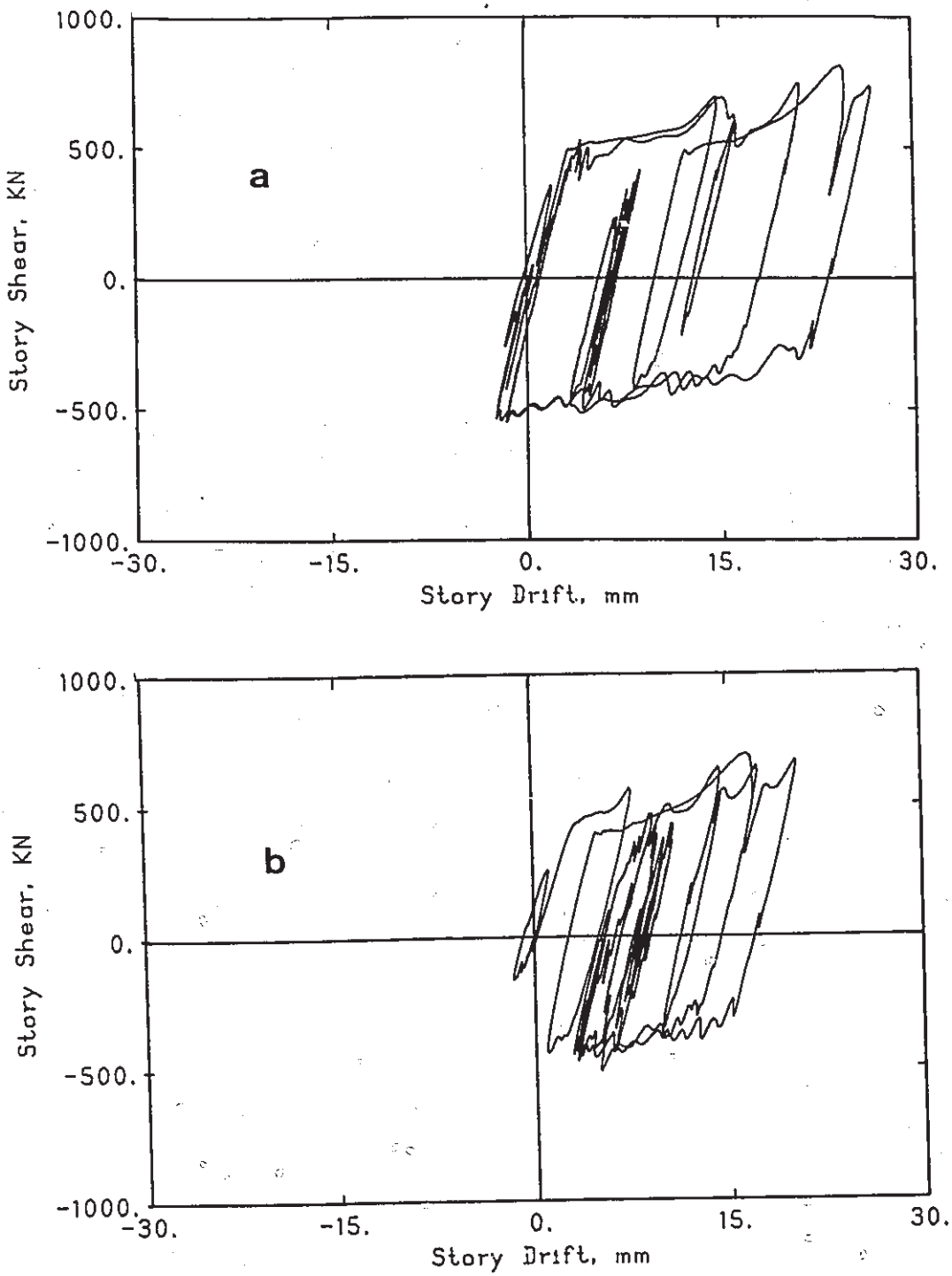

Fig (3.27) Fifth Story Force Deformation Curve;
a- Frame Tube, b- Frame

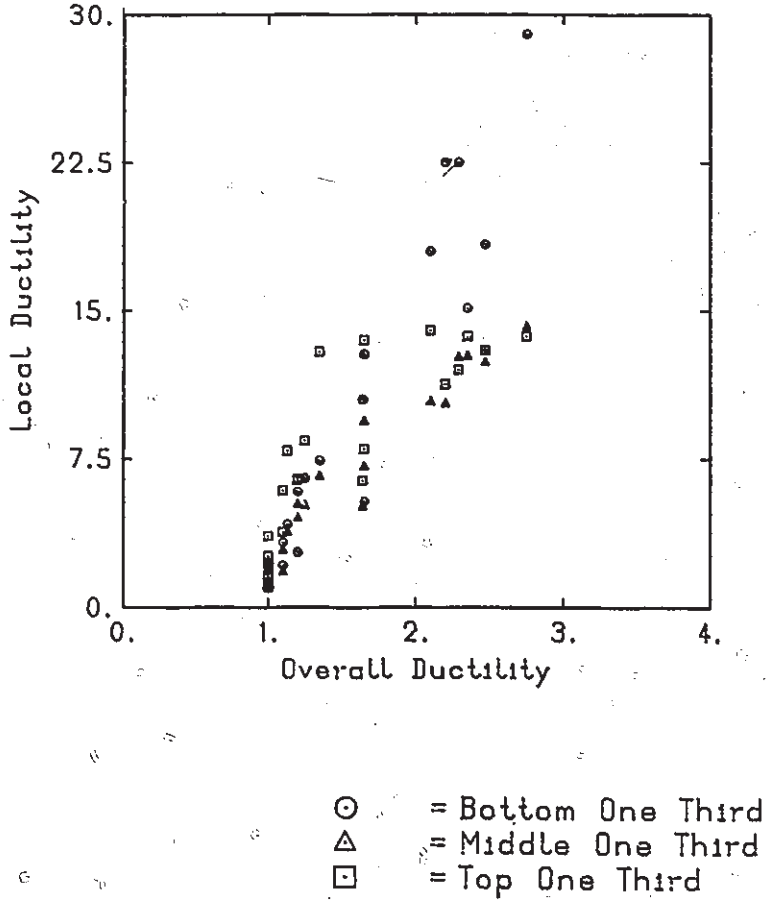

Fig (3.28) Relationship between Overall and Local Ductility

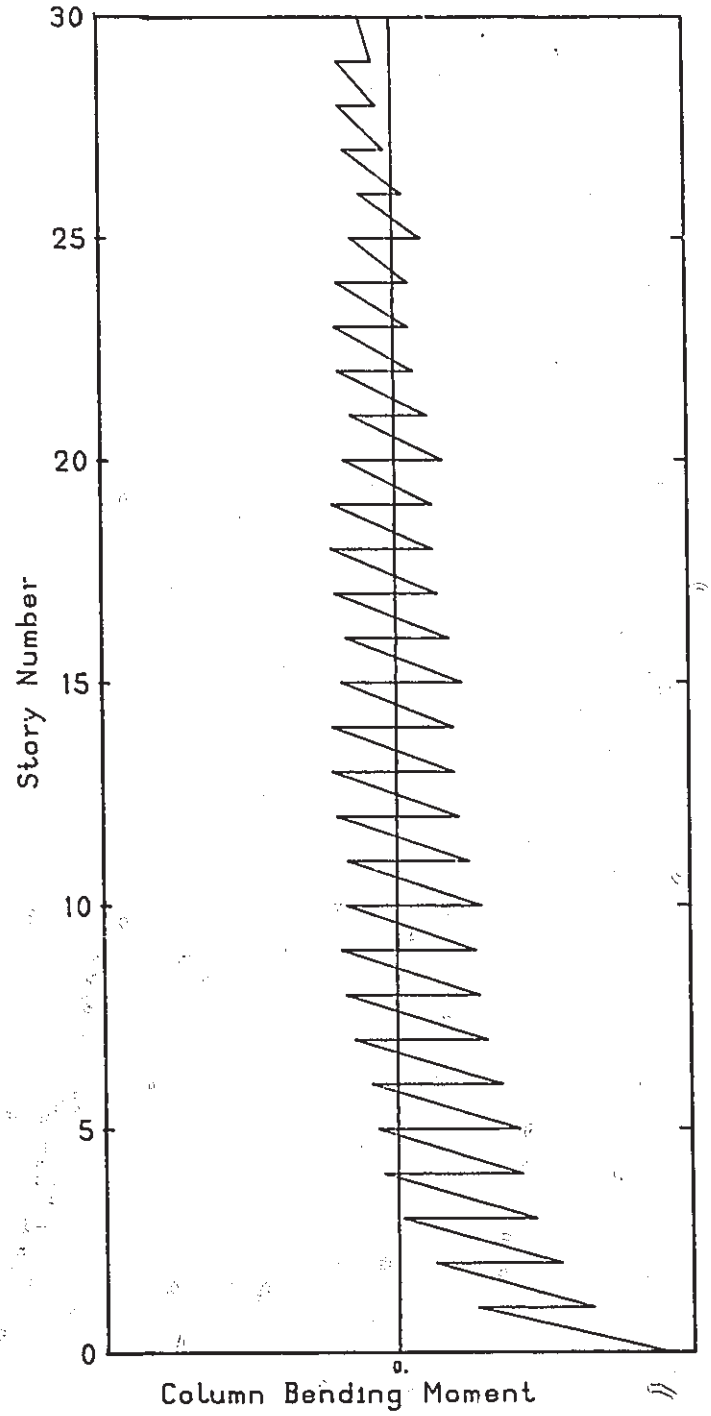

Fig (3.29) Corner Column Moment Diagram; R= 1.5

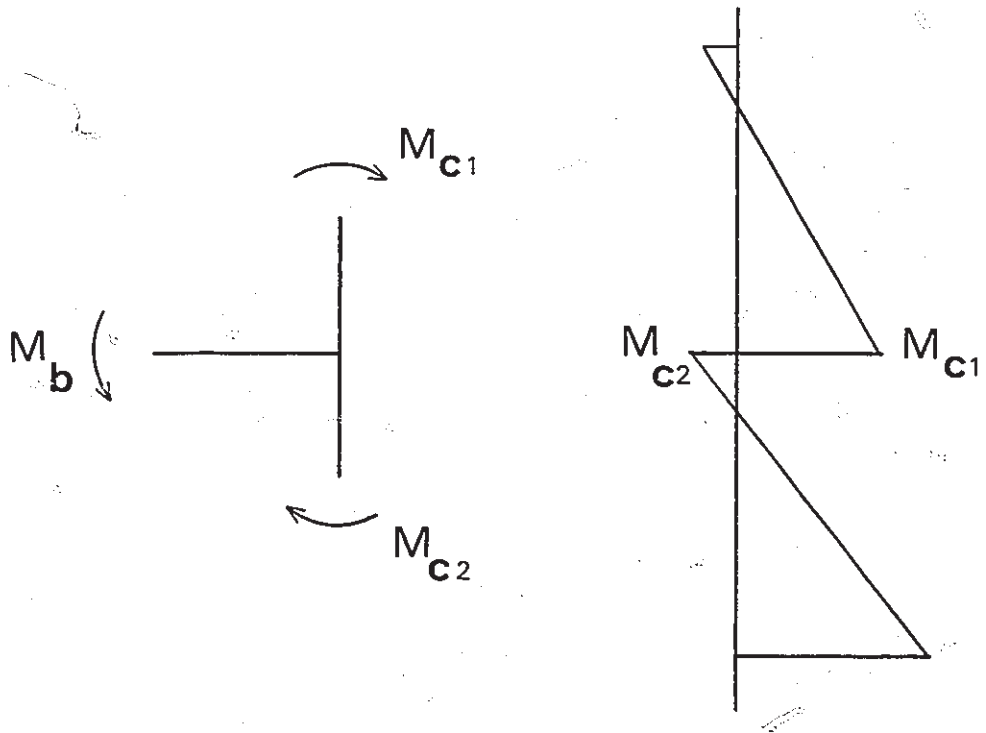

Fig (3.30) Typical Exterior Joint

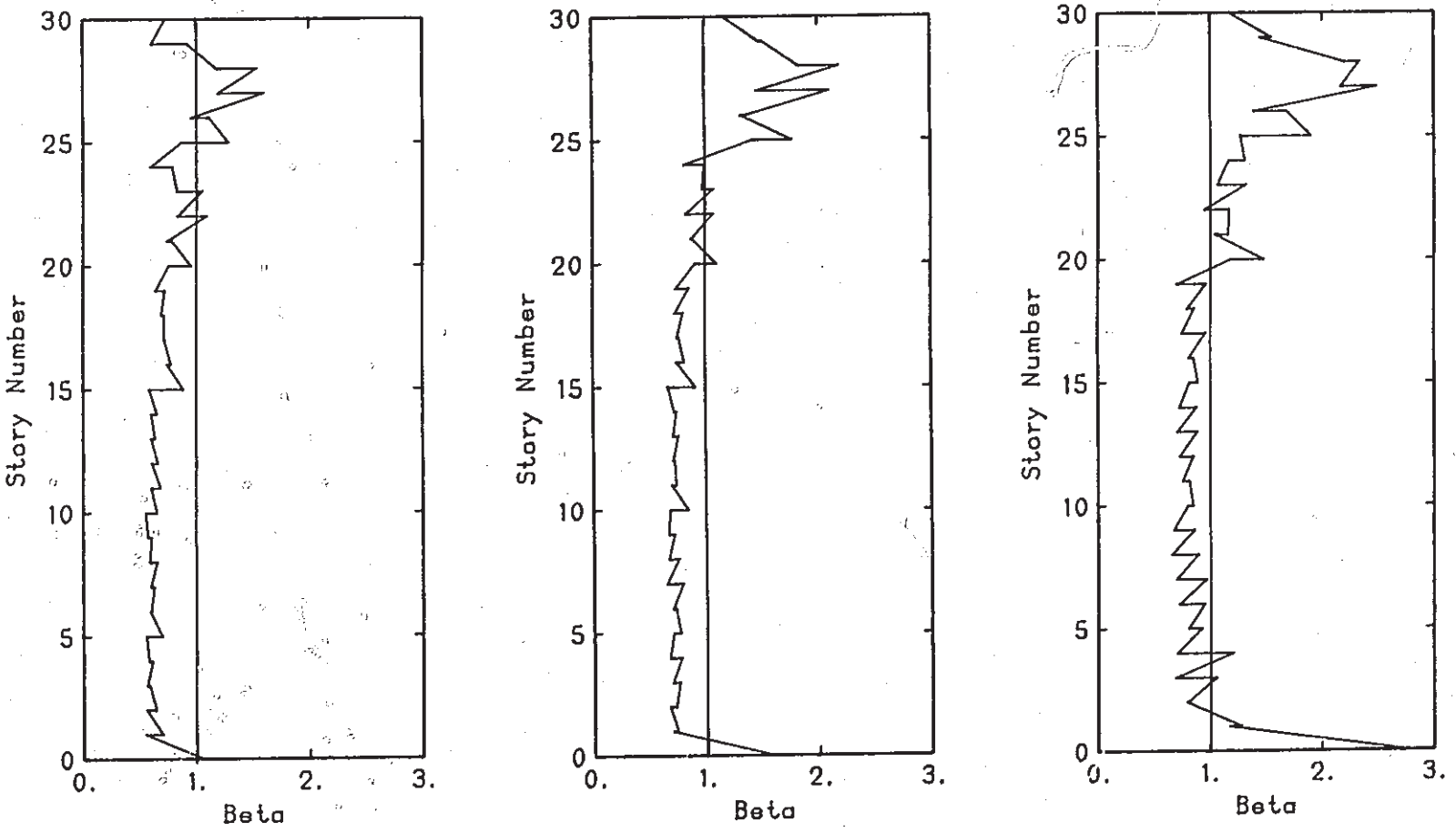

Fig (3.31) Corner Column Flexural Capacity Demand 1940, ELCentro N-S Component

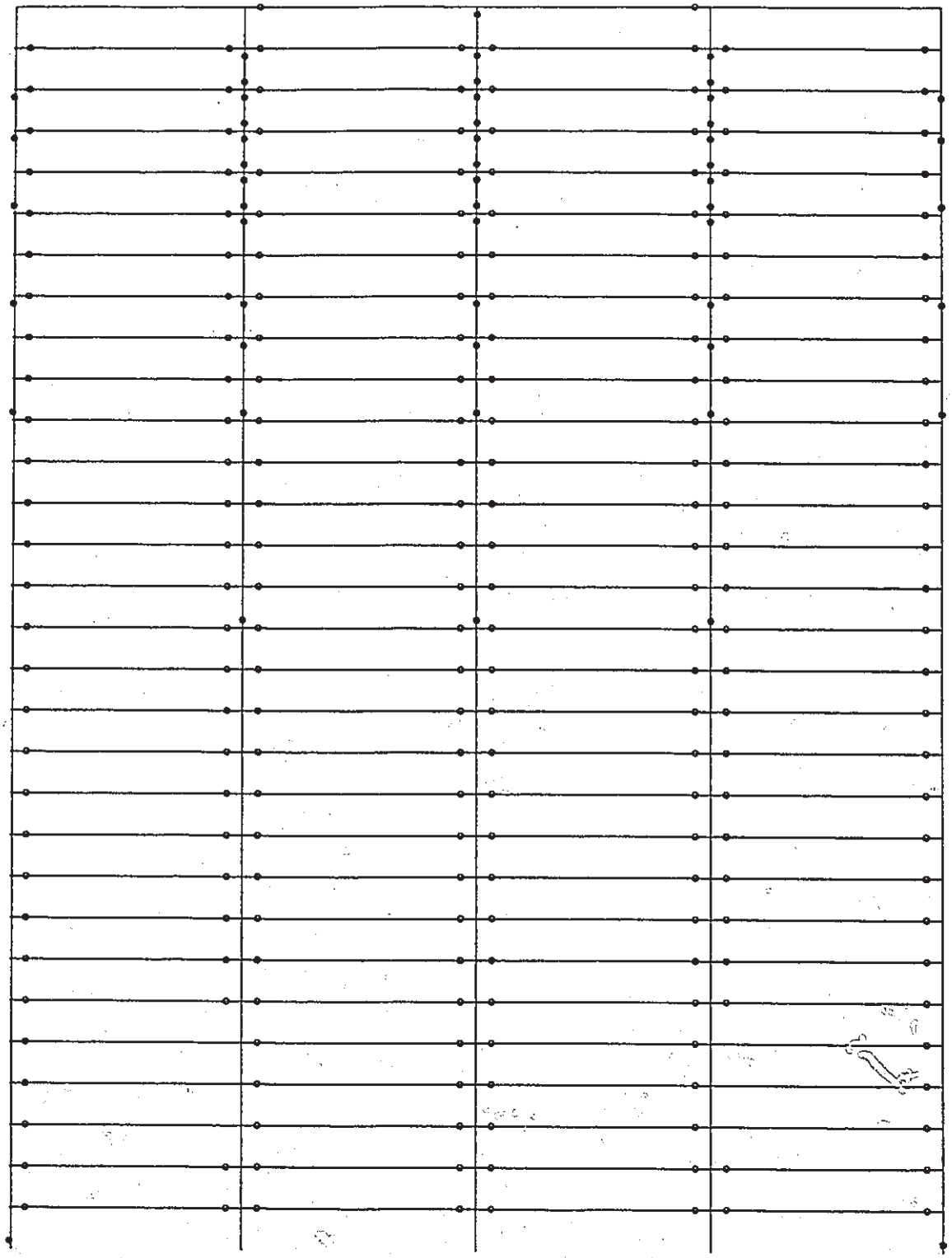

o Hinges in Beams ● Hinges in Columns

Fig (3.32) Distribution of Plastic Hinges Throughout the Longitudinal Frame

CHAPTER FOUR

STATIC AND DYNAMIC ANALYSIS OF FRAME TUBE STRUCTURES WITH UNEQUAL BEAM STRENGTHS AMONG BAYS

4.1 INTRODUCTION

The behavior of frame tube structures discussed in the previous chapter indicate that: (a) Under static lateral loading, the tube action becomes ineffective when the frame tube is loaded into the inelastic range. (b) Under earthquake loading, when the frame tube is excited well into the inelastic range, the bottom stories suffered large interstory drift. A hypothesis was suggested that this large interstory drift was the result that the bottom stories act more like a series of soft stories.

The objectives of this chapter are three folds: First, to provide guidelines on how the tube action of a frame tube structure can be extended beyond first yielding. Second, to lend further credibility to the proposed hypothesis that the large story drifts in the lower stories of the frame tube is due to a small ratio of story stiffness, and finally, to study the dynamic inelastic behavior of the frame tube designed with an enhanced tube action in the inelastic range. For this purpose, the static lateral response of frame tube structures with a modified distribution of beam strengths among bays is initially carried out and the tube action is examined beyond yield. Then, the dynamic inelastic behavior of a frame tube with distributed beam strengths is investigated in detail.

4.2 DESCRIPTION OF THE MODIFIED FRAME TUBE MODELS

To accomplish the objectives stated in the introduction, three frame tube models will be used in this chapter. The first model is the frame tube described in section 3.3 in the

previous chapter. The floor weights, member stiffnesses and beam capacities are summarized in table 4.1. The beam capacities are uniform across the bays. This model will be referred to as the frame tube with uniform beam capacities.

The second model is the same as the first except that the beam capacities in the external bays are increased so that they remain elastic. This model will be referred to as the frame tube with elastic beams in the external bays. Finally, to achieve a balance in the use of material between the first and second model, the third model is taken to be same as the second except that the beams in the internal bays are reduced by a factor alpha. This third model will still have elastic beams in the external bays and will be referred to as the frame tube with distributed beam capacities.

4.3 STATIC INELASTIC ANALYSIS OF THE MODIFIED FRAME TUBE MODELS UNDER LATERAL LOAD

As discussed in the previous chapter, the loss of the tube action beyond yield, when the frame tube is loaded with its design lateral load, is due to yielding of the beams. The yielding of these beams prevented the transferral of forces to the transversal frames under additional applied lateral loading. As a result, no benefit can be obtained from the transversal frames.

One alternative to make use of the transversal frames in frame tube structures is to increase the strength of the beams in the external bays only so that they remain elastic. As a result, any additional applied loading causes the axial force to be developed in the corner column which, in turn, enhances the tube action.

To verify that keeping the beams elastic in the external bays enhances the tube action, the behavior of the frame tube with elastic beams in the external bays and the one with uniform beam strengths are compared. Both structures are loaded with the design lateral load

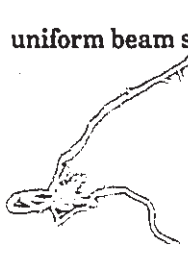

which is increased monotonically. The load ratio R versus the drift at the fifth story is shown in fig. 4.2. The post elastic story stiffness is larger for the frame tube with elastic beams in the external bays than the frame tube with uniform beam strengths. The increase in the post elastic story stiffness, in turn, results in an increase in the ratio of story stiffnesses as shown in table 4.2.

The increase in the post elastic story stiffness is caused by: first, the additional strength provided by the elastic beams in the external bays, and second, the tube action is effective beyond yield. The contribution of the tube action beyond yield is illustrated by comparing the post elastic story stiffness of the frame tube with elastic beams in the external bays with those of the frame structure in which the beams are elastic in the external bays. From table 4.3, the larger post elastic story stiffness of the frame tube with elastic beams in the external bays is caused by the tube action.

A second alternative to enhance the tube action beyond yield is obtained by distributing the beam strengths across the bays so that the inelastic action is restricted to the beams in the internal bays, while the beams in the external bays remain elastic. In this case, the frame tube with distributed beam strengths is used. The beam strengths in the internal bays are reduced by a factor alpha < 1. A reduction factor of 0.5 is selected to illustrate the discussion next. Fig. 4.3 shows the load ratio R versus story drift at the fifth story for the frame tube with distributed beam strengths and for the frame tube with elastic beams in the external bays. The post elastic story stiffness for the two models are the same. Therefore, the tube action should be effective beyond yield using this configuration of beam strength. From fig. 4.3, the elastic limit occurs at $R = 1$ for the frame tube with elastic beams in the external bays and at $R = 0.5$ for the frame tube with distributed beam strengths. For the frame tube with elastic beams in the external bays, first yield occurs in the beams of the internal bays whose capacities are obtained from the design lateral load. By reducing those capacities (frame

tube with distributed beam strengths), the elastic limit would then be reduced proportionally to R = 0.5.

So far, it has been shown that the tube action can be extended beyond yield. However, the distribution of beam strengths between the external and internal bays is still unknown. Specifically, the required capacity that keeps the beams in the external bays elastic, and the appropriate reduction in the beam capacities in the internal bays are not defined. A lengthy calculation presented in Appendix D, shows that a proper distribution of beam capacities can be obtained by reducing the beam capacities in the internal bays by a factor of two, and increasing those in the external bays by two.

4.4 DYNAMIC INELASTIC RESPONSE OF FRAME TUBE STRUCTURES WITH DISTRIBUTED BEAM STRENGTHS

The dynamic inelastic response of frame tube structures with distributed beam strengths is carried out in two parts. First, the verification of the proposed hypothesis is presented, then the dynamic response is investigated in detail.

4.4.1 Hypothesis Verification

As concluded in the previous chapter, the ratio of story stiffness given by

$$\text{R.S.S.} = K_p / K_e \tag{4.1}$$

where K_p, K_e are the post elastic and elastic story stiffness, plays an important role in controlling the dynamic inelastic response of frame tube structures. A hypothesis has been proposed that a small ratio of story stiffness would imply that the bottom stories act as soft stories.

To lend credibility to the proposed hypothesis, the ratio of story stiffness is modified and the effect of this modification on the frame tube behavior is investigated. It was shown in

the previous section that the frame tube with distributed beam strengths possesses a higher ratio of story stiffness. The frame tube with distributed beam strengths (beam capacities in the internal bays are halved, and beam capacities in the external bays are doubled) is subjected to the 1940 ElCentro N-S component corresponding to excitation level eight. The story drift along the height of the frame tube is shown in fig. 4.4. Also, the story drift along the height of the frame tube with uniform beam strengths subjected to the 1940 Elcentro, corresponding to excitation level eight, is plotted in the same figure. The drift is no longer concentrated in the bottom stories, but is distributed more uniformly throughout the height of the structure.

4.4.2 Dynamic Response

The hypothesis being verified, the detailed dynamic response is now examined. The frame tube with distributed beam strengths is considered. The beam capacities in the external bays were increased by two and those in the internal bays are reduced by two. In this analysis, the columns are no longer assumed elastic. The interior column flexural capacities are derived from

$$\sum_{i=1}^{2} M_{ci} = 1.4 \sum_{j=1}^{2} M_{bj} \tag{4.2}$$

The corner column fexural capacities are set equal to the adjoining beam capacities for the first twenty five stories and twice the adjoining beam capacities for the top five stories. A greater factor of safety against corner column hinging is expected in this frame tube with distributed beam capacities.

The purpose of this section is to implement all the above modifications and to carry out the dynamic response of such structure. The response parameters of interest are the local ductility and yielding of the corner column. The ground motion used corresponds to the 1940 ElCentro N-S component with excitation level four.

The rotational ductility throughout the longitudinal frame is shown in fig. 4.5. From this figure, the followings can be observed: (1) the inelastic action is restricted to the internal bays with very few hinges occuring in the external bays in the top five stories. As a result, this observation verifies the proposed method to distribute the beam capacities across the bays so that the inelastic action is restricted to the internal beams. (2) The corner column did not show any yielding throughout its height. This would also verify the proposed estimate of the corner column flexural capacity to avoid yield. (3) The rotational ductility in the internal bays ranges from a value of six up to a value of twenty five. However, what is interesting to note is that the rotational ductility has its lowest value at the first floor, and then increases monotonically as we move upward along the height of the structure. The consequences of this observation is that maximum rotations occur near the top of the structure. To further discuss this observation, a comparison is carried out between the rotational ductility of the frame tube under consideration with the frame tube with uniform beam capacities across the bays.

The rotational ductility throughout the longitudinal frame of the frame tube with uniform beam strengths is shown in fig. 4.6. The rotational ductility is almost uniform along the height of the structure. From the comparison of fig. 4.5 and fig.4.6, the frame tube with distributed beam strengths exhibits a different behavior from the frame tube with uniform beam capacities. Due to the distribution of beam strength across the bays so that the inelastic action is restricted to the internal bays, the frame tube behaved like a coupled shear wall where the walls are represented by the exterior elastic bays coupled by the weaker beams in the interior bays.

One final observation concerning the ductility demand of the frame tube with distributed beam strengths, it is apparent that the ductility demand for this frame tube is much higher than the ductility demand in the frame tube with uniform beam strengths. The high

ductility demand is due to (a) the distribution of beam strengths across the bays, and (b) the reduction of the internal beam capacities by a factor of two. The latter has the effect of reducing the yield rotations by a factor of two which leads to doubling the ductility ratio.

4.5 CONCLUSIONS

The static and dynamic lateral response of frame tube structures with distributed beam strengths are examined in this chapter. The main objective of this study is to enhance the tube action beyond yield, and to improve the dynamic inelastic response. Based on the results and discussion presented in the chapter, the following conclusions can be drawn:

A. Static

(1) Keeping the beams in the external bays elastic enhances the tube action beyond the elastic limit. As a consequence, it also increases the ratio of story stiffness.

(2) Distributing the beam strengths across the internal and external bays, so that the inelastic action is restricted to the internal bays while the external bays remain elastic, also enhances the tube action beyond the elastic limit.

B. Dynamic

(1) The hypothesis that is proposed in the previous chapter is verified in this chapter. By increasing the ratio of story stiffness, the interstory drift is no longer concentrated in the bottom stories but it is more evenly distributed throughout the height of the frame tube. The increase of the ratio of story stiffness is achieved by reducing the beam strengths by a factor of two in the internal bays, and doubling those in the external bays in this study.

(2) The improved inelastic dynamic behavior of the frame tube with distributed beam strengths is attributed to the continued effectiveness of the tube action.

(3) The dynamic response of the frame tube with distributed beam strengths, indicates that the rotational ductility is restricted to the interior bays, and increases monotonically along the height of the frame tube. The behavior of such frame tube resembles the behavior of a coupled shear wall, where the exterior elastic bays behave like shear walls coupled by the weak beams in the interior bays.

(4) The rotational ductility demand of the frame tube with distributed beam strengths is higher than that for the frame tube with uniform beam strengths.

Story No	Beam Inertia $cm^4\ 10^6$	Column Inertia $cm^4\ 10^6$	Column Area $cm^2\ 10^2$	Beam Capacity KN-m	Floor Weight KN
1-5	1.69	1.27	26.3	270	691
6-10	1.53	1.14	23.7	239	691
11-15	1.36	1.02	21.1	212.4	691
16-20	1.19	.891	18.4	176.5	691
21-25	1.02	.736	15.8	129	691
26-30	.848	.636	13.3	66	691

Modulus of Elasticity E = 30500 MPa

Table 4.1 Member Properties and Story Weights for the Frame Tube.

Story No	Ratio of Story Stiffness	
	Uniform Beam Capacities	Distributed Beam Capacities
1	.0708	.302
5	.029	.142
11	.034	.12

Table 4.2 Ratio of Story Stiffness, Frame Tube.

Story No	Post Elastic Story Stiffness with distributed beam strengths Frame Tube KN/m	Frame KN/m
1	152002	140269
5	35199	28859
11	18387	14359

Table 4.3 Comparison of Post Elastic Story Stiffness for Frame Tube and Frame

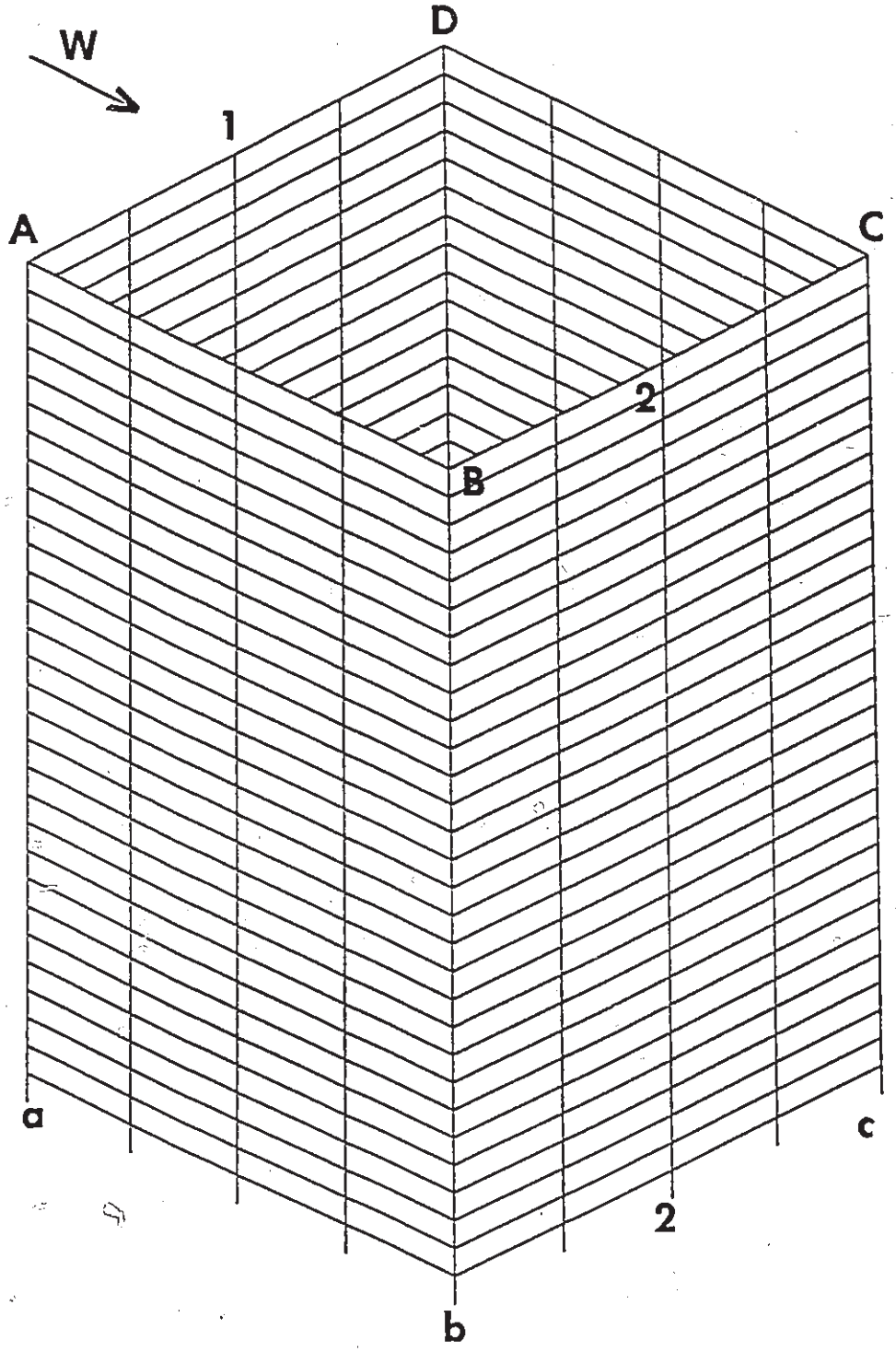

Fig (4.1) Frame Tube Structure

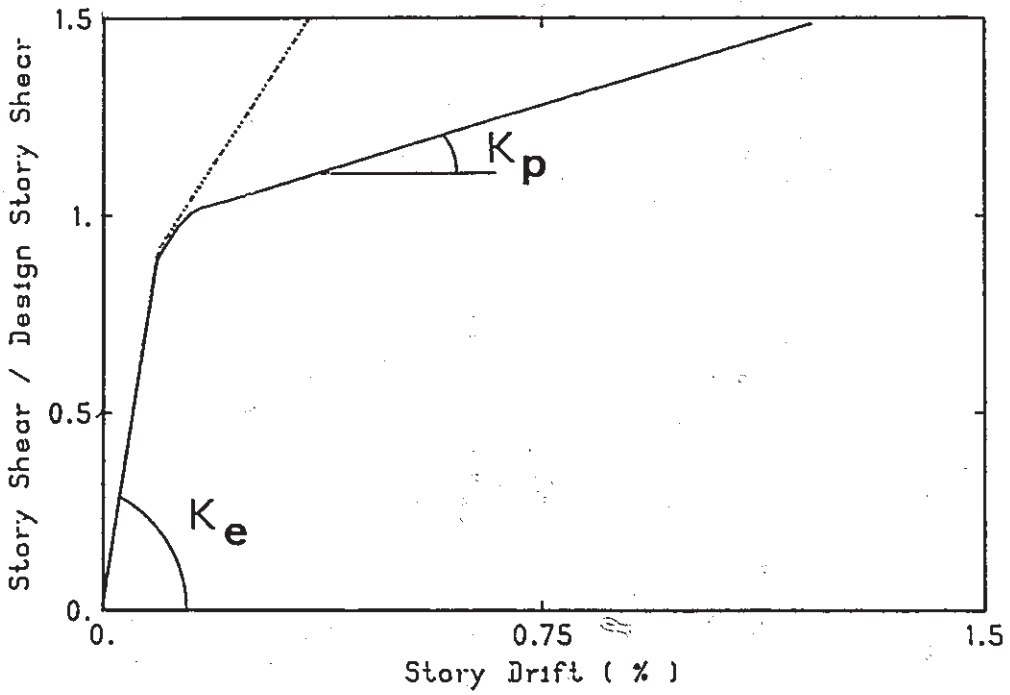

——— = Tube with uniform beam strengths
- - - - - - - - - - = Tube with distributed beam strengths

Fig (4.2) Load Deformation Curve for Frame Tube
Having Uniform and Distributed Beam Strength

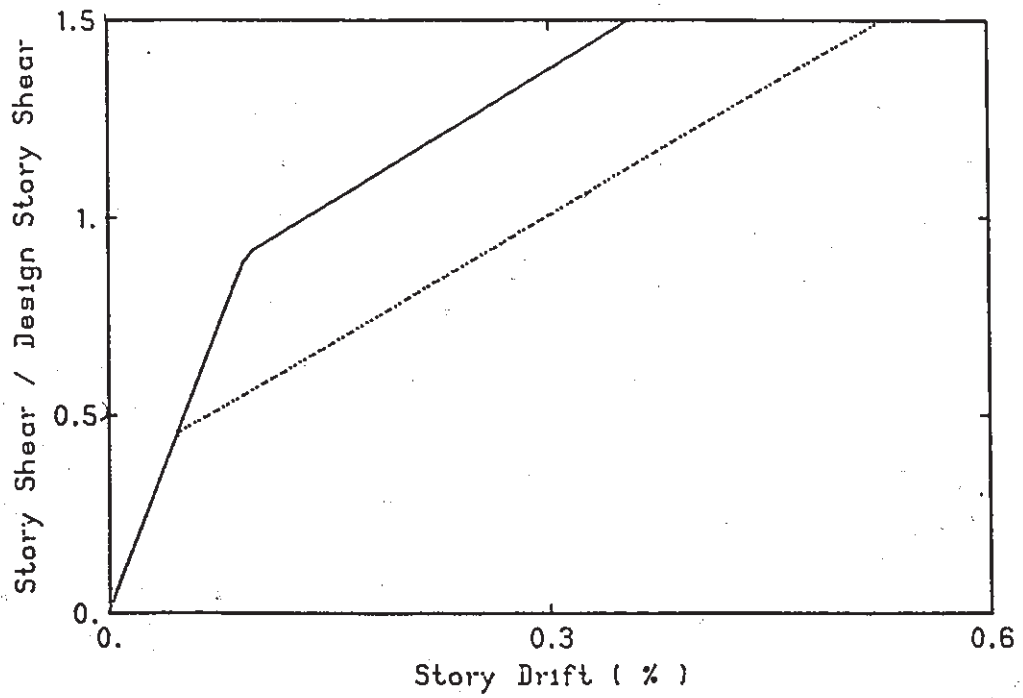

Fig (4.3) Load Deformation Curve for Frame Tube having Elastic Beams in the External Bays and Uniform Beam Strength

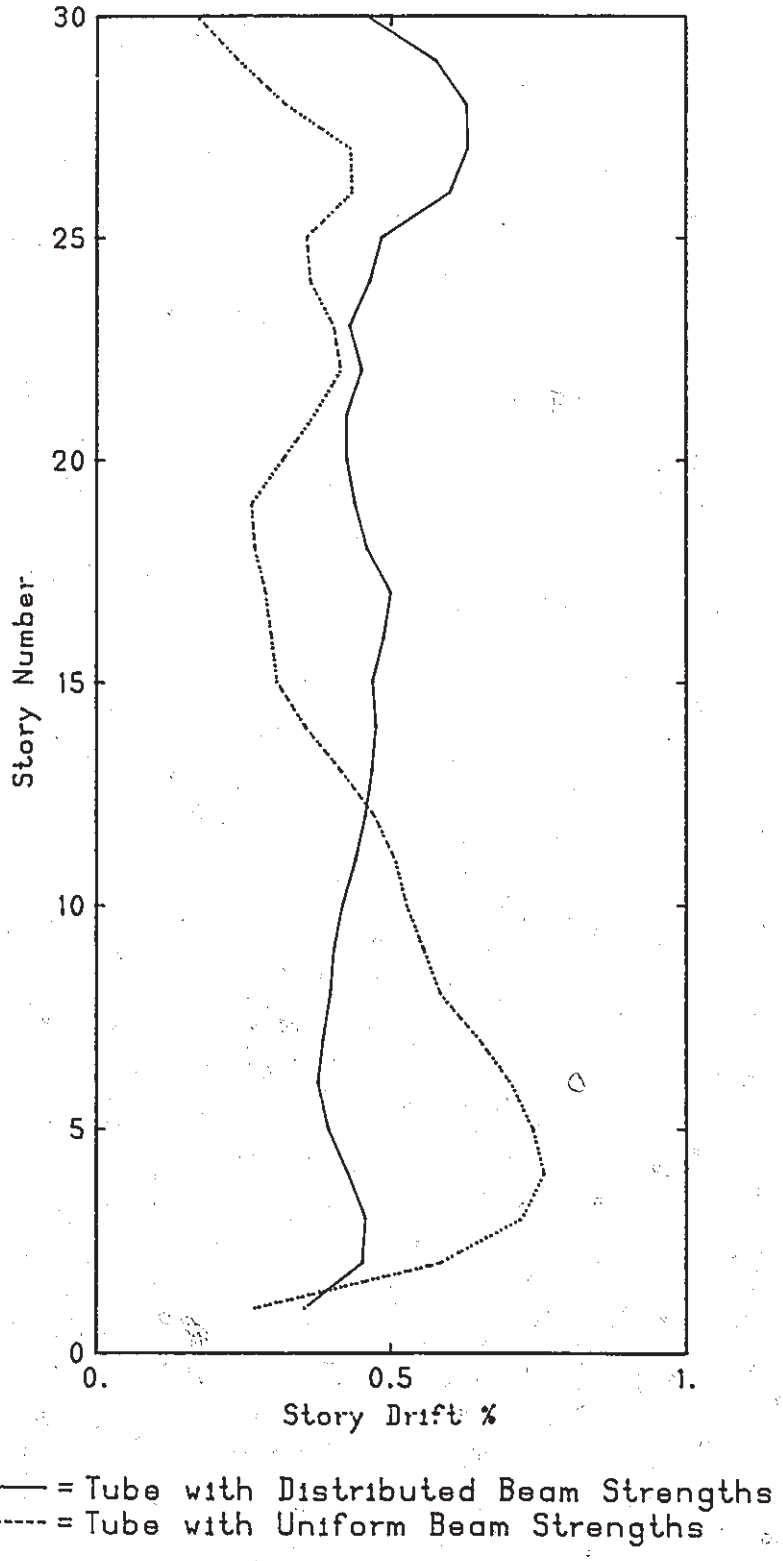

Fig (4.4) Effect of the Ratio of Story Stiffness on the Dynamic Inelastic Behavior of the Frame Tube

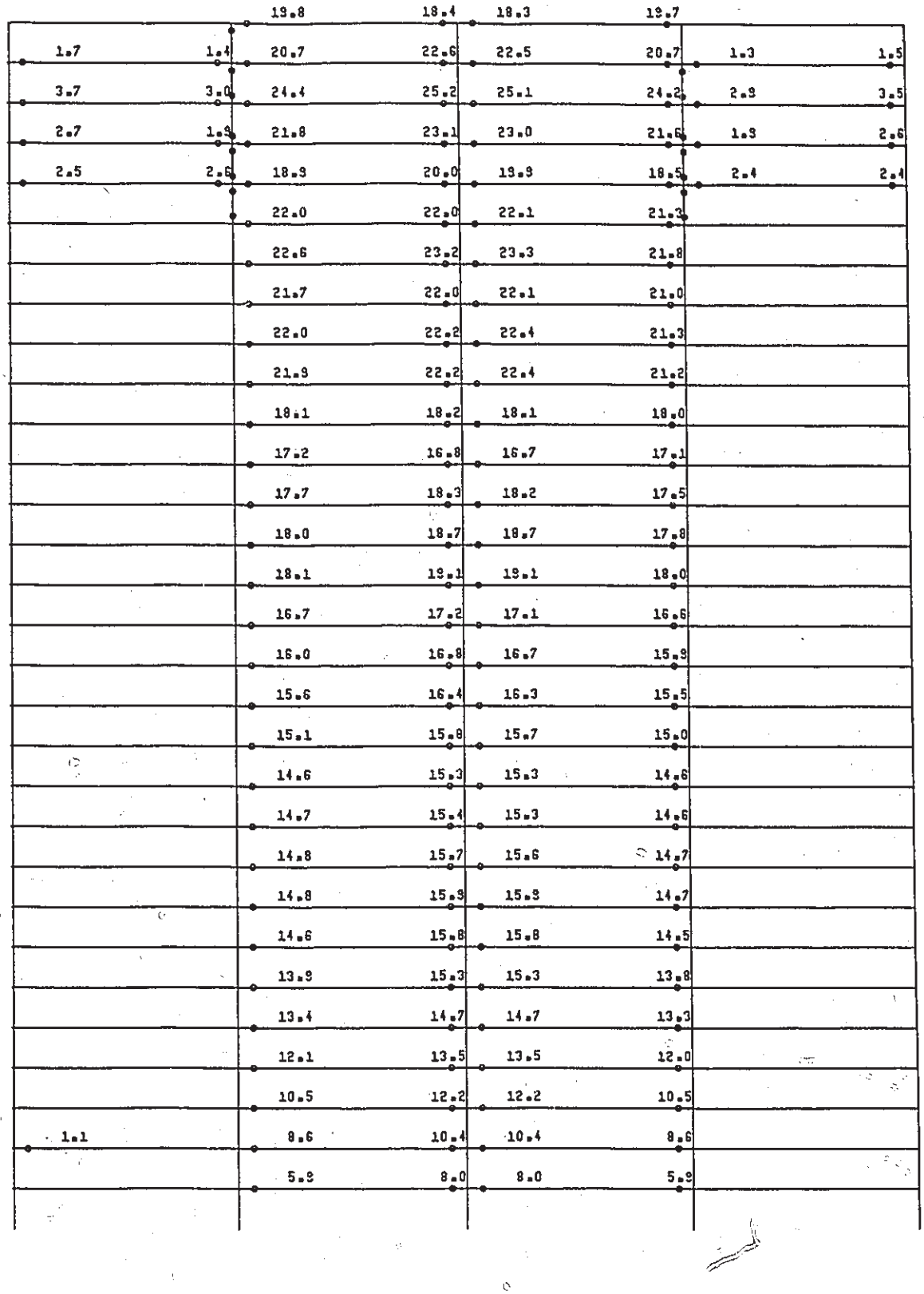

Fig (4.5) Rotational Ductility for Frame Tube with Distributed Beam Strength

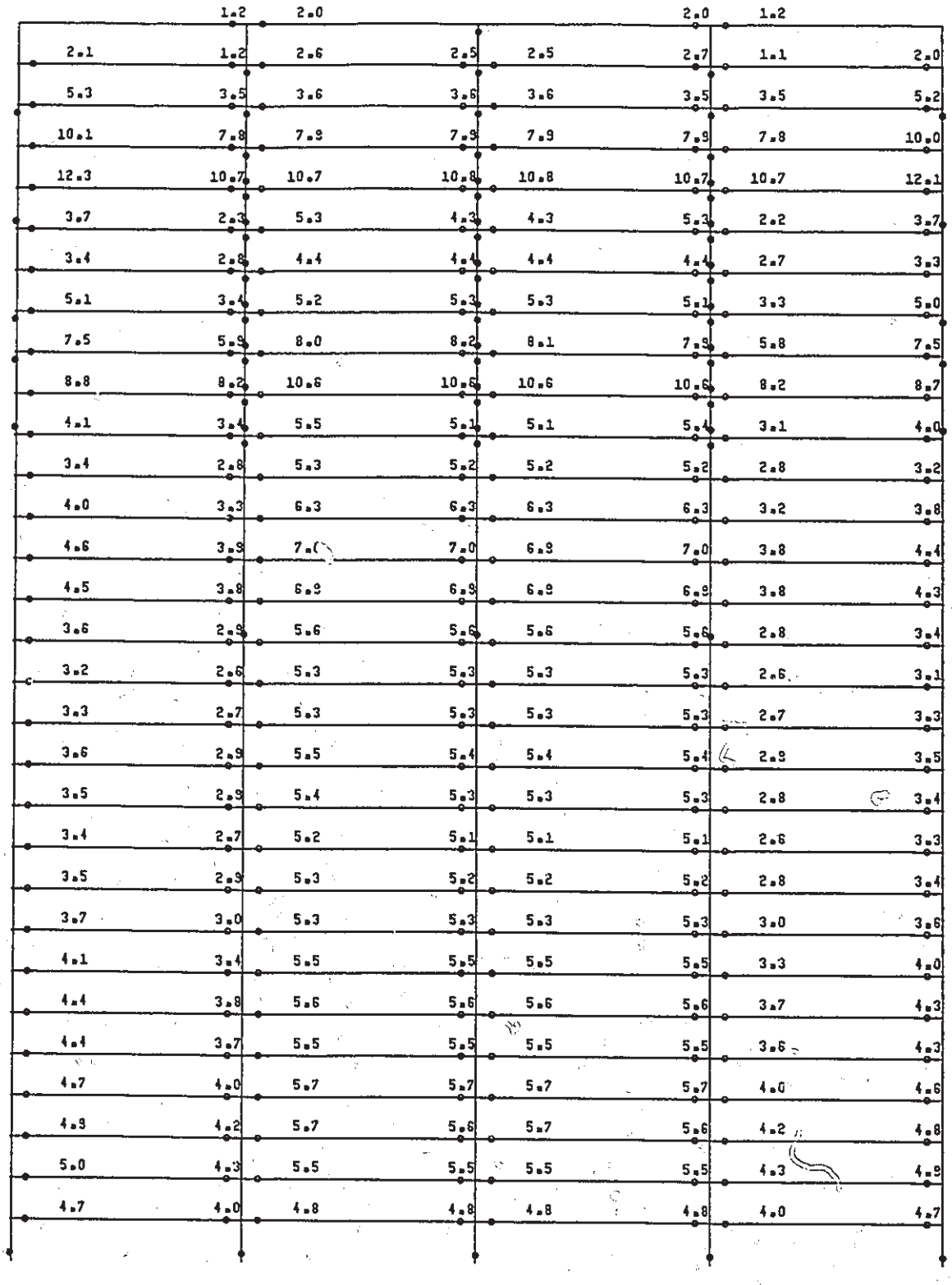

Fig (4.6) Rotational Ductility for Frame Tube with Uniform Beam Strength

CHAPTER FIVE

STATIC RESPONSE UNDER LATERAL LOAD IN AN ARBITRARY ORIENTATION AND DYNAMIC BIDIRECTIONAL RESPONSE OF FRAME TUBE STRUCTURES

5.1 INTRODUCTION

In a frame-tube structure, due to the tube action, ground motions in one direction will induce forces and moments in the frames that are perpendicular to the ground motion direction. However, design codes suggest that for any given three dimensional structure subjected to multiple components of earthquake ground motions, one can analyze the structure by considering planar responses of the structure, assuming the ground motions to occur at one direction at a time. These planar responses are then combined to give the final response estimate for design purposes. This procedure is based on the superposition principle which is valid only in the elastic range of behavior. However, due to its simplicity, this procedure is often used in design, even the structures are expected to yield during the earthquake.

The consequences of applying the design code analysis procedure to frame tube structures excited by ground motions beyond the elastic limit are examined in this chapter. First, the static inelastic response of frame tube structures under lateral loadings in an arbitrary orientation is presented. Then, the dynamic inelastic bidirectional response is investigated. Approximate methods to estimate the radial displacement and corner column axial force are discussed. It is shown that combining the two planar responses according to current practice underestimates the response. A more realistic combination scheme is suggested for frame tube structures.

5.2 DESCRIPTION OF THE ANALYTICAL MODEL

A thirty story frame tube with four bays on each side is selected as a representative frame tube for the present study (fig. 5.1). The bay width is 3 m in frame panels AabB & CcdD and 2.2 m in frame panels BbcC & AadD. This frame tube is similar to the one analyzed in chapter three, except that the bay width in frame panels AabB & CcdD is reduced to 2.2 m so that the frame tube is rectangular in plan and has unequal periods in the two principal directions. The member stiffnesses and story weights of this frame tube are summarized in table 5.1.

A plan view of the frame tube is shown in fig. 5.2. The frame panels with the longer dimension are considered to be parallel to the X axis. The fundamental periods in the X and Y directions are found to be $T_x = 2.5$ and $T_y = 3.43$ sec. The design base shear in the X and Y directions are computed according to,

$$V = vSKIFW \tag{5.1}$$

where, $v = .4$, $S = .22/\sqrt{T}$, T is the fundamental period, based on the fundamental periods in the X and Y directions, respectively, $K = .7$, $I = 1$, $F = 1$, and $W = 20736$ KN. The base shears are 808 KN and 690 KN in the X and Y directions, respectively. The design lateral load distribution is obtained according to the distribution suggested by the NBCC 1985. To obtain the yield capacities of the beams in the frames that are parallel to the X axis, the frame tube is loaded in the X direction with the design lateral load in the X direction. The beam capacities, grouped over intervals of five stories, are set to the largest beam moment in each interval. Similarly, the beam capacities in the frames parallel to the Y axis are obtained by loading the frame tube in the Y direction, with the design lateral load in the Y direction. To be consistent with the limit state design, the design loads (base shear and lateral forces) are factored by 1.5 and, accordingly, the beam capacities are increased by 1.5. The interior columns flexural capacities are derived from the relation

$$M_{yc} = 1.4\, M_{yb} \qquad (5.2)$$

where M_{yb} is the beam capacity. The corner column flexural capacities are set equal to the larger of the adjoining beam capacity. The axial capacity of the columns are assigned a large value so that axial yielding of the columns does not occur. An elaborate discussion on the axial capacity of the columns is presented later in this chapter. The member capacities are summarized in table 5.2. The effect of gravity loads is ignored in this analysis.

5.3 STATIC INELASTIC RESPONSE OF FRAME TUBE STRUCTURES UNDER LATERAL LOADING IN AN ARBITRARY ORIENTATION

The loading P_{0xy} consists of the design lateral load in the X direction applied at an angle θ from the principal structural axis. The load is decomposed into two components P_{0x} and P_{0y}, acting along each of the principal structural axis, as shown in fig. 5.2. In the elastic range, the answer can be obtained by analysing the structure under the action of one component at a time, then superposing the planar responses. Due to its simplicity, however, it became a common practice to use such a technique even when the behavior is in the inelastic range. It is the purpose of this section to examine such superposition procedure for the inelastic response of frame tube structures subjected to static lateral loading.

Three values of the angle of orientation of the lateral load are considered, namely, $\theta = 30$, 45 and 60 degrees. For each value of θ, three loading cases are carried out; first, considering the response under the simultaneous action of the two components, or loading P_{xy}. The response quantity associated with this case will be denoted by r_{xy}. Second, considering the response under the action of loading one component at a time. The response quantity is denoted by r_x or r_y, depending whether the load component is acting along the X or Y direction. In each case, the load is increased monotonically forcing the frame tube to respond beyond its elastic limit. For the case where the two components are considered simultaneously, the load is

increased bearing the same proportion between the two components. The response parameters of interest in this analysis are the radial displacement and the corner column axial force.

5.3.1 Radial Displacement

Let R be the ratio of the total applied load P_{xy}, and the design load P_{0xy}. R is also the ratio of the total applied load P_x and the total load P_{0x}, or the ratio of the total applied load P_y, and the total load P_{0y}, when considering the response under the action of one component at a time. A plot of R versus the normalized radial roof displacement is shown in fig. 5.3 for the three loading cases when $\theta = 45$ degrees. The normalizing factor for the radial displacement is the total height of the structure. For the planar responses under P_x or P_y, the radial displacement is the same as the displacement in the direction of the load.

To apply the superposition principle, the radial displacement is obtained from the two planar responses according to

$$d_r = \sqrt{d_x^2 + d_y^2} \tag{5.3}$$

where d_x is the roof displacement when the structure is subjected to P_x only, and d_y is the roof displacement when the structure is subjected to P_y only. d_r, computed from equation 5.3, is also plotted in fig. 5.3 and corresponds to the curve labeled 'Estimated'. By comparing the estimated radial displacement with the one corresponding to the response under the simultaneous action of the two components (exact value), it is clear that: (1) In the elastic range of behavior, the two curves coincide with each other verifying the superposition principle, and (2) in the inelastic range, the estimated radial displacement is smaller than the exact value. Therefore, one concludes that the superposition principle resulted in an unconservative radial displacement when the behavior is in the inelastic range.

Inspection of the load-displacement curves for the three loading cases shown in fig. 5.3, indicates that the elastic limit for the two planar responses is higher than that of the exact

response. As an example, for an R value of 1.1, the two planar responses are elastic, while the exact response shows yielding has occured in the structure. Therefore, the structure posseses more strength in the planar response cases. This reserved strength, in turn, resulted in underestimating the exact radial displacement.

To consider angles of orientations of the lateral load other than 45 degrees from the structural principal axes, the ratios of the estimated and exact radial displacement for $\theta = 30$ and 60 degrees are shown in fig. 5.4. For $\theta = 0$ or 90 degrees, the lateral load coincides with the structural principal axis. Hence, the exact and planar responses are the same. For $\theta = 30$ and 60, the estimated radial displacements are also smaller than the exact value, but the underestimation is not as large as when $\theta = 45$ degrees.

5.3.2 Corner Column Axial Force

One of the most important design quantity for frame tube structures is the corner column axial force. The interaction between the longitudinal and transversal frames takes place at the corner column undergoing axial deformation. If the design axial force is underestimated, the corner column would yield axially and this may lead to the collapse of the structure. One procedure to estimate the corner column axial force from the two planar responses is

$$F = F_x + F_y \tag{5.4}$$

where, F_x and F_y are the corner column axial force corresponding to the loading component in the X and Y directions, respectively. For corner column C, the ratio of F/F_{xy} where, F_{xy} is the exact value, is calculated and plotted in fig. 5.5 for the first, sixth and eleventh story when $\theta = 30$, 45 & 60 degrees, and for different values of the load level R. From this figure, the followings can be observed: (1) the ratio F/F_{xy} is always less than one, (2) for a particular R

value, the ratio F/F_{xy} is the smallest, when $\theta = 45$ degrees, and (3) for a particular θ, the ratio F/F_{xy} decreases as R increases.

To understand the previous findings, fig. 5.6 shows the three loading cases. For the two planar responses, when the load is increased, the beams in the longitudinal frames will yield, while the beams in the transversal frames remain elastic. Under additional applied loading, any increase in the axial force in the corner column will be shared by the other columns in the transversal frames since the beams in those frames are elastic. As a result, only a small increase will occur in the corner column axial force. However, when the two components of the load act simultaneously, the beams in all the frames will yield, and any increase in the corner column axial force is not shared by the other columns leading to a large corner column axial force. As a result, the exact axial force becomes larger than the estimated value. In particular, the smallest ratio of F/F_{xy} occurs at $\theta = 45$ because the two loading components being equal, cause the beams in any two orthogonal frames to yield almost at the same time. Any further increase in the applied load will lead to a large increase in the corner column axial force.

Finally, the estimated corner column based on the superposition principle diverges from the exact value as the load is increased. In other words, the accuracy of the estimate using the superposition principle decreases as the load beyond the elastic limit is increased.

In summary, the superposition principle when applied beyond the elastic limit to predict the static lateral response of frame tube structures, underestimates the radial displacement and corner column axial force. The degree of inaccuracy depends on the orientation of the lateral load with respect to the structural principal axis, and on the load level beyond the elastic limit.

5.4 DYNAMIC BIDIRECTIONAL RESPONSE OF FRAME TUBE STRUCTURES

5.4.1 Ground Motions

The ground motions considered are the two components of the 1940 ElCentro, and 1971 San Fernando (Hollywood storage) Earthquake recordings as shown in fig. 5.7. The angle of orientation of the ground motion axes is measured from the X structural axis in an anti-clockwise direction, as shown in fig. 5.8. Label 1 represents the N-S, or E-W component, of ElCentro and San Fernando earthquakes, respectively (strong components in terms of peak ground acceleration), while label 2 represents the second component. When $\theta_g = 0$, the strong component acts along the X direction. To investigate the inelastic dynamic bidirectional response, the strong component of each record is scaled so that the frame tube dynamic elastic base shear, when subjected to the strong component alone and acting in the X direction is four times the design base shear in the X direction. The other component is then scaled by the same factor. The scaling factors are summarized in table 5.3.

5.4.2 Effect of Orientation of Ground Motions

It has been the practice in seismic design to consider the seismic loading to act along the principal structural axes. To examine the effect of the earthquake forces acting in a direction, other than the structural principal axes, the frame tube is subjected to the two components of the ground motions with the orientation angle θ_g being varied from zero to 90 degrees. The response parameters of interest are the radial displacement and corner column axial force.

Fig. 5.9 shows the radial displacement along the height of the structure for five values of θ_g, namely, 0, 30, 45, 60 and 90 degrees. The radial displacement is more sensitive to ElCentro than to San Fernando earthquake record for the different values of θ_g. However, the

orientation of ground motion is not significant on the radial displacement which lies in a narrow band for the whole range of θ_g.

Fig. 5.10 shows the maximum axial force among all four corner columns along the height of the structure for the different values of θ_g. The orientation of ground motion is not significant either on the corner column axial force. Therefore, one concludes that the response of the structure when subjected to seismic loading along the two principal structural axes is a good representation of the response under an excitation in an arbitrary orientation.

5.4.3 Approximate Estimate

An elaborate inelastic response of structures subjected to multiple components of ground motions is complex, and often costly. Therefore, it is desirable to have simple approximate methods to estimate such inelastic response.

One common approach to consider the orthogonal effects of the earthquake forces is to analyze the structure along the two principal axes using the stronger component of the earthquake one at a time. The planar responses are then combined. The combination schemes suggested by design codes are:

1. ATC-06 [4] and UBC 88 [42]

$$r = \max \begin{matrix} 100\%\, r_x + 30\%\, r_y \\ 30\%\, r_x + 100\%\, r_y \end{matrix} \qquad (5.5)$$

2. UBC 88 [42]

$$r = \sqrt{r_x^2 + r_y^2} \qquad (5.6)$$

where r is the response quantity under consideration, and r_x,r_y are the response quantities when the strong component of the ground motion acts in the X and Y directions, respectively.

The purpose of this section is to check the validity of the above approximate combination schemes (eq. 5.5 and 5.6), and to suggest an alternative if these prove inaccurate. The investigation is carried out by comparing the approximate estimate with the exact value. This exact value is obtained from the response of the structure, when subjected to the simultaneous action of the two components of the earthquake, and corresponds to the maximum response quantity over the entire range of θ_g. The response parameters considered, herein, are the radial displacement, corner column axial force, and rotational ductility.

Corner column axial force

For the ElCentro earthquake, the ratios of F_x/F^* and F_y/F^*, where F_x,F_y is the axial force in the corner column, when the ground motion is acting in the X and Y directions and F^* is the exact value, are plotted in fig. 5.11-a, for column A. All along the structures height, these two ratios hovered around a value of half. As a result,the use of their sum as the possible combination scheme would lead to a better estimate than the one suggested by equation 5.5 or 5.6 which underestimate the exact value. For the same column line, similar curves are plotted in fig. 5.11-b, when the structure is subjected to San Fernando earthquake. In this case, the proposed summation rule resulted in good accuracy in the top and bottom of the structure, while the estimate is on the conservative side in the middle portion of the structure. Similar observations are made for column lines B, C and D for ElCentro and San Fernando earthquakes as shown in fig. 5.12 a,b,c,d,e,f.

Radial Displacement

The radial displacement is estimated from the two planar responses using the square root of the sum squares (SRSS). Specifically

$$d_r = \sqrt{d_x^2 + d_y^2} \tag{5.7}$$

The ratios of d_r to d_r^*, where d_r^* is the exact value are plotted in fig. 5.13 for ElCentro and San Fernando earthquakes. Such ratios hovered around unity indicating that the SRSS rule proved accurate in predicting the radial displacement. It is worth to mention that the SRSS rule is suggested by the UBC 88 [42].

Rotational Ductility

The rotational ductility in the beams of the frame AabB of fig. 5.8 is investigated. The rotational ductility was defined by

$$\mu_\theta = 1 + \theta_p / \theta_y \tag{5.8}$$

where θ_p is the plastic hinge rotation, and θ_y is the yield rotation given by

$$\theta_y = M_y L/6EI \tag{5.9}$$

The estimated rotational ductility is obtained by subjecting the frame tube to the strong component alone and acting in the X direction. No combination rule is attempted because when the ground motion is acting in the Y direction, the frame AabB remains elastic. Fig. 5.14 a&b shows the exact and estimated rotational ductility for the ElCentro earthquake, where it is clear that the distribution pattern of the plastic hinges are similar. In addition, the magnitude of the rotational ductulity are comparable. Therefore, one concludes that the rotational ductility demand can be realistically estimated using a unidirectional analysis.

5.5 CONCLUSION

The static response of a frame tube structure under lateral loads acting in an arbitrary orientation, and the seismic bidirectional response of the same frame tube structure, are investigated in this chapter.

The main objective of the static analysis is to assess the degree of approximation if the superposition principle was used beyond the elastic limit. For this purpose, analysis was

done on a thirty story frame tube subjected to an inverted triangular distribution lateral load, which acts at an angle θ from the principal structural axis. The load is decomposed into two components acting along the principal structural axes. The frame tube is analyzed under the action of the two load components. First, the two components are applied simultaneously, then they are applied one at a time. The response parameters of interest are the radial displacement and the corner column axial force. Based on the results and discussions in this chapter, the following conclusions can be drawn:

(1) When applied beyond the elastic limit, the superposition principle underestimates the radial displacement and corner column axial force.

(2) The difficulty arising from predicting the exact response from the two planar responses is due to the difference in the overall strength of the structure for the various loading cases.

The main objectives of the dynamic analysis are to assess the effect of orientation of ground motion with respect to the structural principal axes, and to quantify the bi-directionality effect of excitation on the response of frame tube structures. For this purpose, the thirty story frame tube is subjected to the simultaneous actions of the two components of the 1940 ElCentro and also the 1971 San Fernando earthquakes. Planar responses under the action of the stronger component are carried along both structural principal axes. The response parameters of interest are the radial displacement, corner column axial force, and the beam rotational ductility. Based on the results presented in this chapter the following can be drawn:

(1) The orientation of the bidirectional ground motion with respect to the structural principal axes showed little effects on the radial displacement and corner column axial force.

(2) The approximate estimate suggested by design codes to consider the bidirectionality of excitation underestimates the corner column axial force.

(3) A more realistic estimate of the corner column axial force which will take into account the bidirectionality of excitation is the simple summation rule, namely, the sum of the corner column axial force obtained from the two planar responses.

(4) The SRSS rule produced good accuracy to estimate the radial displacement. Such rule is suggested by the UBC 88 [42].

(5) The bidirectionality of excitation showed little effect on the rotational ductility in the beams. Therefore, the rotational ductility demand in the beams can be realistically estimated using a unidirectional excitation analysis.

Story No	Beam Moment of Inertia cm^4 10^6	Column Moment of Inertia cm^4 10^6	Column Area cm^2 $1-2$	Story Weight KN
1-5	1.697	1.27	26.3	691
6-10	1.53	1.14	23.7	691
11-15	1.36	1.02	21.1	691
16-20	1.19	.89	18.4	691
21-25	1.02	.736	15.8	691
26-30	.848	.636	13.2	691

Table 5.1 Member Stiffnesses and Story Weights

	Frames with longer dimensions		
Story No	Beam Capacities KN-m	Interior Column Capacities KN-m	Corner Column Capacities KN-m
1-5	307	430	307
6-10	285	400	285
11-15	261	365	261
16-20	225	315	225
21-25	175	246	175
26-30	112	157	112

Table 5.2-a Member Capacities for Frames With Longer Dimensions

Story No	Frames with smaller dimensions Beam Capacities KN-m	Interior Column Capacities KN-m	Corner Column Capacities KN-m
1-5	270	378	307
6-10	248	347	285
11-15	231	323	261
16-20	200	280	225
21-25	156	219	175
26-30	100	140	112

Table 5.2-b Member Capacities for Frames With Smaller Dimensions

Earthquake	Scaling Factor
El Centro	.92
San Fernando	1.32

Table 5.3 Scaling Factors for The Earthquake Records.

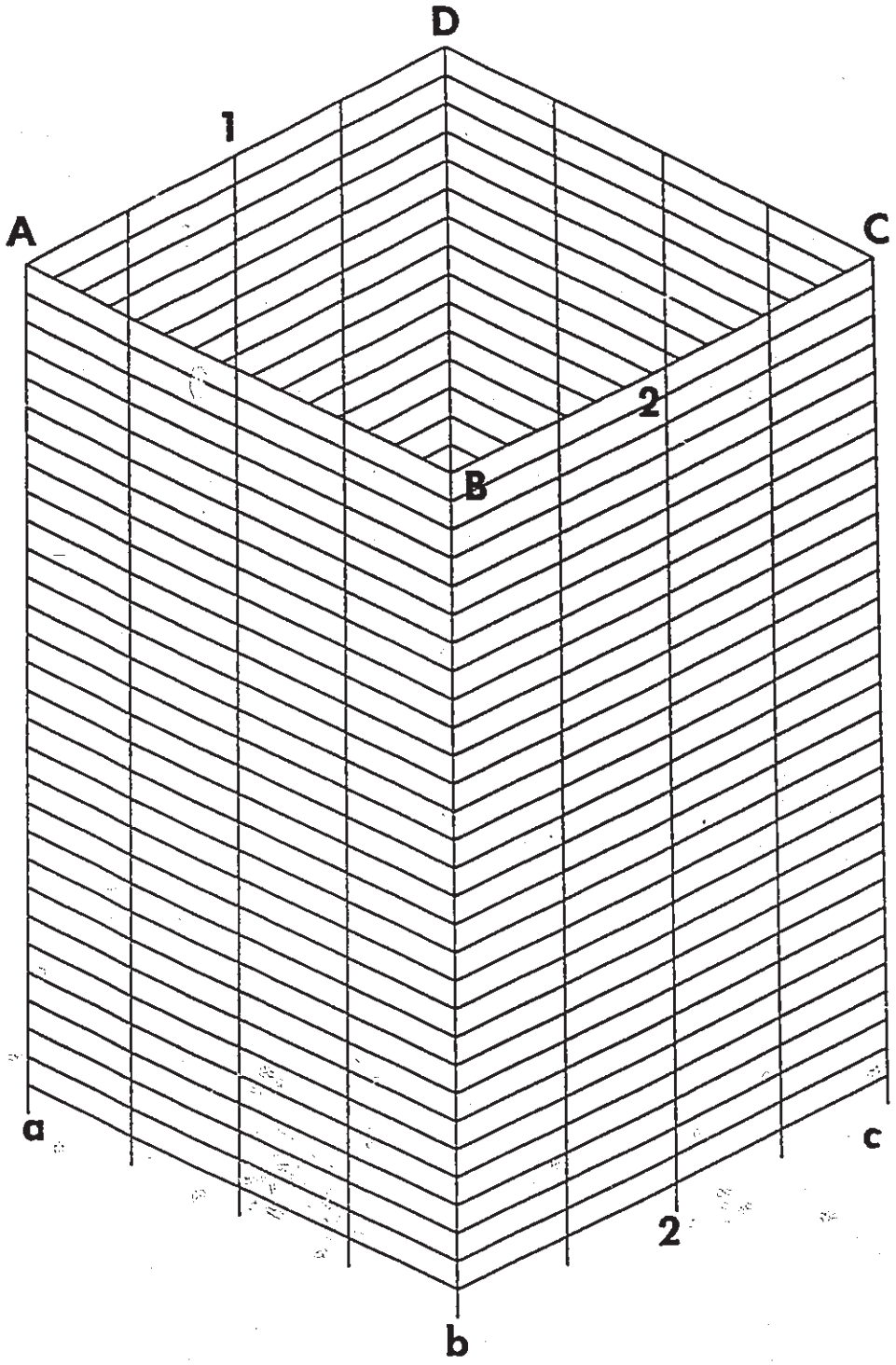

Fig (5.1) Frame Tube Structure

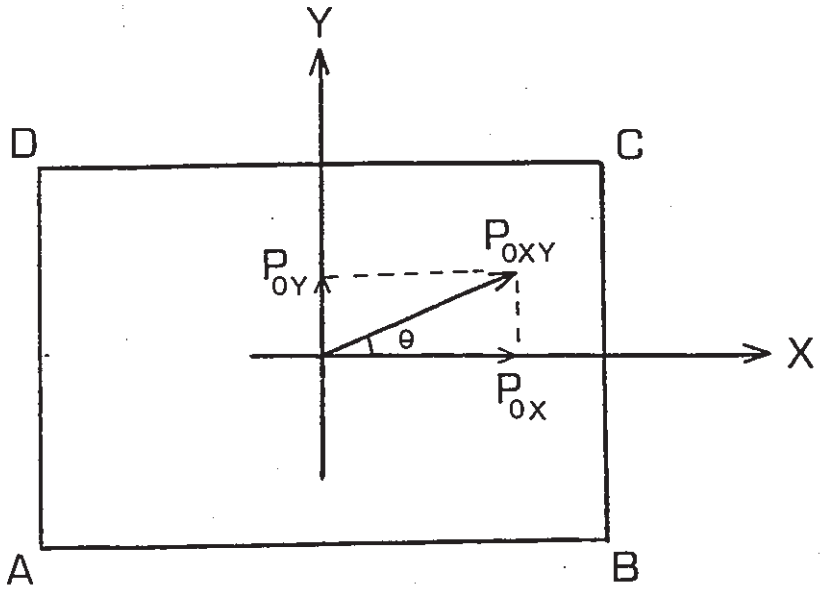

Fig (5.2) Plan View of Frame Tube Structure

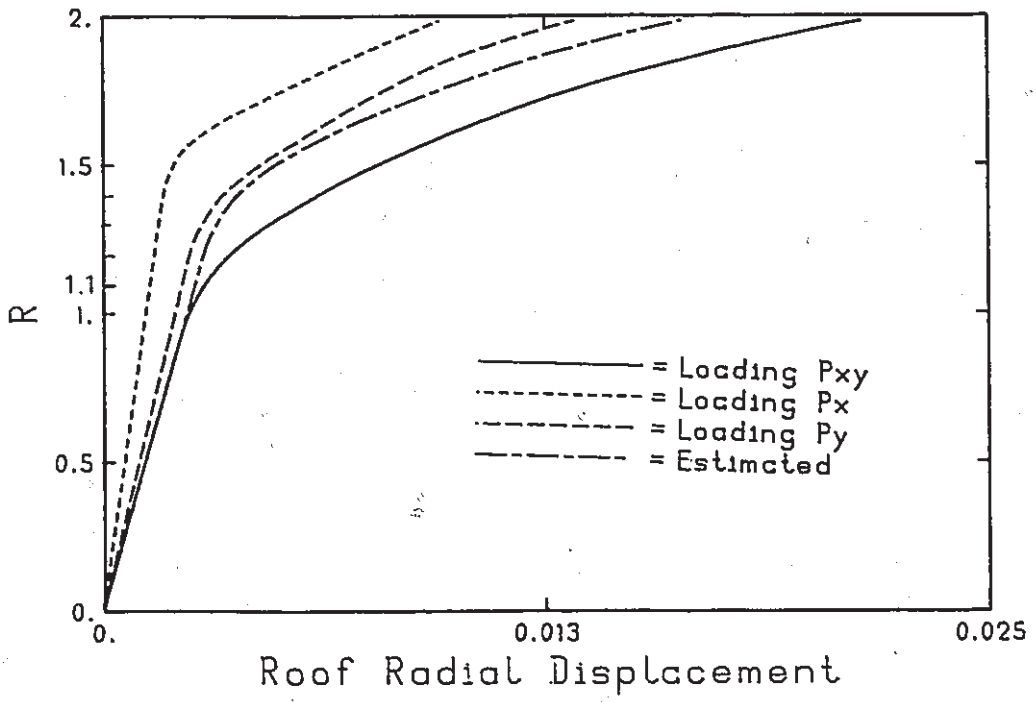

Fig (5.3) Top Story Load Displacement Curve; θ= 45

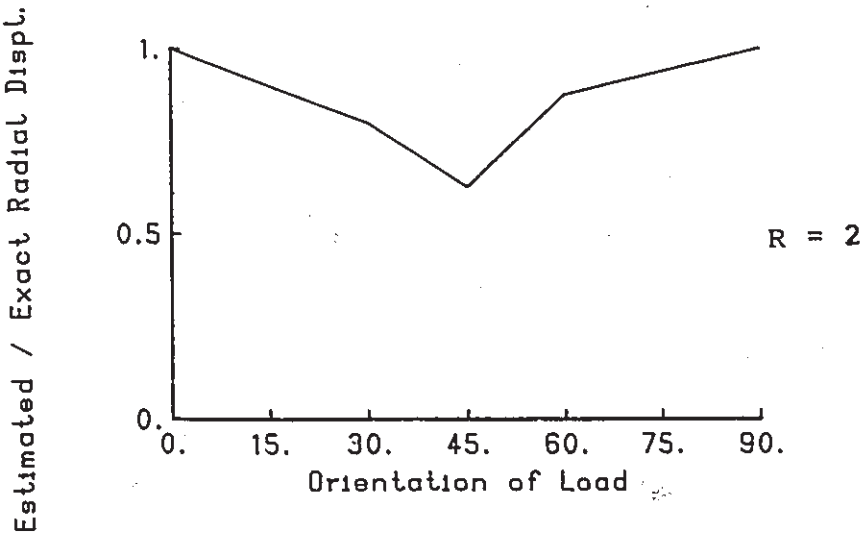

Fig (5.4) Ratio of Estimated and Exact Radial Displacement for Top Story

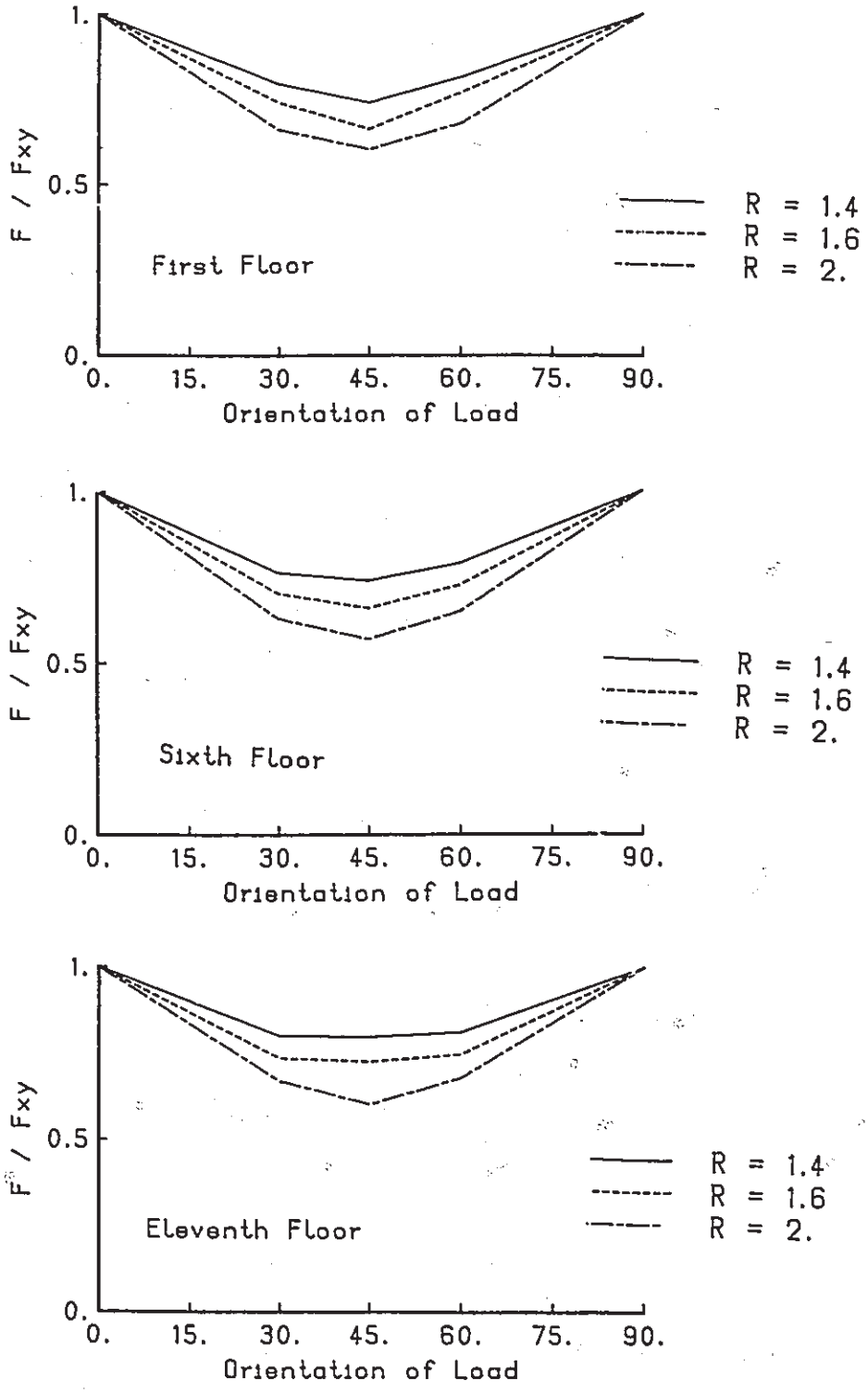

Fig (5.5) Ratio of Estimated and Exact Axial Force

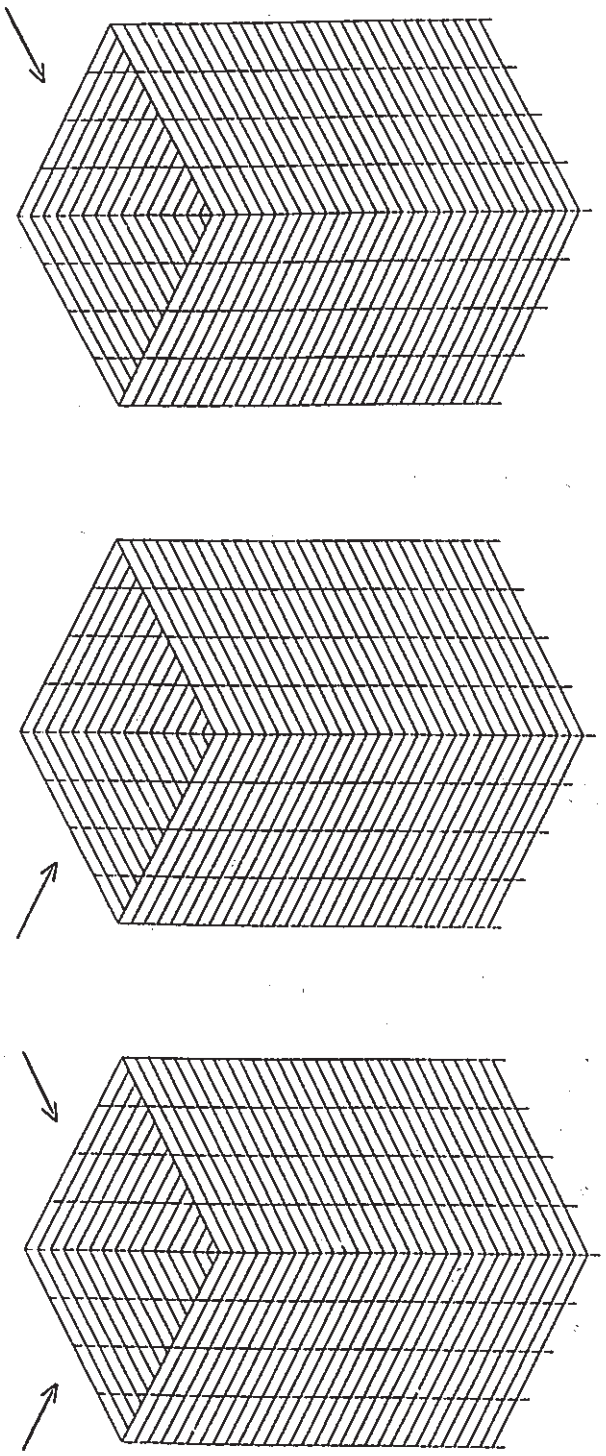

Fig (5.6) Frame Tube with the Three Loading Cases

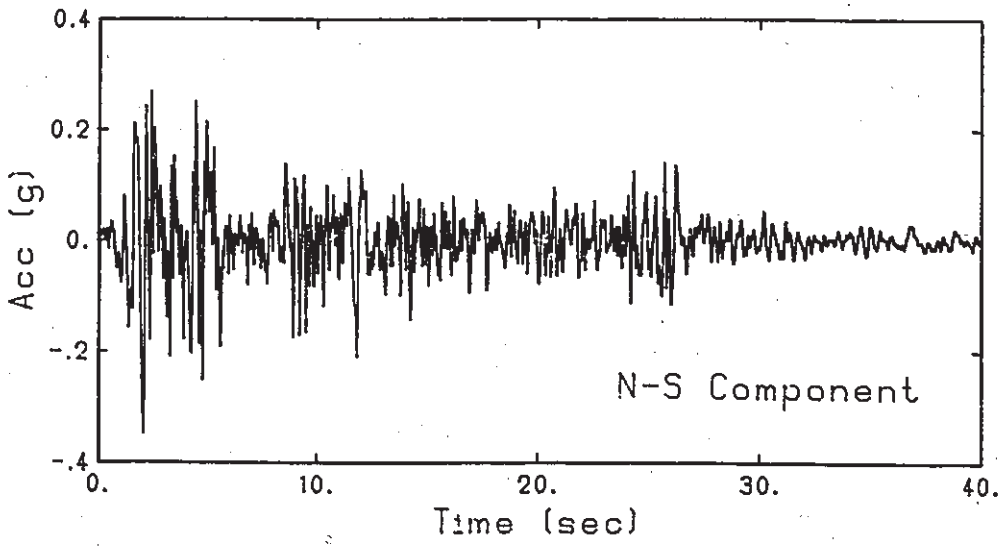

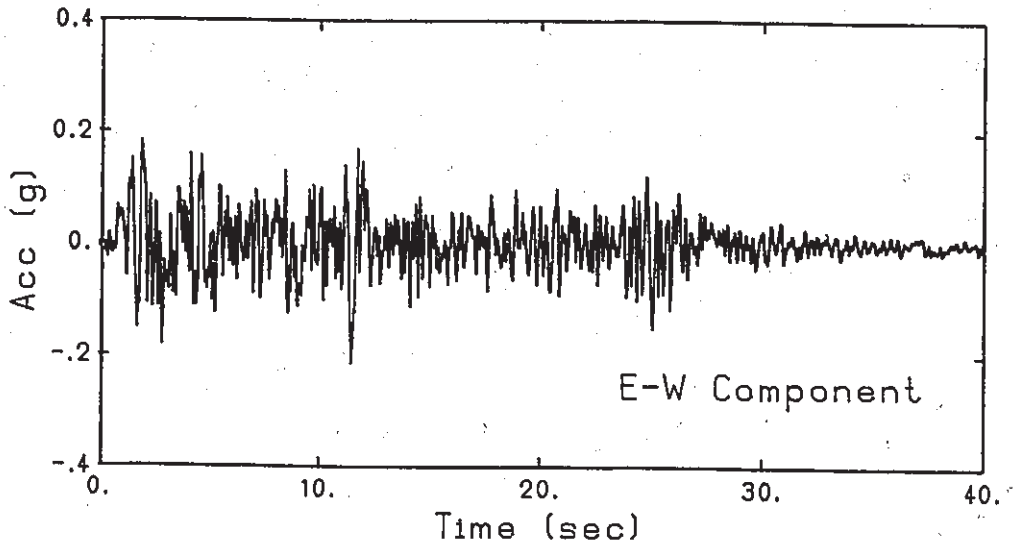

Fig (5.7a) Acceleration Time History, 1940 ELCentro

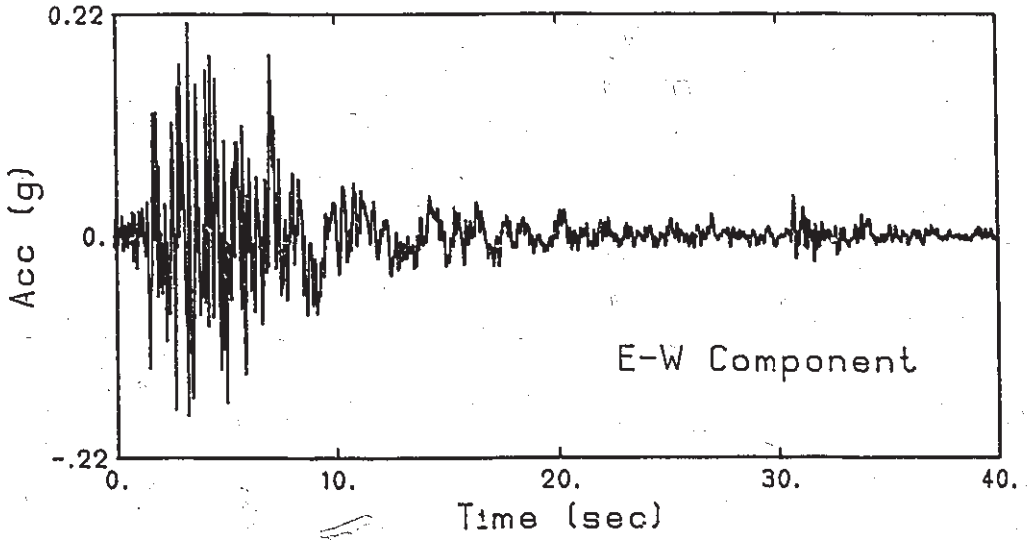

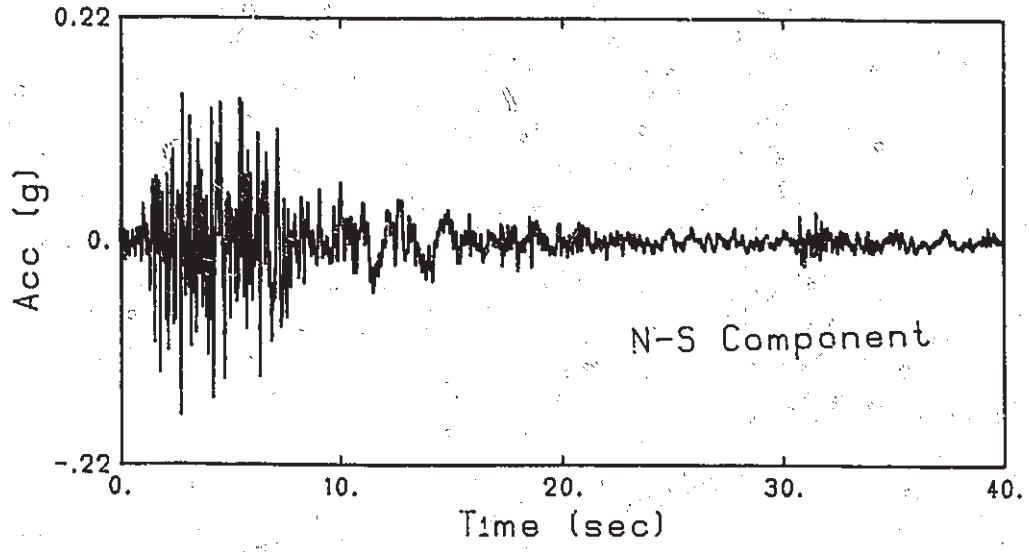

Fig (5.7b) Acceleration Time History, 1971 San Fernando

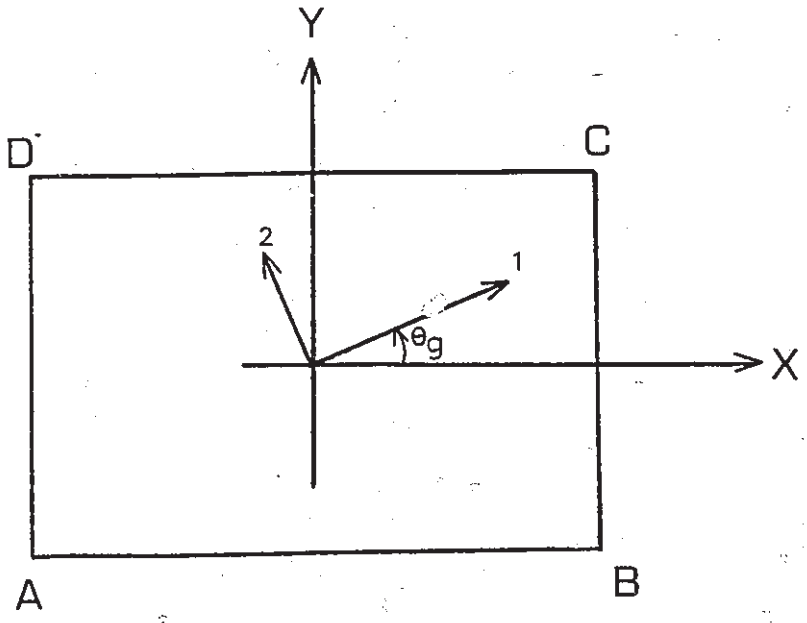

Fig (5.8) Plan View of Frame Tube

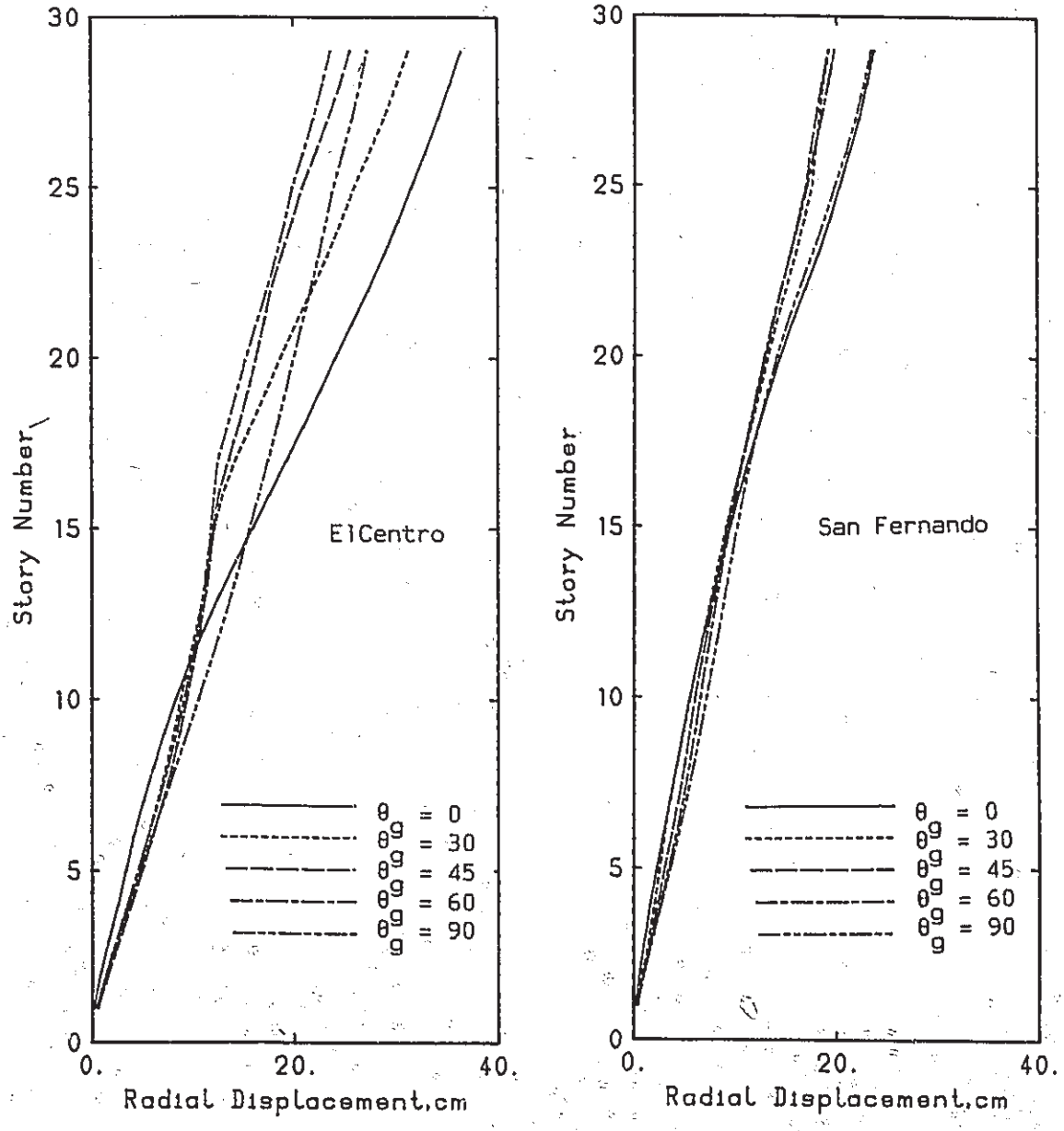

Fig (5.9) Effect of Orientation of Ground Motion on Radial Displacement

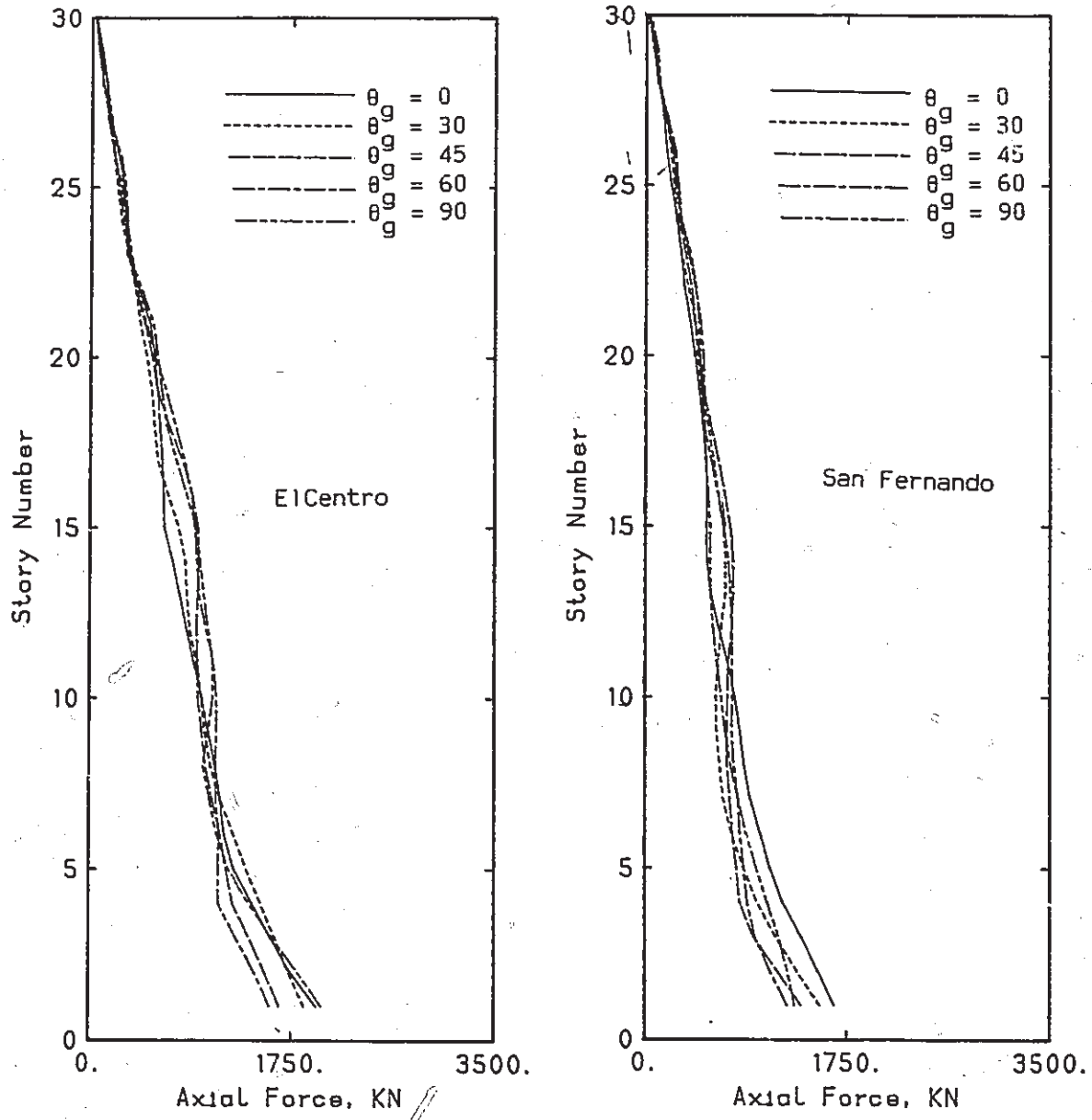

Fig (5.10) Effect of Orientation of Ground Motion on Column Axial Force

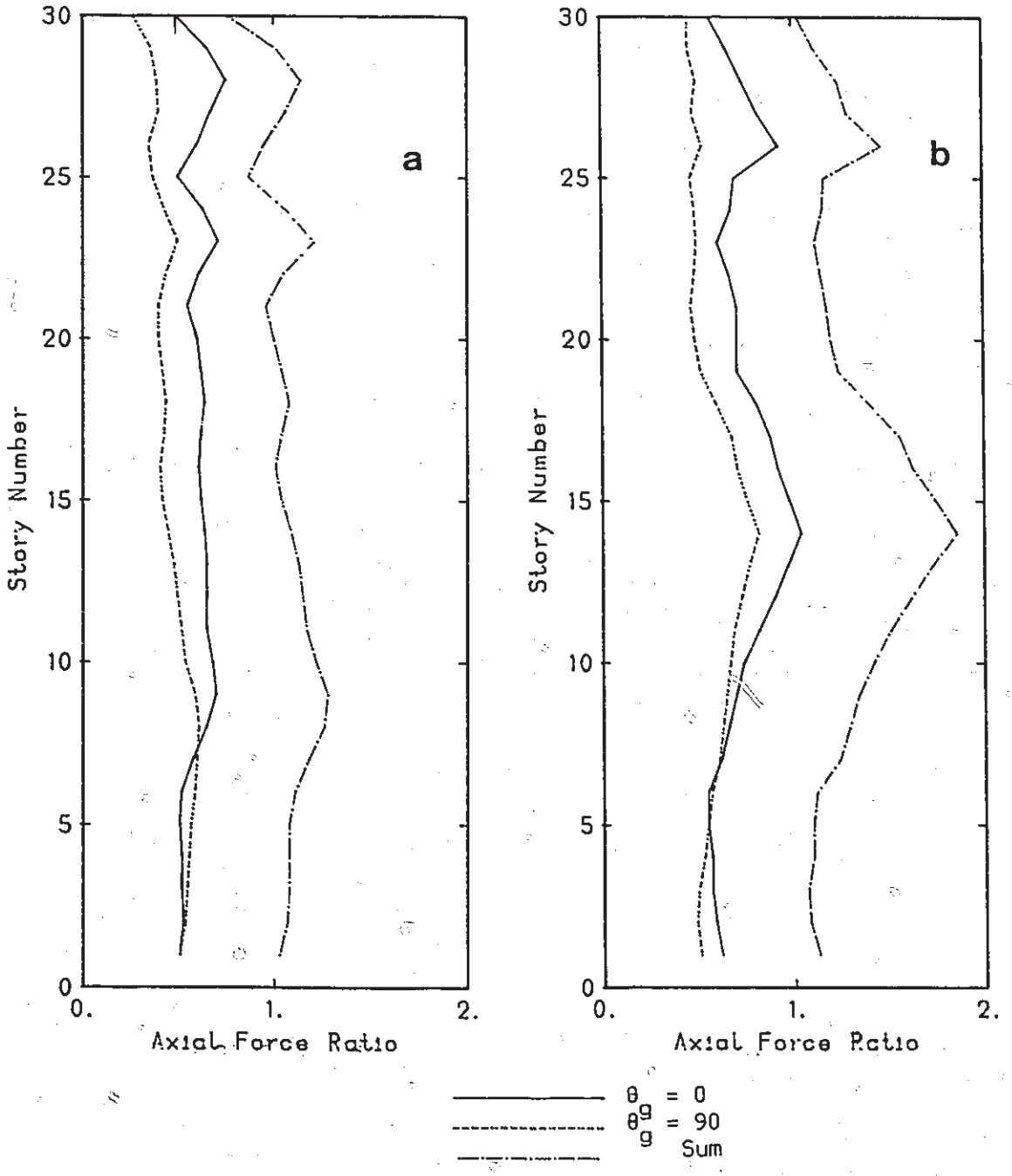

Fig (5.11) Estimation of Column Axial Force, Corner Column A; a- ELCentro, b- San Fernando

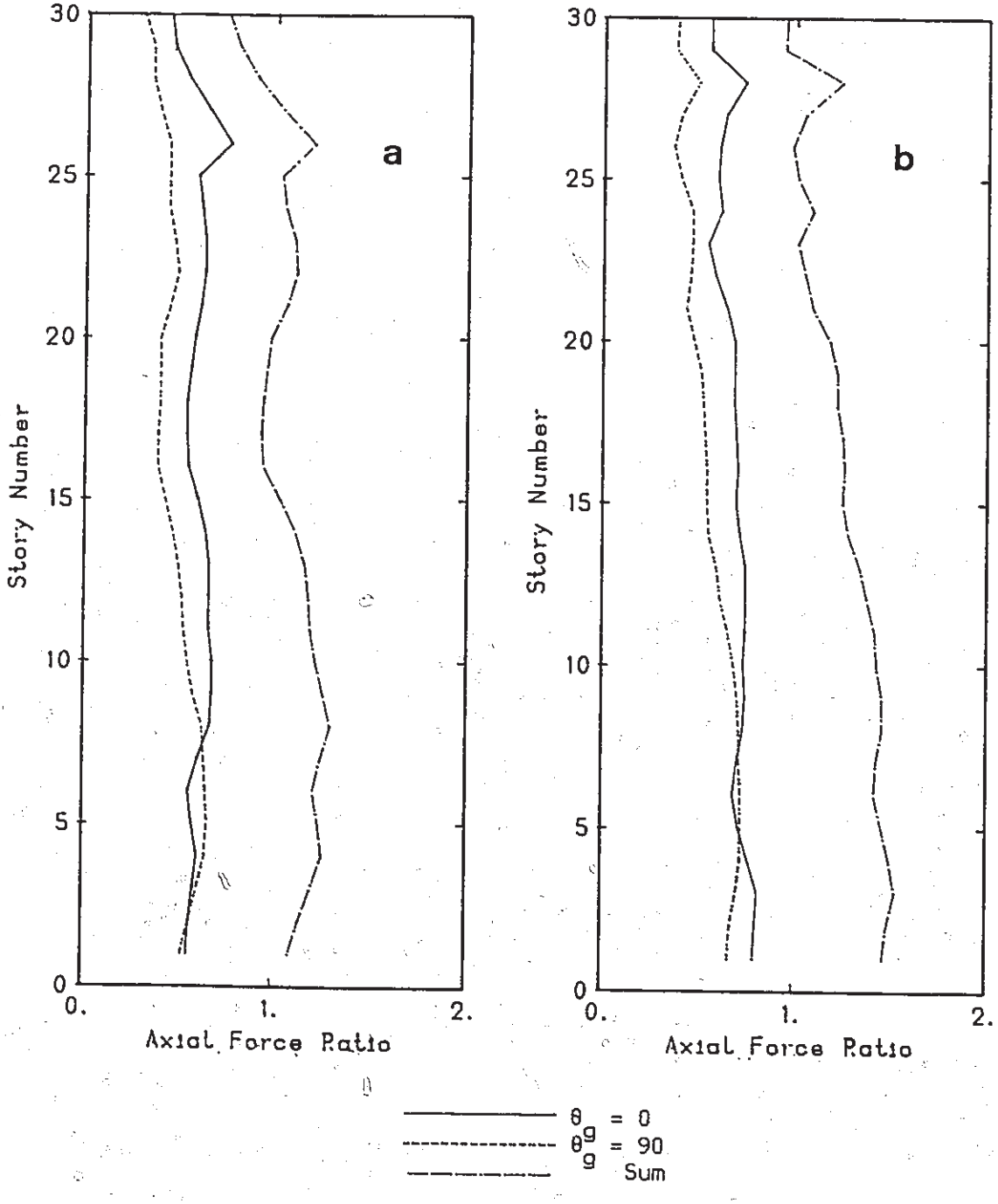

Fig (5.12a,b) Estimation of Column Axial Force, Corner Column B; a- ELCentro, b- San Fernando

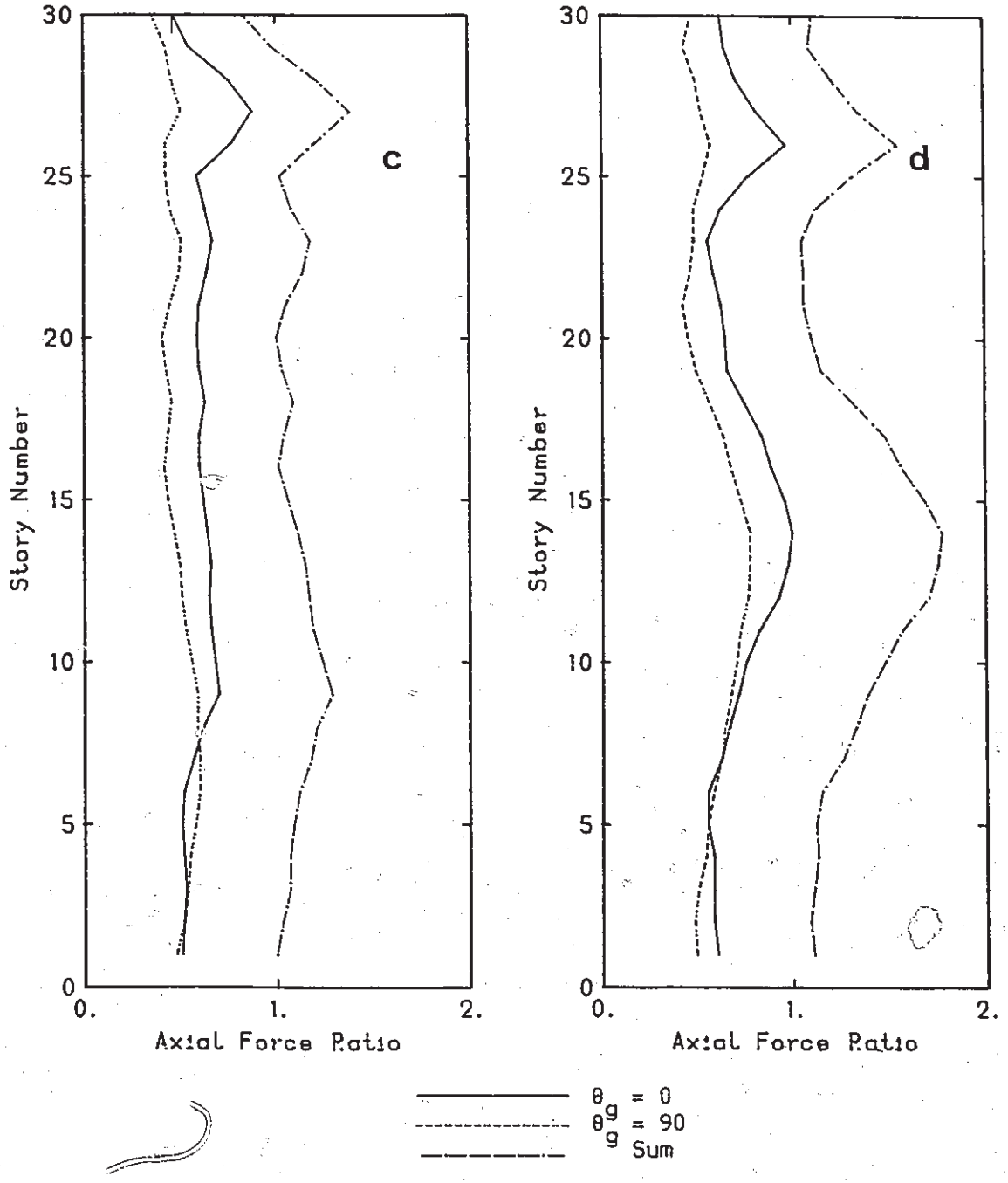

Fig (5.12c,d) Estimation of Column Axial Force, Corner Column C; c- ELCentro, d- San Fernando

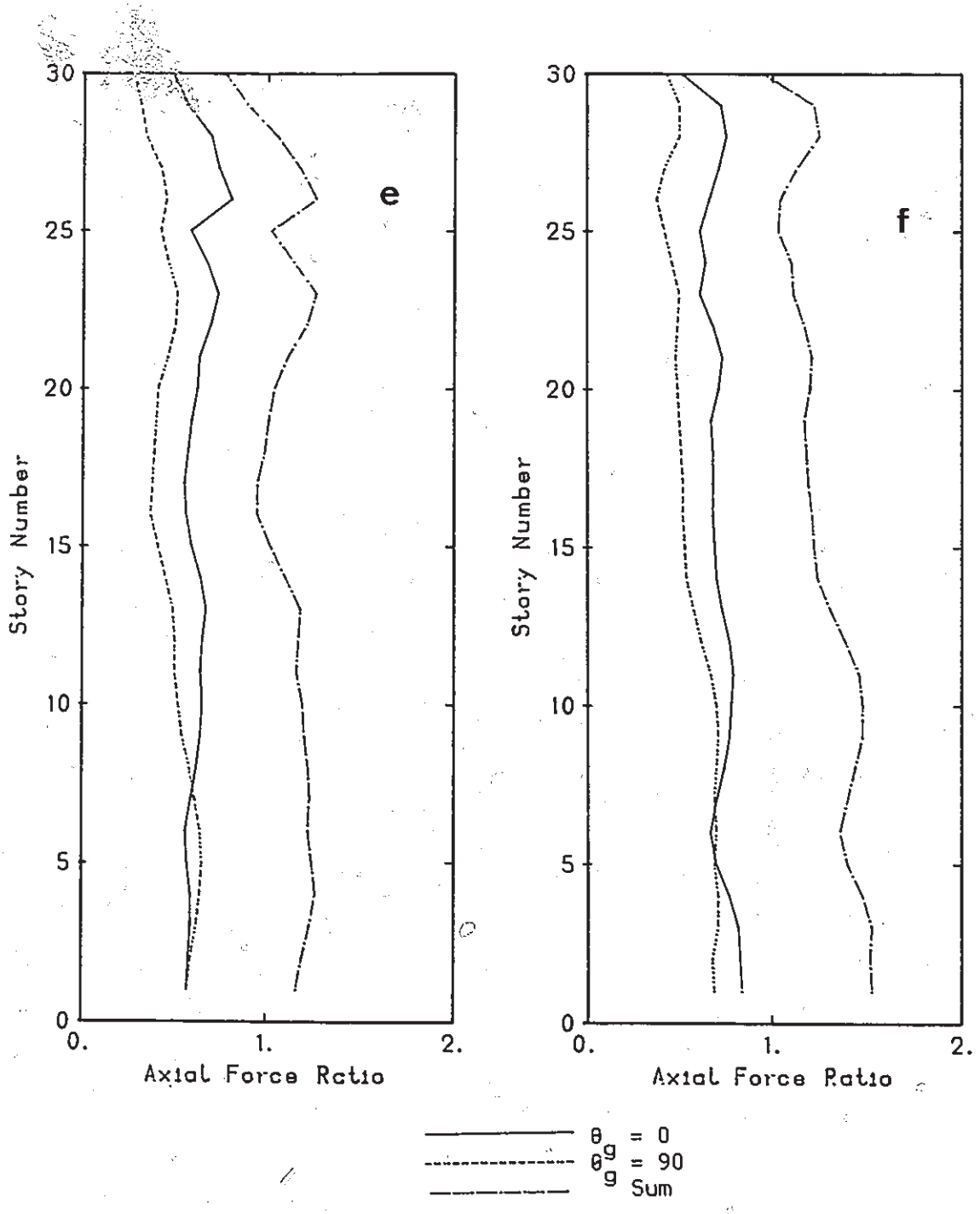

Fig (5.12e,f) Estimation of Column Axial Force, Corner Column D; e- ELCentro, f- San Fernando

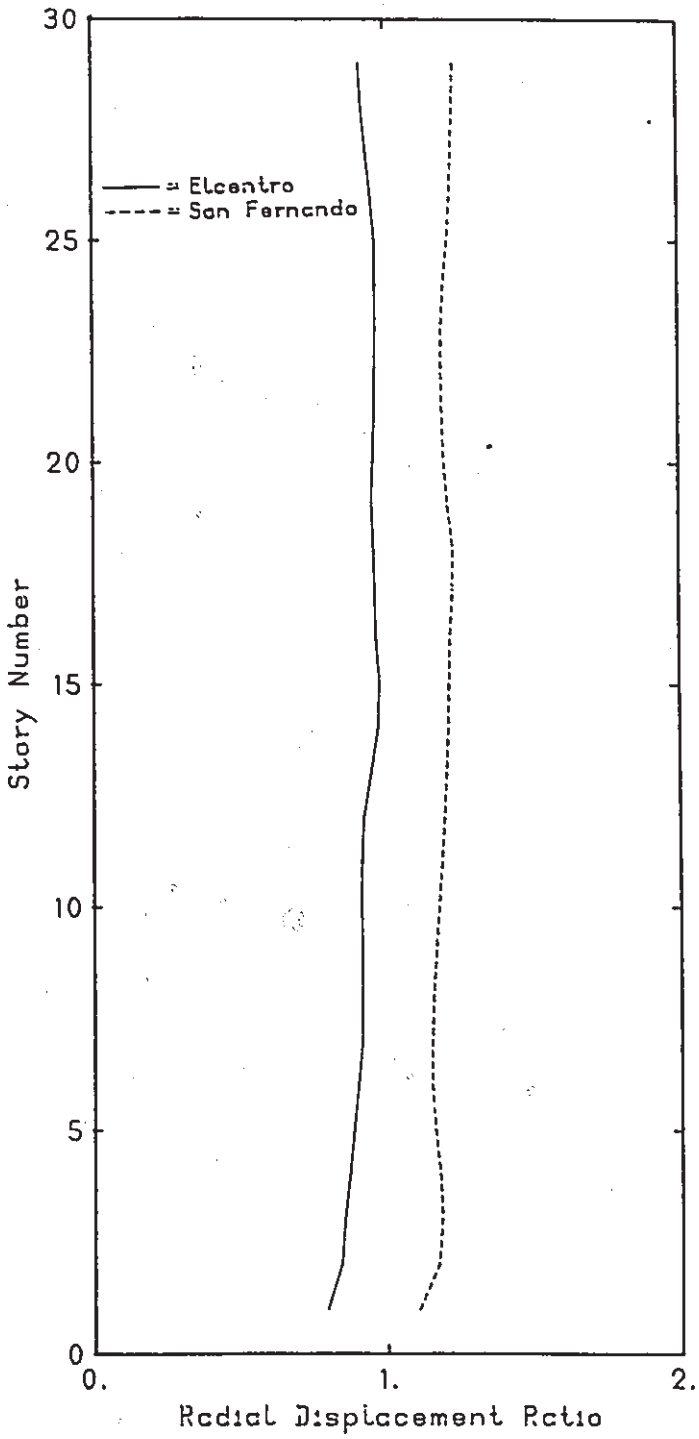

Fig (5.13) Estimation of Radial Displacement

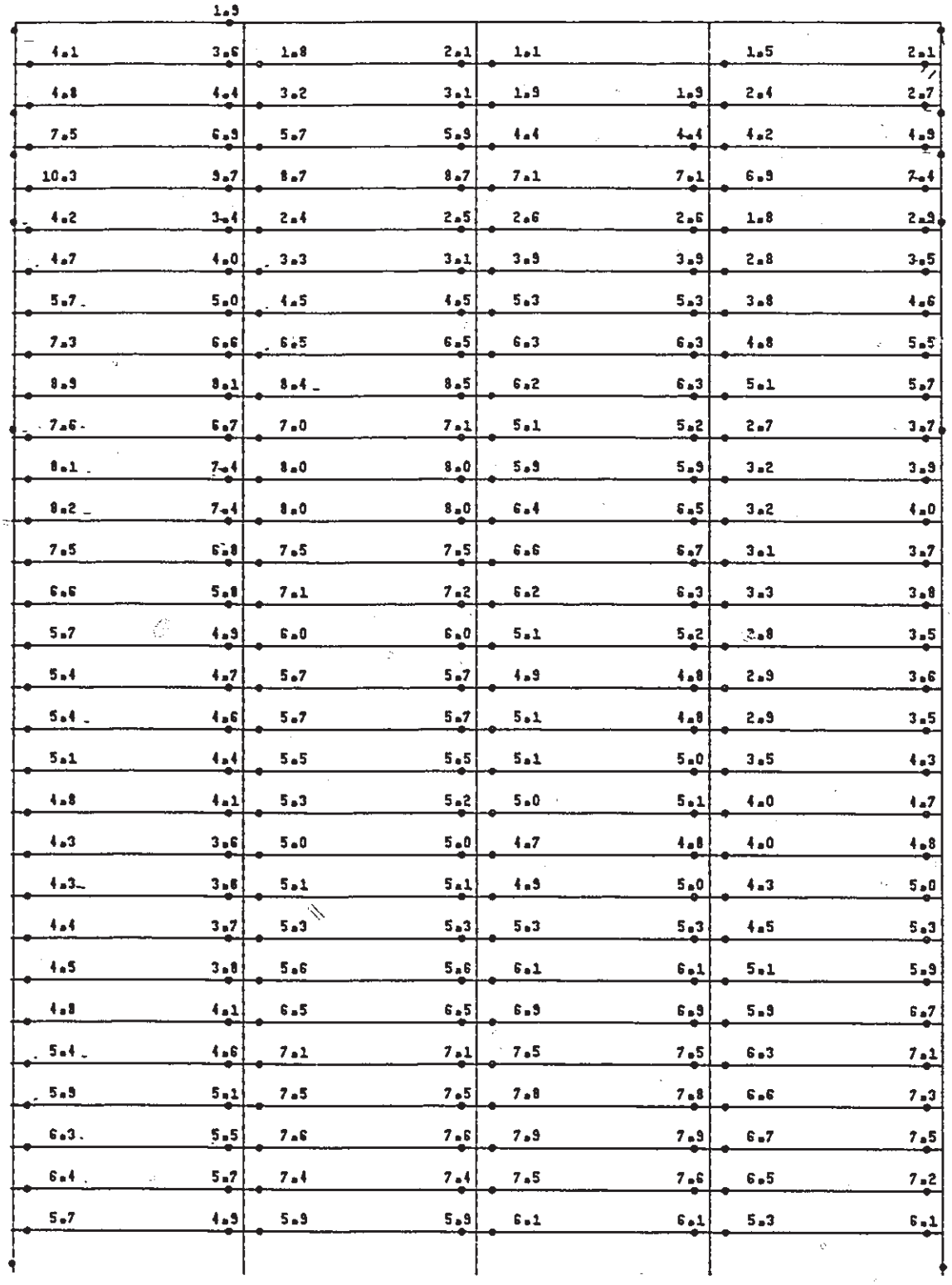

Fig (5.14a) Exact Rotation Ductility

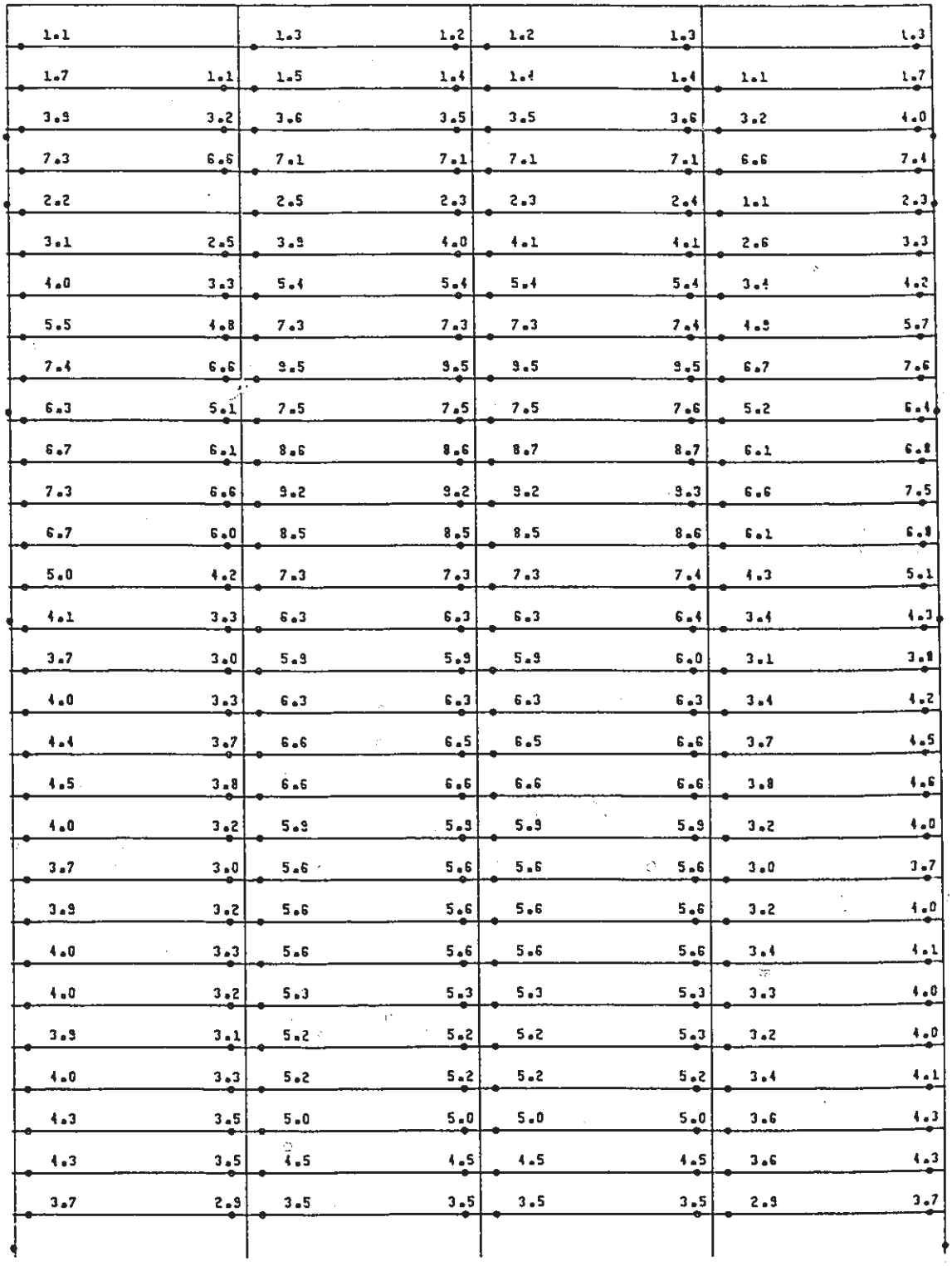

Fig (5.14b) Estimated Rotational Ductility

CHAPTER SIX

SUMMARY AND CONCLUSIONS

6.1 SUMMARY

In this investigation, a study has been made for the inelastic response of frame tube structures subjected to static loading as well as dynamic excitation. The intent of this investigation was (i) to identify the parameters that govern the behavior of frame tube structures, (ii) to assess the significance of the tube action on the elastic as well as inelastic responses, and (iii) to provide guidelines as how to account for the bidirectionality of ground motions.

Since a large amount of computation is involved in such parametric studies, a simplified model for frame tube structures was introduced capable of computing both elastic and inelastic response of such structures subjected to lateral loadings.

The simplified model is based on replacing the three dimensional frame structure by a set of interconnected plane frames. The inelasticity that can occur in these frames are modelled by plastic hinges at the end of frame members, similar to the model used in the DRAIN-2D inelastic plane frame program. A complete three dimensional beam column element is developed to represent the common column joining any two orthogonal frames. Inelastic actions at this common element are also taken to be concentrated at its ends. Both static and dynamic loading are considered, and the accuracy of this simplified model was checked by comparing results obtained from a complete three dimensional inelastic computer program ANSR.

The key parameters involved in characterizing the frame tube behavior are the stiffness ratio and the spandrel shear stiffness factor. The stiffness ratio is defined as the ratio

of the beam bending stiffness to the column bending stiffness. The spandrel shear stiffness factor is taken as the ratio of the beam shear stiffness to the column axial stiffness. The static elastic response of a thirty story frame tube structure was discussed for different combinations of the stiffness ratio and spandrel shear stiffness factor values under lateral loading. The response parameters are taken to be the lateral displacement along the height of the structure and the axial force in the columns of the first story.

Tube action is commonly referred as the forces developed in the two frames that are orthogonal to the direction of loading which provide partial resistance to the applied loading. To quantify the effects of this tube action on the behavior of the frame tube, an associated frame system is analyzed in conjunction with the frame tube. First, the static behavior under an inverted triangular lateral load distribution of the frame tube and its associated frame system are compared and the benifits of the tube action are evaluated. Next, a response spectrum analysis is presented to examine the dynamic characteristics and the elastic dynamic response of such systems. Finally, the inelastic dynamic response based on the average response to an ensemble of six recorded earthquakes is investigated.

The behavior of a frame tube with beams capacity such that the beams always remain elastic in the external bays is examined. First, the static behavior under an inverted triangular lateral load is carried out and the tube action is examined. Then, the dynamic behavior of the frame tube with distributed beam strengths is presented.

Finally, the static inelastic response of a frame tube under an inverted triangular lateral load acting in an arbitrary orientation is discussed. The superposition principle to combine the planar responses in the inelastic range is assessed. Then, the inelastic response of the thirty story frame tube subjected to the simultaneous action of the two horizontal components of earthquake ground motions is discussed. Two pairs of recorded ground motions are used as input. Attention is focused on the radial displacement and corner column axial

force. The effects of the orientation of ground motion components with respect to the structural axes are examined. Approximate formulae to estimate the radial displacement and corner column axial force are presented.

6.2 CONCLUSIONS

By the end of each chapter, the related conclusions are included. An overall view of the findings of the present study are presented in the following.

Based on the planar model for the lateral load inelastic analysis of frame tube structures presented in chapter two, the following conclusions can be made:

(1) The proposed planar model of frame tube structures, used to obtain the lateral displacement along the height of the structure, the axial force in the corner column, and the plastic hinge rotation in the beams, showed good accuracy in each case when compared with the results based on a three dimensional model.

(2) The computer time involved with the planar model is at least one third that for the three dimensional model.

(3) The proposed model is a viable tool to be used to study the inelastic behavior of frame tube structures subjected to lateral loading.

Based on the discussion in chapter three on the static and dynamic behavior of frame tube structures, the following can be made:

A. Static

(1) In order for the tube action to be effective, the frame tube should deflect like a cantilever column with a linear variation of axial force in the columns of the longitudinal frames and almost uniform axial force in the columns of the transversal

frames. This is obtained by using relatively stiff beams both in flexure and in shear. (Stiffness ratio less than 1.6 and spandrel shear stiffness factor greater than .1)

(2) Even for a frame tube with the above properties, the tube action is effective only when the behavior is elastic. This tube action becomes ineffective when the frame tube is loaded beyond the elastic limit, and leads to a small ratio of story stiffness.

B. Dynamic

Based on the results of the elastic response spectrum analysis, the following can be made:

(1) The tube action leads to a reduction of the contribution of higher modes to the base shear.

(2) The tube action leads to a significant increase in story shears only in the middle portion of the structure.

(3) The modal contribution of higher modes to story shears is significant in the top portion of the structure and to a less extent in the lower portion of the structure. However, negligible contribution of higher modes occured in the middle portion of the frame tube.

Based on the results on the dynamic inelastic analysis, the following can be made:

(1) The tube action leads to a large interstory drift in the bottom stories when the frame tube is subjected to a dynamic excitation beyond the elastic limit.

(2) The parameter governing the inelastic dynamic response of the frame tube is the ratio of story stiffness.

Based on the discussion in chapter four on the dynamic behavior of frame tube structures with unequal beam strengths among bays, the following can be made:

A. Static

(1) Keeping the beams in the external bays elastic enhances the tube action beyond the elastic limit. As a consequence, it also increases the ratio of story stiffness.

(2) Distributing the beam strengths across the internal and external bays, so that the inelastic action is restricted to the internal bays while the external bays remain elastic, also enhances the tube action beyond the elastic limit.

B. Dynamic

(1) By increasing the ratio of story stiffness, the interstory drift is no longer concentrated in the bottom stories but it is evenly distributed throughout the height of the frame tube. The increase of the ratio of story stiffness can be achieved by reducing the beam strength by a factor of two in the internal bays, and doubling those in the external bays.

(2) The improved inelastic dynamic behavior of the frame tube with distributed beam strengths is attributed to the continued effectiveness of the tube action.

(3) The dynamic response of the frame tube with distributed beam strengths, indicates that the rotational ductility is restricted to the interior bays, and increases monotonically along the height of the frame tube.

(4) The rotational ductility demand of the frame tube with distributed beam strengths is higher than that for the frame tube with uniform beam strengths.

Based on the discussion in chapter five on the bidirectional response of frame tube structures, the following can be made:

A. Static Response

(1) The superposition principle, when applied beyond the elastic limit, underestimates the radial displacement and the corner column axial force.

(2) The difficulty arising from predicting the exact response using the planar responses is due to the difference in the overall strength of the structure for the various loading cases.

B. Dynamic Response

(1) The orientation of the bidirectional ground motion with respect to the structural principal axes showed little effects on the radial displacement and corner column axial force.

(2) The approximate estimate suggested by design codes to consider the bidirectionality of excitation would underestimate the corner column axial force.

(3) A more realistic estimate of the corner column axial force which takes into account the bidirectionality of excitation is the simple summation rule, namely, the sum of the corner column axial force obtained from the two planar responses.

(4) The SRSS rule produced good accuracy to estimate the radial displacement. Such rule is suggested by the UBC 88 [42].

(5) The bidirectionality of excitation showed little effects on the rotational ductility in the beams. Therefore, the rotational ductility demand in the beams can be realistically estimated using a unidirectional analysis.

REFERENCES

1. Amin N. and Lowie J. "Design of Multiple Frame Tube High Rise Structures in Seismic Zones", Proceedings Eighth World Conference on Earthquake Engineering, San Francisco, 1984.

2. Anagnosto P., Haviland R.W. & Biggs J.M. "Use of Inelastic Spectra in a Seismic Design", Journal of the Structural Division, ASCE, No. ST1 pp 95, Jan 1978.

3. Andreaus U. and D'Asdia P. "Incremental Analysis of Elastic PLastic Frames at Finite Spread of Yielding Zones", Engineering Fracture Mechanics, V 21 n4 pp 827, 1985.

4. Applied Technology Council, Tentative Provisions for the development of Seismic Regulations for Buildings, ATC3-06, Washington, D.C., National Bureau of Standards, 1978.

5. Associate Committee on the National Building Code, National Building Code of Canada, 1985, ottowa, Ontario, National Council of Canada.

6. Blume J.A. "Dynamic Characteristics of Multi Story Buildings", Journal of the Structural Division, ASCE, Feb 1968, pp 377.

7. Bathe K.J., Wilson E.L. and Peterson F.E. "SAP IV, a Structural Analysis Program for Static and Dynamic Response of Linear systems", Earthquake Engineering Research Center, University of California Berkeley, EERC 73/11, June 1973

8. Borges J.F. and Ravara A. "Seismic Design of Traditional and Prefabricated Reinforced Concrete Buildings", Proceedings, Fourth World Conference on Earthquake Engineering, Santiage, Chile, 3,B-5 pp 13, 1968.

9. Chopra A.K., Clough D.P. and Clough R.W. "Earthquake Resistance of Buildings with a Soft First Story", Earthquake Engineering and Structural Dynamics, Vol 1 pp 347, 1973.

10. Clough R.W., Benuska K.L. and Wilson E.L. "Inelastic Earthquake Response of Tall Buildings", Proceedings, Third World Conference on Earthquake Engineering, Wellington, New Zealand, Vol II, 1965.

11. Clough R.W., King I.P. and Wilson E.L. "Large Capacity Multistory Frame Analysis Programs", Journal of the Structural Division, ASCE, pp 179, Aug. 1963.

12. Coull A. and Subedi N.K. "Frame Tube Structures for High Rise Buildings", Journal of the Structural Division, ASCE, pp 2097, Aug. 1971.

13. Cruz E.F. and Chopra A.K. "Simplified Methods of Analysis for Earthquake Resistant Design of Buildings", Earthquake Research Center, University of California Berkeley, EERC 85/01, Feb 1985.

14. Farhoomand F. and Wen R.K. "Dynamic Analysis of Inelastic Space Frames", Journal of the Engineering Mechanics Division, ASCE, 96(EM5), pp667, Oct 1970.

15. Fintel M. and Khan F.R. "Shock Absorbing Soft Storey Concept for Multi Storey Earthquake Structures", American Concrete Institute, 381-390, 1969.

16. Halabieh B.A. and Tso W.K. "Simplified Procedure for Lateral Load Inelastic Analysis of Frame Tube Structures", accepted for publication in Computers and Structures.

17. Heidebreicht A.C. and Smith S. "Approximate Analysis of Tall Wall Frame Structures", Journal of the Structural Division, ASCE Vol 99 No ST2 pp 199.

18. Heidebreicht A.C., Naumoski N. and Tso W.K. "A Selection of Representative Strong Motion Earthquake Records Having Different A/V Ratios", Earthquake Engineering Research Group, McMaster University, EERG 88/01, 1988.

19. Hilmy H.I. and Abel J.F. "Material and Geometric Nonlinear Analysis of Steel Frames Using Computer Graphics", Computers and Structures, Vol 21, No 4, pp 825, 1985.

20. Israel R.G. and Powell G.H. "DRAIN-TABS, A Computer Program for Inelastic Earthquake Response of Three Dimensional Buildings", Earthquake Engineering Research Center, University of California Berkeley, EERC 77/08, 1977.

21. Kanaan A. and Powell G.H. "DRAIN-2D, a General Purpose Computer Program for Dynamic Analysis of Inelastic Plane Structure", Earthquake Engineering Research Center, University of California Berkeley, EERC 75/37, 1975

22. Khan F.R. and Amin N.R. "Analysis and Design of Frame Structures for Tall Concrete Buildings", American Concrete Institute, Paper SP 36-3, Detroit Michigan 1973.

23. Lin J. and Mahin S.A. "Effect of Inelastic Behavior on the Analysis and Design of Earthquake Resistant Structures", Earthquake Engineering Research Center, University of California Berkeley, EERC 85/08, June 1985.

24. Mazzeo A. and De Fries A. "Perimetral Tube for the 37 Storey Steel Buildings", Journal of the Structural Division, ASCE, pp 1255, June 1972.

25. Miller R.K. "The Steady State Response of Multi Degree of Freedom Systems with a Spacially Localized Nonlinearity", Earthquake Engineering Research Laboratory, California Institute of Technology Pasadena, EERL 75/03 1975.

26. Mondkar D. and Powell G.H. "ANSR-1, General Purpose Computer Program for Analysis of Nonlinear Structural Response", Earthquake Engineering Research Center, University of California Berkeley, EERC 75/37, 1975.

27. Naumoski, N "SPEC, Calculation of Response Spectra", McMaster Earthquake Engineering Software Library, Jan 1985.

28. Newmark N.M "Fundamentals of Earthquake Engineering", Prentice Hall, 1971.

29. Newmark N.M and Hall W.J. "Vibration Handbook", Second Edition, McGrawhill, 1976, pp 29-1.

30. Nigam N.C. "Inelatic Interaction in the Dynamic Response of Structure", Ph.D. Thesis, California Institute of Technology, Pasadena, 1967.

31. Nigam N.C. "Yielding in Frame Structures Under Dynamic Loading", Journal of the Engineering Mechanics Division, ASCE, 96(EM5) pp687, 1970.

32. Park R. and Pauley T. "Reinforced Concrete Structures", John Wiley and Sons, 1975.

33. Powell G.H. and Clerq H. "Analysis and Design of Tube-Type Tall Buildings Structures", Earthquake Engineering Research Center, University of California Berkeley, EERC 76/05 1976.

34. Powell G.H. and Allahabadi R. "DRAIN-2DX a General Purpose Computer Program for the Dynamic Analysis of Inelastic Plane Structures", Earthquake Engineering Research Center, University of California Berkeley, EERC 88/06, 1988.

35. Riahi A., Row D. and Powell G.H. "Three Dimensional Inelastic Frame Elements for the ANSR-1 Program", Earthquake Engineering Research Center, University of California Berkeley, EERC 78/06, 1978.

36. Sadek A.W. "Seismic Response of Inelastic Structures Subjected to Bidirectional Excitations", Ph.D. Thesis, McMaster University 1985.

37. Schueller W. "High Rise Building Structures", John Wiley and Sons, 1977.

38. Smith A. and Wilson C.A. "Wind Stresses in the Steel Frames of office Buildings", Journal of the Western Society of Engineers, pp 365, April 1915.

39. Strang G. "Linear Algebra and Its Application", Academic Press, 1980.

40. Taranath B.S. "Structural Analysis and Design of Tall Buildings", McGrawhill 1988.

41. Tso W.K."A Proposal for the Compatibility of Static and Dynamic Seismic Base Shear Provisions of the National Building Code", Canadian Journal of Civil Engineering, Vol 9 pp 308, 1982.

42. Uniform Building Code, International Conference of Building Officials, Whittier, California, 1988.

43. Uzgider E.A. "Inelastic Response of Space Frames to Dynamic Loads", Computers and Structures, Vol 11 pp 97, 1980.

44. Wilson C.A. "Wind Bracing with Knee Braces or Gusset Plates", Engineering Records, pp 272, 1908.

45. Wilson E.L. and Bathe K.J. "Numerical Methods in Finite Element Analysis", Prentice Hall, New Jersey, 1976.

46. Wilson E.L. and Dovey H.H. "Three Dimensional Analysis of Building Systems; TABS", Earthquake Engineering Research Center, University of California Berkeley, EERC 72/08 1972.

47. Wilson E.L. and Dovey H.H. "Static and Earthquake Analysis of Three Dimensional Frame and Shear Wall Buildings", Earthquake Engineering Research Center, University of California Berkeley, EERC 72/01 1972.

48. Wilson E.L., Hollings, J.P. and Dovey H.H. "Three Dimensional Analysis of Building Systems (Extended Version)", Earthquake Engineering Research Center, University of California Berkeley, EERC 75/13, 1975.

APPENDIX A

DERIVATION OF THE TANGENT STIFFNESS MATRIX

The tangent stiffness is derived to relate increments of end forces to increments of end deformations for the elastic perfectly plastic component. That is

$$dS = k_t\, dv \tag{A.1}$$

in which dS = vector of element action increments,

dv = vector of element deformation increments, and

k_t = element tangent stiffness matrix.

The following basic assumptions are necessary for development of the theory.

a. Element deformation increments can be decomposed into elastic and plastic components. That is,

$$dv = dv_e + dv_p \tag{A.2}$$

in which dv_e = vector of elastic deformation increments, and

dv_p = vector of plastic deformation increments.

b. Element action increments are related to the elastic deformation increments by the elastic action deformation relationship. That is

$$dS = k_e\, dv_e \tag{A.3}$$

in which k_e = initial elastic stiffness matrix.

c. The plastic increment of deformation is normal to the yield surface, directed outwards. For a hinge, at, say element end i, this assumption can be expressed as

$$dv_{pi} = \phi_{i,s} \cdot \lambda_i \tag{A.4}$$

in which $\phi_{i,s}$ = gradient vector of yield function at end i, each term being partial derivative of the yield function with respect to the corresponding element action; and λ_i = a scalar which determines the magnitude of the plastic deformations.

With these three assumptions, the tangent stiffness matrix for an element with hinges at either or both ends is formed as follows.

For the hinges at end i and j, from eq. A.4

$$dv_{pi} = \phi_{i,s} \cdot \lambda_i \tag{A.5-a}$$

and

$$dv_{pj} = \phi_{j,s} \cdot \lambda\phi_j \tag{A.5-b}$$

Eqs. A.5-a and A.5-b can be combined to give

$$\begin{bmatrix} dv_{pi} \\ dv_{pi} \end{bmatrix} = \begin{bmatrix} \phi_{i,s} & 0 \\ 0 & \phi_{i,s} \end{bmatrix} \begin{bmatrix} \lambda_i \\ \lambda_j \end{bmatrix} \tag{A.6}$$

or

$$d\underline{v}_p = \phi_{,s}\,\underline{\lambda} \tag{A.7}$$

At each hinge, the value of the yield function must remain constant that is,

$$d\,\phi_i = 0 \tag{A.8-a}$$

and

$$d\,\phi_j = 0 \tag{A.8-b}$$

or

$$\phi_{i,s}^T \cdot dS_i = 0 \tag{A.9-a}$$

and

$$\phi_{j,s}^T \cdot dS_j = 0 \tag{A.9-b}$$

Eqs. A.9-a and A.9-b can be combined to give

$$\begin{bmatrix} \phi_{i,s} & 0 \\ 0 & \phi_{i,s} \end{bmatrix} \begin{bmatrix} dS_i \\ dS_j \end{bmatrix} = 0 \tag{A.10}$$

or

$$\Phi_{,S}^{T} \cdot dS = 0 \tag{A.11}$$

Substitution of eq. A.2 into A.3 gives

$$dS = k_e(dv - dv_p) \tag{A.12}$$

and substituting eq. A.7 into eq. A.12 gives

$$dS = k_e(dv - \Phi_{,S}\,\lambda) \tag{A.13}$$

Premultiplication of eq. A.13 by $\Phi_{,S}^{T}$ gives

$$\Phi_{,S}^{T}\,dS = \Phi_{,S}^{T}\,k_e(dv - \Phi_{,S}\,\lambda) \tag{A.14}$$

Hence from eq. A.11

$$\Phi_{,S}^{T}\,k_e(dr - \Phi_{,S}\,\lambda) = 0 \tag{A.15}$$

or

$$(\Phi_{,S}^{T}\,k_{e\,,s}) = (\Phi_{,S}^{T}\,k_e)dv \tag{A.16}$$

Eq. A.16 can be solved for λ to give

$$\lambda = (\Phi_{,s}^{T}\,k_e\,\Phi_{,S})^{-1}\,(\Phi_{,S}^{T}\,k_e)dv \tag{A.17)}$$

Substitution of eq. A.17 into eq. A.13 yields the elasto plastic stiffness relationship

$$dS = [k_e - (k_e\,\Phi_{,S})(\Phi_{,S}^{T}\,k_e\,\Phi_{,S})^{-1}\,(\Phi_{,S}^{T}\,k_e)]dv \tag{A.18}$$

or

$$dS = k_t\,dv \tag{A.19}$$

which is the required tangent stiffness relationship.

The gradient matrix in equation A.11 and for the yield function given by equation 2.2 can be written as

$$\Phi_{,s}^{T} = \begin{bmatrix} \frac{2M_1}{M_{01}^2} & \frac{2M_2}{M_{02}^2} & \frac{2P}{P_0^2} & 0 & 0 & 0 \\ 0 & 0 & 0 & \frac{2M_1}{M_{01}^2} & \frac{2M_2}{M_{02}^2} & \frac{2P}{P_0^2} \end{bmatrix} \tag{A.20}$$

APPENDIX B

INPUT DATA FOR THE THREE DIMENSIONAL BEAM COLUMN ELEMENT

The structure and loading data are consistent with DRAIN-2D user's guide. The input data for the three dimensional beam column element has the following format

B7(a) CONTROL INFORMATION FOR GROUP (3I5)

Columns	5:	Punch 7 (to indicate that group consists of 3-D beam column element)
	6-10:	Number of elements in group
	11-15:	Number of different element stiffnesses types. max(40)

B7(b) STIFFNESS TYPES (I5,5F10.0) – ONE CARD FOR EACH STIFFNESS TYPE

Columns	5:	Stiffness type number, in sequence beginning with one
	6-15:	Young's modulus of elasticity.
	16-25:	Strain hardening modulus as a proportion of Young's modulus
	26-35:	Average cross sectional area.
	36-45:	Moment of inertia I1
	46-55:	Moment of inertia I2

B7(c) CROSS SECTION YIELD INTERACTION SURFACE (I5,3f10.0)

Columns	5:	Yield Surface Number in sequence beginning with one
	6-15:	Ultimate moment corresponding to I1
	16-25:	Ultimate moment corresponding to I2

21-30: Ultimate axial force

B7(d) ELEMENT GENERATION COMMANDS (6I5)

Element must be specified in increasing numerical order. Cards for the first and last element must be included.

Columns 5: Element number or number of first element in a sequentially numbered series of elements to be generated by this command

6-10: Node number at element end i.

11-15: Node number at element end j.

16-20: Node number increment for element generation.If zero or blank assumed to be one.

21-25: Stiffness type number.

26-30: Time history output code.If time history of element results is not required for element covered by this command ,punch zero or leave blank. If a time history printout is required punch one.

APPENDIX C

DERIVATION OF CORNER COLUMNS SIZES

The corner columns and interior columns have the same moment of inertia and cross-sectional area. The corner column, however, possesses identical properties in the longitudinal and transversal frame directions. For this reason, the corner column must have a circular, square or L shape cross section. One possibility is the section shown below for the first five stories.

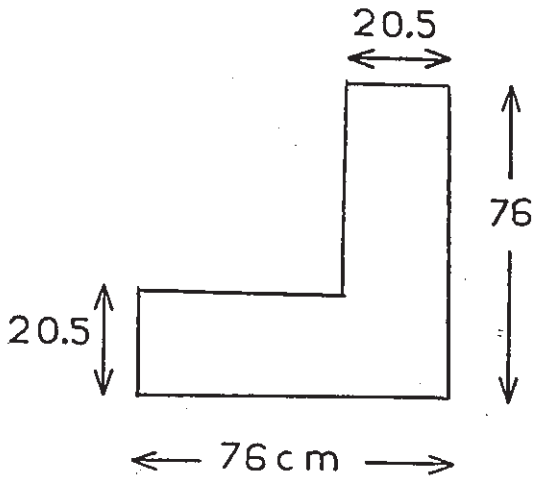

APPENDIX D

DISTRIBUTION OF BEAM STRENGTHS BETWEEN THE INTERNAL AND EXTERNAL BAYS

D.1 DISTRIBUTION OF BEAM CAPACITIES

The distribution of beam capacities between the external and internal bays is illustrated by considering the frame tube with distributed beam capacities with alpha being unknown. The objective of this study is to provide guidelines on the proper selection of the reduction factor alpha and the required capacity of the beams in the external bays.

The load displacement curve for the frame tube with distributed beam capacities and the one with uniform beam capacities are schematically represented in fig. D.1 for one particular story. These curves are similar to the ones shown in fig. 4.2 and 4.3. In the post elastic range, the equations of the two curves are:

Frame Tube with uniform beam capacities

$$V_A = V_d + K_A(d - d_d) \tag{D.1}$$

Frame Tube with distributed beam capacities

$$V_B = \alpha V_d + K_B(d - \alpha d_d) \tag{D.2}$$

where V_d is the design story shear,

V_A, V_B are the story shear for the frame tube with uniform and distributed beam capacities,

K_A, K_B are the post elastic story stiffness corresponding to the frame tube with uniform and distributed beam capacities respectively,

d_d is the drift corresponding to the first yield of the frame tube with uniform beam capacities and for the story under consideration, and

d is the story drift.

The restriction that is imposed on alpha is such that the story shear in the frame tube with distributed beam strengths is at least equal to the story shear of the frame tube with uniform beam strengths. In this way, one can have no penalty by reducing the beam capacities in the internal bays. The story shear of the frame tube with distributed beam strengths will be larger than that of the frame tube with uniform beam strengths as the story drift increases. However, the story drift should be controlled and a second restriction on alpha is imposed. Mathematically, the restrictions on alpha are:

$$V_B >= V_A \tag{D.3}$$

for required

$$d <= d_L \tag{D.4}$$

where d_L is an upper limit on story drift.

Substituting D.1, D.2 into D.3 yield

$$\alpha V_d + K_B(d-\alpha d_d) >= V_d + K_A(d-d_d) \tag{D.5}$$

or considering the equality

$$\alpha V_d + K_B(d-\alpha d_d) = V_d + K_A(d-d_d) \tag{D.6}$$

It is worth to note that α cannot be computed directly from equation D.6 because d is unknown. However, values of α are selected in advance ($\alpha=.25$, $\alpha=.5$, and $\alpha=.75$) and the corresponding drift is computed. If the drift d is such that

$$d <= d_L,$$

The value of α is admissible. The restriction presented by equation D.4 should be satisfied at every story throughout the height of the structure.

The selection of the reduction factor alpha depends on the choice of the drift limit. Therefore, there no unique solution for alpha.

D.2 RELATIONSHIP BETWEEN BEAM STRENGTH OF THE INTERNAL AND EXTERNAL BAYS

To compute the required capacity of the beams in the external bays, one needs to understand the relationship between the beam capacities in the internal and external bays.

Fig. D.2 shows a typical one story section of the frame tube. Beam ab is elastic. Therefore, the moment can be computed using the slope deflection equation given by;

$$M_{ab} = 4EI/L(\theta_a) + 2EI/L(\theta_b) - 6EI/l(\rho_{ab}) \tag{D.7}$$

where, θ_a is the rotation at node a,

θ_b is the rotation at node b, and

ρ_{ab} is the relative vertical displacement between node a and b divided by the beam length.

Equation D.7 can be rearranged

$$M_{ab} = 4EI/L(\theta_a - \rho_{ab}) + 2EI/L(\theta_b - \rho_{ab}) \tag{D.8}$$

in which the terms

$\theta_a - \rho_{ab}$ represents the rotation at end a of beam ab which is the result of the rotation at node a and the relative vertical displacement of nodes a and b, similarly

$\theta_b - \rho_{ab}$ represents the rotation at end b of beam ab.

As for the case of story shear versus story drift, the normalized story shear versus rotation for the frame tube with distributed beam strengths is schematically plotted in fig. D.3, where the curves of interest are the rotation at end a of beam ab, the rotation at end b of beam ab, and the rotation at end b of beam bc.

The rotation at the end b of beam bc can be decomposed into elastic and plastic components. That is

$$(\theta_b - \rho_{bc}) = (\theta_b - \rho_{bc})_y + \theta_p \tag{D.9}$$

where, $(\theta_b - \rho_{bc})_y$ is the rotation at the end b of beam bc when the beam reaches its yield moment, and

θ_p is the plastic hinge rotation at the end b of beam bc.

The rotation at the ends of beam ab can be related to the plastic hinge rotation by

$$(\theta_a - \rho_{ab}) = (\theta_a - \rho_{ab})_y + k_1/k_2(\theta_p) \quad (D.10)$$

$$(\theta_b - \rho_{ab}) = (\theta_b - \rho_{ab})_y + k_1/k_3(\theta_p) \quad (D.11)$$

where, $(\theta_a - \rho_{ab})_y$ is the proportional limit rotation at beam end a,

$(\theta_b - \rho_{ab})_y$ is the proportional limit rotation at beam end b,

k_1 is the post elastic slope of curve $\theta_b - \rho_{bc}$

k_2 is the post elastic slope of curve $\theta_a - \rho_{ab}$, and

k_3 is the post elastic slope of curve $\theta_b - \rho_{ab}$.

Substituting all the terms in equation D.8 yields

$$M_{ab} = 4EI/L(\theta_a - \rho_{ab})_y + 2EI/L(\theta_b - \rho_{ab})_y + 2EI/L(2k_1/k_2 + k_1/k_3)\,\theta_p \quad (D.12)$$

Hence the beam moment of the external bays depends on the plastic hinge rotation in addition to the yield capacity of the beam of the internal bays. The plastic hinge rotation can be related to story shear. From fig. D.3, the equation of curve $\theta_b - \rho_{bc}$ can be written as

$$V = \alpha V_d + k_1(\theta_p) \quad (D.13)$$

It has been shown earlier (Equation D.2)

$$V = \alpha V_d + K_B(d - \alpha d_d)$$

Solving for θ_p yields

$$\theta_p = K_B(d - \alpha d_d)/k_1 \quad (D.14)$$

Substituting equation D.14 into D.12 yields

$$M_{ab} = 4EI/L(\theta_a - \rho_{ab})_y + 2EI/L(\theta_b - \rho_{ab})_y + 2EI/L(1/k_3 + 2/k_2)(K_B)(d - \alpha d_d) \quad (D.15)$$

In summary, the reduction factor of beam capacities of the internal bays can be selected such that the drift limit is satisfied. Then, those capacities as well as the proportional

limit rotations can be computed. Finally the required capacity to keep the beams in the external bays elastic can be obtained from equation D.15 after the story stiffnesses and the post elastic rotational slopes are computed.

In developing the proposed procedure to distribute the beam strength accoss the bays, an upper limit for the interstory drift is assumed. The beam capacities of the external bays computed guarantee that the inelastic action is restricted to the beams in the internal bays such that the drift limit is satisfied. However, if the lateral load is further increased, the drift limit is violated and the beams of the external bays would yield.

D.3 EXAMPLE

The following example will be presented to illustrate the proposed procedure of distributing the beam capacities across the bays. The example structure used is the frame tube with uniform and distributed beams strengths. First, the reduction factor α needs to be selected such that the drift limit is satisfied. According to equation D.6, the drift along the height of the structure can be obtained as a funtion of α. However, the post elastic story stiffnesses are not known, but those post elastic stiffnesses are independent of α.

Fig. B.4 shows the drift along the height of the structure for $\alpha=.75$, $\alpha=.5$, and $\alpha=.25$ computed using equation D.6. The post elastic story stiffnesses are obtained from the analysis of the frame tube with distributed beam strengths with $\alpha=1$. By choosing the drift limit to be one percent the story height. It can be seen that $\alpha=.25$ is not appropriate since the drift requirement is not satisfied. For $\alpha=.5$, the drift is satisfied except for the top four stories, while $\alpha=.75$ satisfies the drift requirement throughout the structure's height. For this example, a value of half is selected for α with little violation of drift requirement for top four stories.

Second, the post elastic rotational slopes and the proportional limit rotations need to be known. These can be obtained either by analyzing the frame tube with distributed beam strengths with $\alpha = .5$ and plotting the normalized story shear versus rotations, or by plotting those curves (fig. D.5) for the frame tube with distributed beam strengths with $\alpha = 1$. As for the case of the post elastic story stiffness, the post elastic slopes are independent of α. However, the proportional limit rotations are directly proportional to α. In other words, the proportional limit rotation for $\alpha = .5$ will be half the values corresponding to $\alpha = 1$. Once these informations are obtained, the moment in the external bay can be computed using equation D.15.

It is interesting to see the additional capacity as compared to the initial capacity the beams in the external bays should possess to remain elastic. Such information is presented in fig. D.6 where the ratio of the computed capacities of the beams in the external bays and its original value is plotted along the height of the structure for $\alpha = .5$. It is clear that this ratio hovered around the value of two. In other words, a simple rule is that reducing the beam capacities in the internal bays by a factor of two and doubling those in the external bays would restrict the inelastic action to the internal bays.

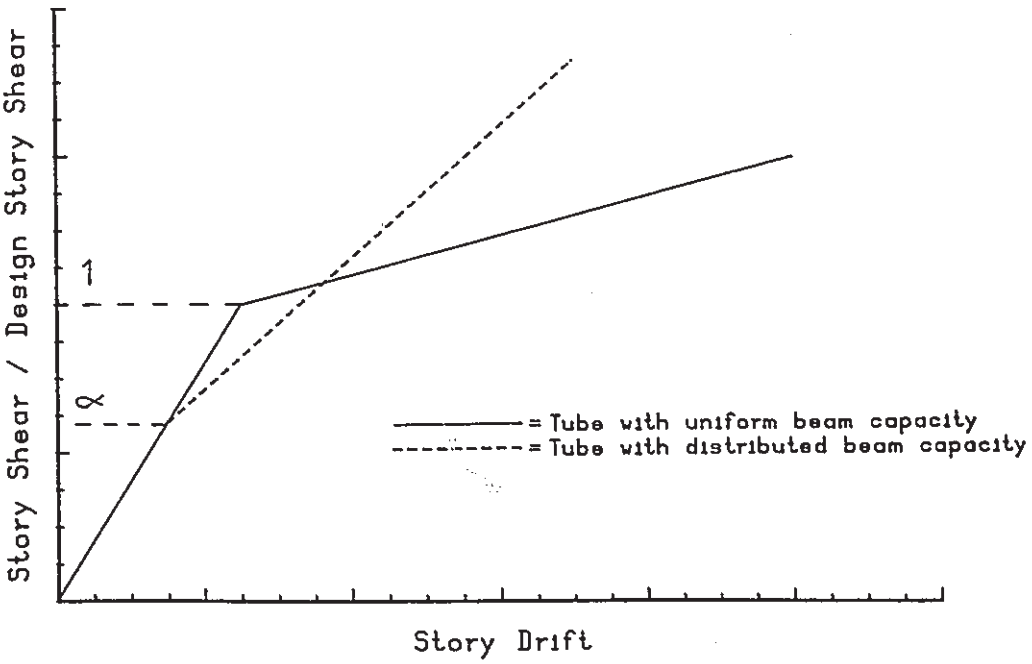

Fig (D.1) Story Shear versus Story Drift for Frame Tube
with Uniform and Distributed Beam Capacities

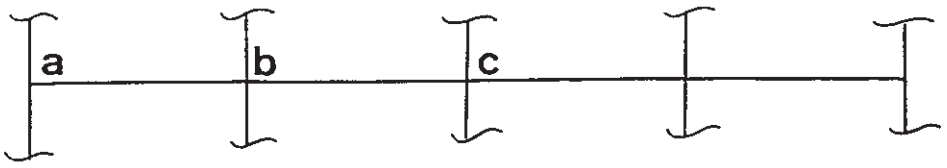

Fig (D.2) Typical One Story Section

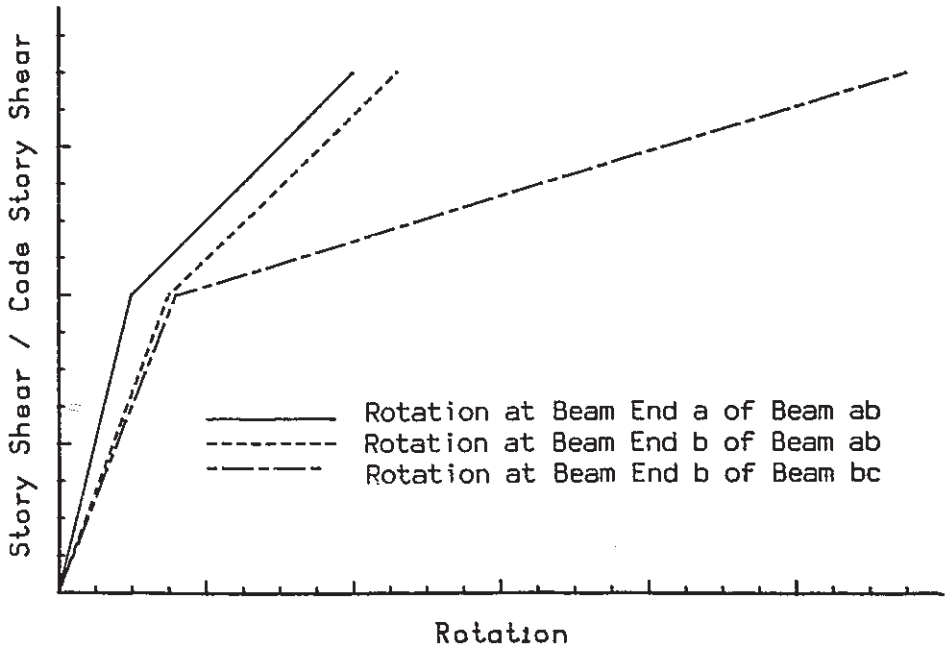

Fig (D.3) Story Shear versus Joint Rotation

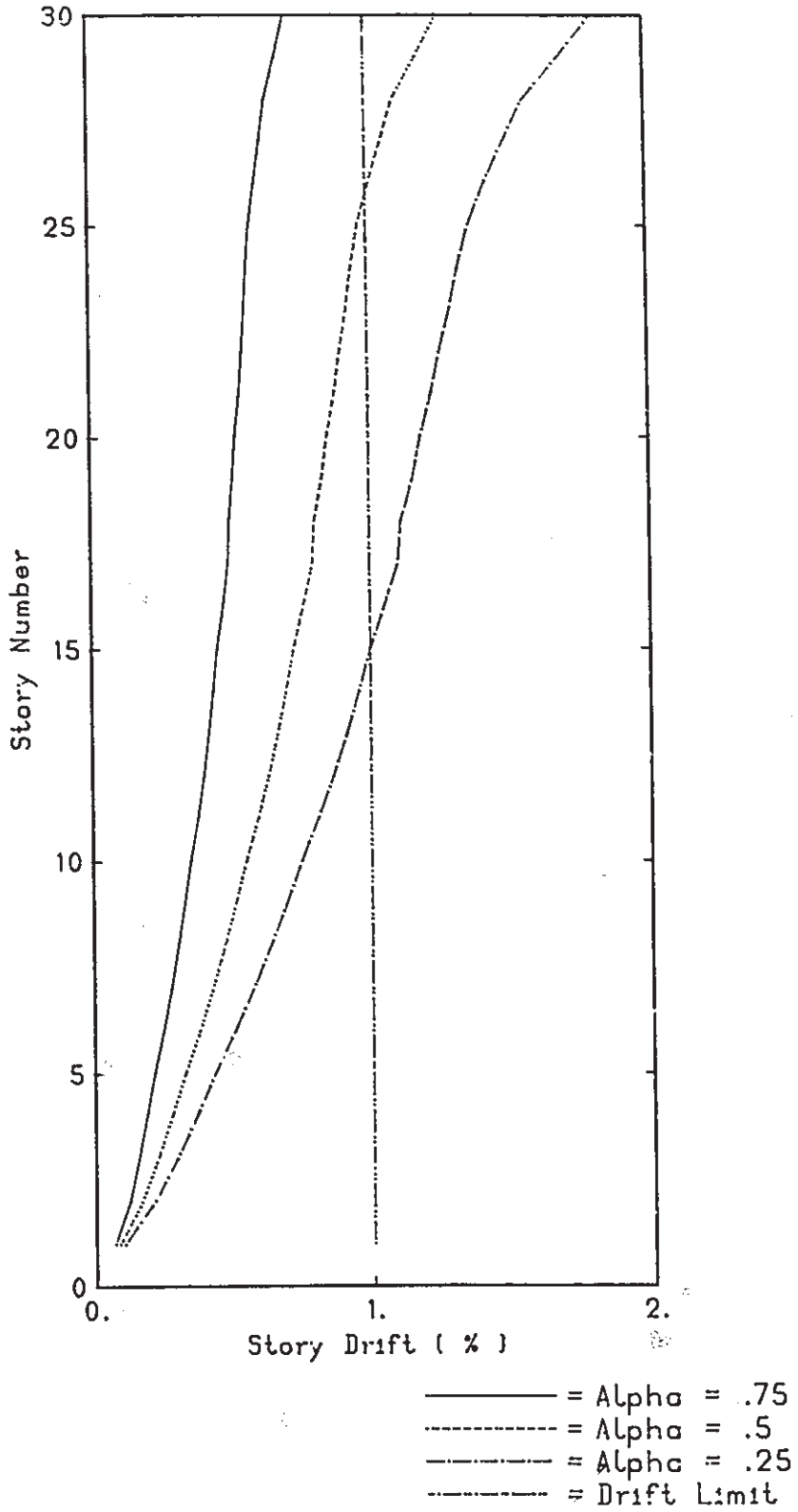

Fig (D.4) Effect of the Reduction of Beam Capacities of the Internal Bays on Story Drift

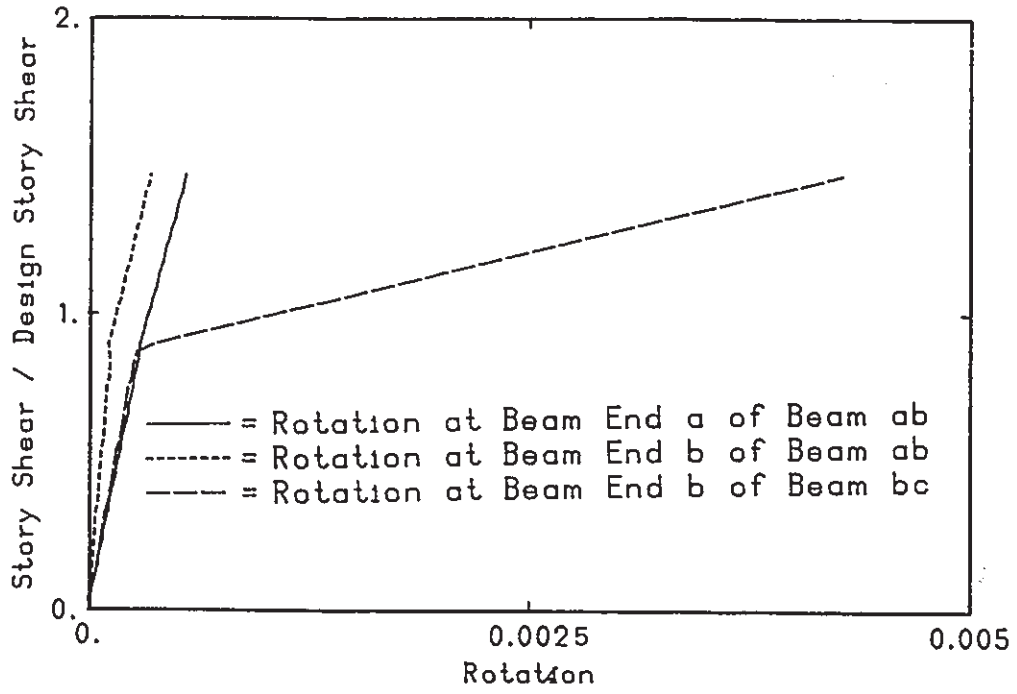

Fig (D.5) Story Shear versus Joint Rotation, Fifth Story

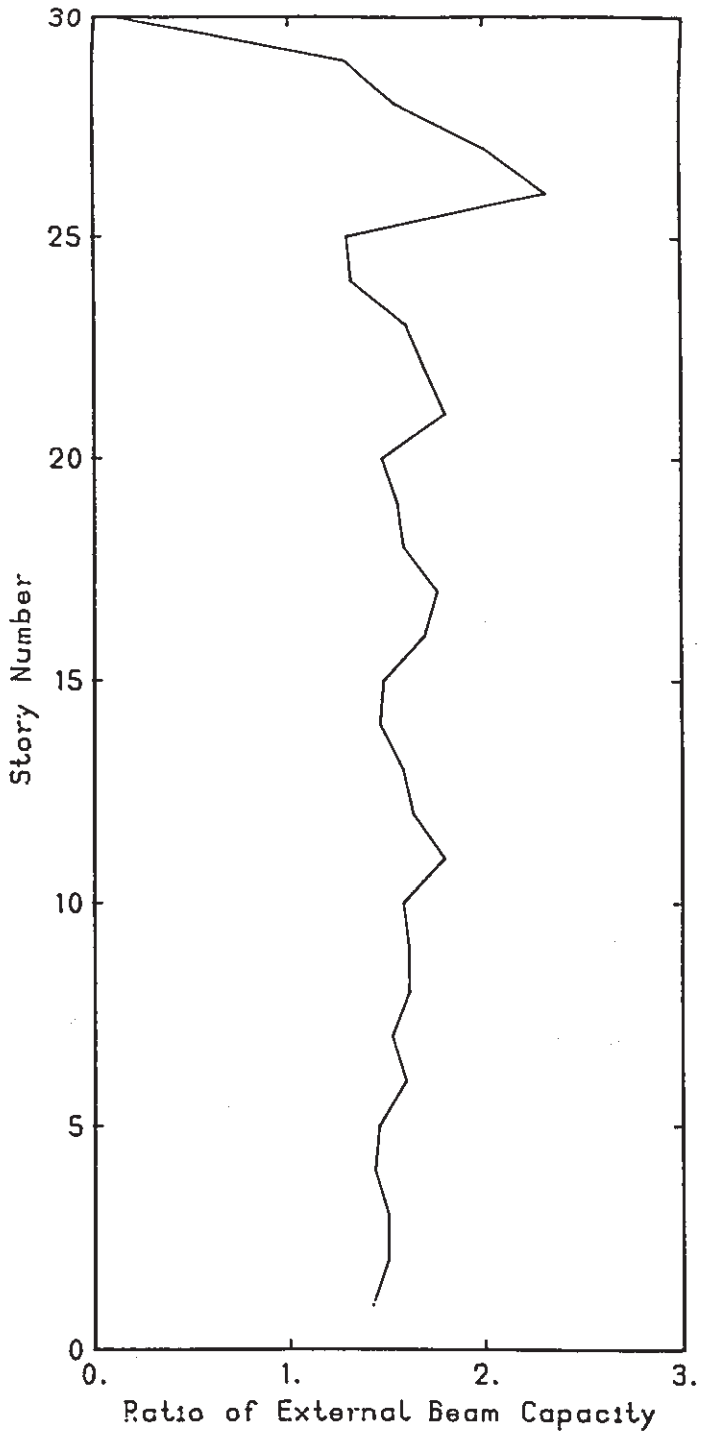

Fig (D.6) Comparison between the Beam Capacities for the Frame Tube with Uniform and distributed Beam capacities